



Zinc based metal–organic framework for nickel adsorption in water and wastewater samples by ultrasound assisted-dispersive-micro solid phase extraction coupled to electrothermal atomic absorption spectrometry

Negar Motakef Kazemi^{a,*}

^{a,*} Department of Medical Nanotechnology, Faculty of Advanced Sciences and Technology, Tehran Medical Sciences, Islamic Azad University, Tehran, Iran

ARTICLE INFO:

Received 14 Sep 2020

Revised form 15 Nov 2020

Accepted 30 Nov 2020

Available online 29 Dec 2020

Keywords:

Metal–organic framework,
Nickel,
Adsorption,
Dispersive- micro solid phase
extraction,
Water sample,
Electrothermal atomic absorption
spectrometry

ABSTRACT

In this research, $Zn_2(BDC)_2(DABCO)$ metal–organic framework (MOF) as a solid phase was used for separation and preconcentration toxic nickel ions (Ni) from water samples by ultrasound assisted-dispersive-micro solid phase extraction coupled to electrothermal atomic absorption spectrometry (USA-D- μ -SPE/ET-AAS). The MOF nanostructure was characterized by field emission-scanning electron microscope (FE-SEM) and transmission electron microscopy (TEM) for presentation of morphology and size of MOF synthesis. By procedure, 25 mg of $Zn_2(BDC)_2(DABCO)$ as MOF adsorbent was added to 25 mL of water samples and then, Ni ions chemically adsorbed based on dative bonding of nitrogen in DABCO (1,4-diazabicyclo [2.2. 2]octane); $N_2(C_2H_4)_3$ at pH=8. The adsorbent was separated from liquid phase by syringe cellulose acetate filters (SCAF, 0.2 μ m) and Ni ions back extracted from MOF adsorbent before determined by ET-AAS. The maximum recovery of MOF for nickel ions as a physically and chemically adsorption was obtained 34.6% and 98.8% at pH=3 and 8, respectively. The capacity adsorption of $Zn_2(BDC)_2(DABCO)$, MOF for nickel was acquired 125.7 mg g⁻¹ at pH=8. By procedure, the preconcentration factor (PF), LOD, and linear range were achieved 48.7, 0.03 μ g L⁻¹ and 0.10-2.88 μ g L⁻¹, respectively (RSD<1.26). The validation of proposed method was successfully obtained by ICP- MS analysis in real samples.

1. Introduction

The water pollution is one of the most important issues in the world today [1-2]. The high concentration of heavy metals in environment has been attributed to population growth, economic

development and rapid industrialization in recent years [3-5]. These toxic metals can enter to the human body after release into the environment. Exposure to heavy metals causes to poisoning, mutagenicity, carcinogenicity and disease in humans, as well as a serious threat to the environment and public health [6]. Nickel is one of the most toxic heavy metal for humans even in

*Corresponding Author: [Negar Motakef Kazemi](mailto:Negar.Motakef.Kazemi@iaups.ac.ir)

Email: motakef@iaups.ac.ir

<https://doi.org/10.24200/amecj.v3.i04.123>

low concentrations. Nickel toxicity causes some disorders in human body such as bone diseases, damage to the liver and the kidney, bronchitis, lung cancer and CNS problem [7, 8]. Nickel ions enter into environment from waste water, water and air from industries and factories such as battery Company, mining and electroplating. Normal range of nickel in human serum ($0.2 \mu\text{g L}^{-1}$) is reported by *American conference of governmental industrial hygienists (ACGIH)*. Also, the nickel values in water samples are ranges from 3 to $10 \mu\text{g L}^{-1}$ and average levels in drinking water is between $2.0\text{--}4.3 \mu\text{g L}^{-1}$ [7,8]. Recently, the different techniques include, flame atomic absorption spectrometry (F-AAS) [9], electrothermal atomic absorption spectrometry (ET-AAS) [10], ultrafiltration [11], ion-exchange [12], chemical precipitation [13], electrodialysis [14], adsorption [15], spectrophotometry [16] and inductively coupled plasma-mass spectrometry (ICP-MS) [17] were used for nickel determination in water and human biological samples. As difficulty matrixes and trace concentration in drinking waters and wastewater, the sample preparation must be used to separation Ni ions from samples. The different procedures for sample preparation of Ni were reported in water samples. For examples, the solid-phase extraction (SPE), the functionalized magnetic SPE [18], the dispersive liquid-liquid microextraction method (DLLME) [19], ultrasound-assisted solid phase extraction (USA-SPE) [20] and micro SPE (D- μ -SPE) [21] were previously presented for preparation of water samples by researchers. Today, the nanotechnology has led to significant advances in different fields of science and product innovation [22]. Nanomaterials have been developed due to their special properties and various application potentials [23, 24]. Recently, the metal-organic frameworks (MOFs) have expanded as porous hybrid organic-inorganic materials [25, 26]. These materials synthesized via self-assembly of primary building blocks including metal ions (or metal clusters) as metal centers, and bridging ligands as linkers [27]. MOFs have been synthesized by different

methods such as solvothermal, hydrothermal, ionic liquids, microwave, sonochemical, diffusion, electrochemical, mechanochemical, and laser ablation [28]. MOFs have received great attention because of their unique properties in many areas [28-29]. The ultrasound assisted-dispersive ionic liquid-suspension solid phase micro extraction is a good candidate method for Ni extraction from waters [30].

In the present study, the nickel absorption is one of the most considerable applications of $\text{Zn}_2(\text{BDC})_2(\text{DABCO})$ MOF in waters. So, The Zn-MOF adsorbent based on USA-D- μ -SPE procedure was used for nickel adsorption/extraction from water samples and the concentration of nickel ions determined by ET-AAS.

2. Experimental

2.1. Materials

All reagents with high purity and analytical grade were purchased from Merck (Darmstadt, Germany). Materials including zinc acetate dihydrate ($\text{Zn}(\text{OAc})_2 \cdot 2\text{H}_2\text{O}$), 1,4 benzenedicarboxylic acid (BDC), 1,4-diazabicyclo [2.2.2] octane (DABCO), dimethylformamide (DMF) were purchased and used for synthesis of $\text{Zn}_2(\text{BDC})_2(\text{DABCO})$ MOF. The syringe cellulose acetate filters (SCAF, $0.2 \mu\text{m}$) purchased from Sartorius, Australia (Minisart® Syringe Filters). The GBC 932, electrothermal atomic absorption spectrophotometer (ET-AAS, model 932, Australia) equipped with a graphite furnace were used for the determination of nickel in water samples. The samples were injected to graphite tube with auto-sampler ($20 \mu\text{L}$). The ICP-MS was used for determining of ultra-trace nickel in water samples (Perkin Elmer, 1200 W; 2.0 L min^{-1} ; 1-1.5 sec per mass; N_2 gas). The pH meter with the glassy electrode was used for measuring pH in water samples (Metrohm, E-744, Switzerland). The shacking of water and wastewater samples were done by vortex mixer (Thermo, USA). The standard solution of nickel nitrate (1%, $\text{Ni}(\text{NO}_3)_2$) was purchased from Sigma, Germany. All of Ni standard 0.5-5 ppb was daily prepared

by dilution of the standard Ni solution with DW. Ultrapure water was prepared from RIPI Co. (IRAN). The pH was adjusted from 5.5 to 8.0 by sodium phosphate buffer solution (0.2 M, Merck, Germany).

2.2. Characterization

The MOF was characterized by scanning electron microscope (FESEM) (SIGMA VP) and transmission electron microscope TEM (EM10C) microscopes from Zeiss Company. X-ray diffraction (XRD) spectrum were prepared by a Seifert TT 3000 diffractometer (Germany) using wavelength 0.15 nm. The Fourier transform infrared spectrophotometer (FTIR, IFS 88, Bruker Optik GmbH, Germany) was used in the 200-4000 cm^{-1} . Determination of nickel was performed with ET-AAS.

2.3. Synthesis of MOF

The $Zn_2(BDC)_2(DABCO)$ MOF was prepared via the self-assembly of Zn^{2+} ion as a connector, DABCO as a bridging ligand, and BDC as a chelating ligand. In a typical reaction, Zn (OAc) $_2$ ·2H $_2$ O (0.132 g, 2 mmol), BDC (0.1 g, 2 mmol), and DABCO (0.035 g, 1 mmol) were added to 25 ml DMF [4]. The reactants were sealed under reflux and stirred at 90 °C for 15 min. Then, the reaction mixture was cooled to room temperature, and filtered. The white crystals were washed with DMF to remove any metal and

ligand remained, and dried in a vacuum. DMF was removed from white crystals with a vacuum furnace at 150 °C for 5 h.

2.4. General procedure of nickel adsorption

By proposed method, the $Zn_2(BDC)_2(DABCO)$ as metal–organic framework (MOF) was used for extraction of toxic nickel ions (Ni^{2+}) from water samples by USA-D- μ -SPE procedure (Fig.1). Firstly, 25 mg of $Zn_2(BDC)_2(DABCO)$ adsorbent added to 25 mL of water samples included Ni standard solution and Ni ions chemically adsorbed based on dative bonding of nitrogen groups in DABCO material after shaking for 10 min at pH=8. Secondly, the $Zn_2(BDC)_2(DABCO)$ adsorbent separated from water samples by SCAF (10 mL, 0.2 μ m) and then the Ni loaded on the MOF was back-extracted from solid-phase based on changing pH by nitric acid solution (0.2 M, 0.25 mL). After dilution, the remained solution was determined by ET-AAS after dilution with DW up to 0.5 mL. Also, the adsorptions of the $Zn_2(BDC)_2(DABCO)$ adsorbent were evaluated in different pH by USA-D- μ -SPE procedure and capacities adsorption was obtained. The proposed procedure was used for a blank solution without any analyte (Ni) for 10 times. The calibration curve for nickel in was prepared from LLOQ to ULOQ ranges (0.1-2.88 μ g L $^{-1}$) and the PF obtained by the curve-fitting rule.

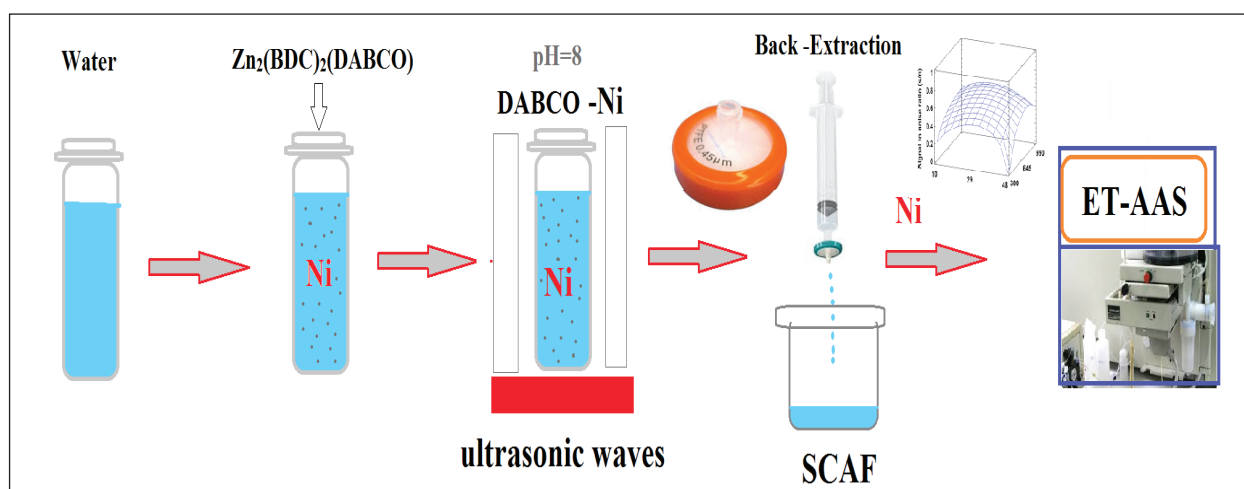


Fig. 1. Extraction procedure for nickel ions in water by $Zn_2(BDC)_2(DABCO)$ adsorbent

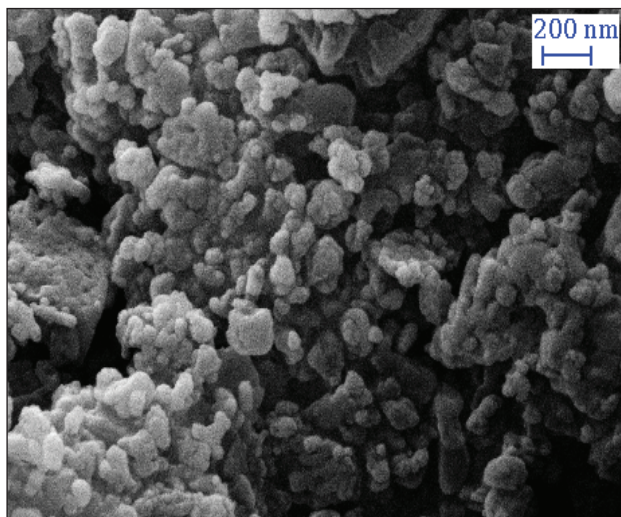


Fig. 2a. FESEM of $Zn_2(BDC)_2(DABCO)$ MOF

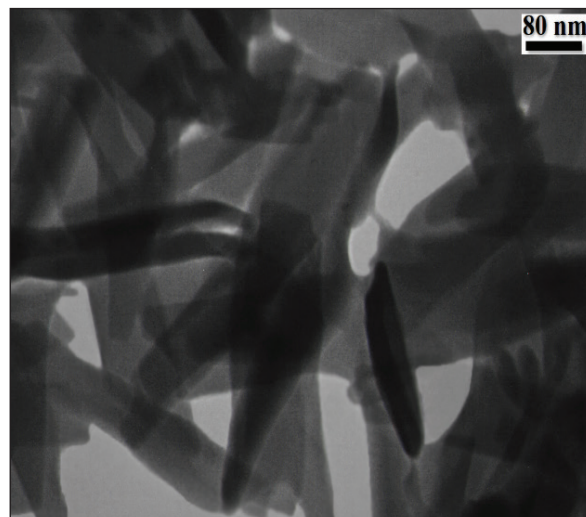


Fig. 2b. TEM of $Zn_2(BDC)_2(DABCO)$ MOF

3. Results and Discussion

3.1. FE-SEM and TEM

Field emission scanning electron microscope (FE-SEM) was used for evaluation of morphology of MOF [$Zn_2(BDC)_2(DABCO)$] with an average diameter of 100 nm (**Fig. 2a**). Transmission electron microscope (TEM) was used for evaluation of nanoparticles size and morphology of the MOF. TEM showed the pore shape and size, the pore has rod-shaped with many pore with different sizes from 20-80 nm (**Fig. 2b**).

3.2. FTIR of $Zn_2(BDC)_2(DABCO)$ MOF

The organic material and functional groups such as NH, CO, SH in different adsorbents were identified by FTIR analysis. The FTIR spectrum of $Zn_2(BDC)_2(DABCO)$ MOF was obtained after calcination in KBr matrix (250 °C). As results, there is no peak based on impurities and and it confirm the completion of the synthesis. Also, various peaks were presented such as 705 cm^{-1} and 1000 cm^{-1} for ZnO bonds, 3000 cm^{-1} - 3500 cm^{-1} for OH of carboxylic acid, 1600 cm^{-1} for CO stretching

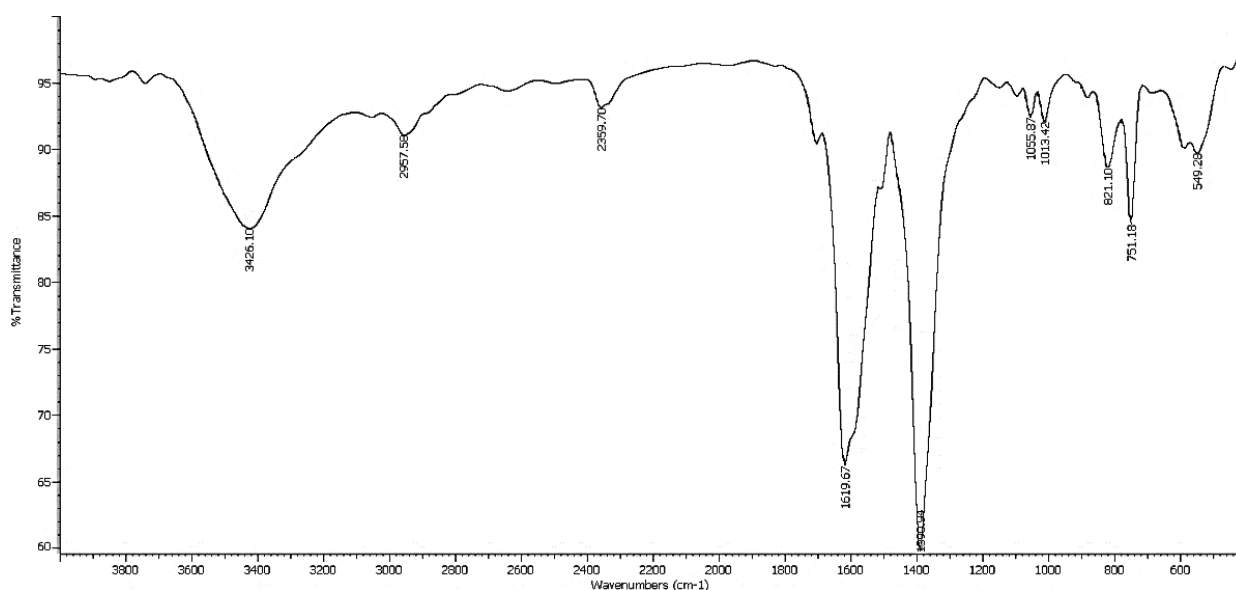


Fig. 3. FTIR spectrum of the $Zn_2(BDC)_2(DABCO)$ MOF.

bond and 1440 cm^{-1} , 1358 cm^{-1} , 1429 cm^{-1} and 1550 cm^{-1} for aromatic compounds (Fig.3).

3.3. XRD of $Zn_2(BDC)_2(DABCO)$ MOF

By application of XRD technique, the essential information can obtain based on crystal structure and product purity by XRD analysis. The XRD pattern for the $Zn_2(BDC)_2(DABCO)$ MOF was shown in Figure 4. By results, all peaks are clear. In addition, the XRD pattern for the $Zn_2(BDC)_2(DABCO)$ has no peak belong to impurities. The crystal structure of the $Zn_2(BDC)_2(DABCO)$ confirm by sharp peaks of XRD pattern. The size of the $Zn_2(BDC)_2(DABCO)$ MOF was achieved about 45 nm by Debye-Scherrer equation.

3.4. The pH optimization

The pH is the effective factor on adsorption and extraction of nickel ions by USA-D- μ -SPE procedure. So, the different pH between 2-10 was studied for extraction of Ni (II) in water and wastewater samples. The experimental results showed us, the $Zn_2(BDC)_2(DABCO)$

MOF was simply extracted Ni (II) ions from water samples in a pH 7.5-8.5. Moreover, the extraction efficiency was achieved about 98.7% in pH of 8 but, the recoveries were reduced at acidic pH less than 7 and basic pH more than 9.0. So, the optimum pH of 8 was used for further works in this study. The extraction mechanism of nickel ions in water samples based on $Zn_2(BDC)_2(DABCO)$ MOF take place by the coordination of dative covalent bond of N group as negative charge with the positively charged Ni ions ($Ni \rightarrow :N$) at pH=8. At lower pH ($pH < pK_{pzc}$), the surface of $Zn_2(BDC)_2(DABCO)$ MOF have positively charged and extraction efficiency decreased as repulsion. Also, the surface of $Zn_2(BDC)_2(DABCO)$ MOF have negatively charged at pH=8 and so the negative charge between nitrogen group and Ni^{2+} caused to increased recovery. At pH more than 8, the Ni ions started to participate ($Ni(OH)_2$) and so, the recovery decreased (Fig. 5). The best pH for physical adsorption was achieved at pH between 3-4 with the mean recovery of 34.6%.

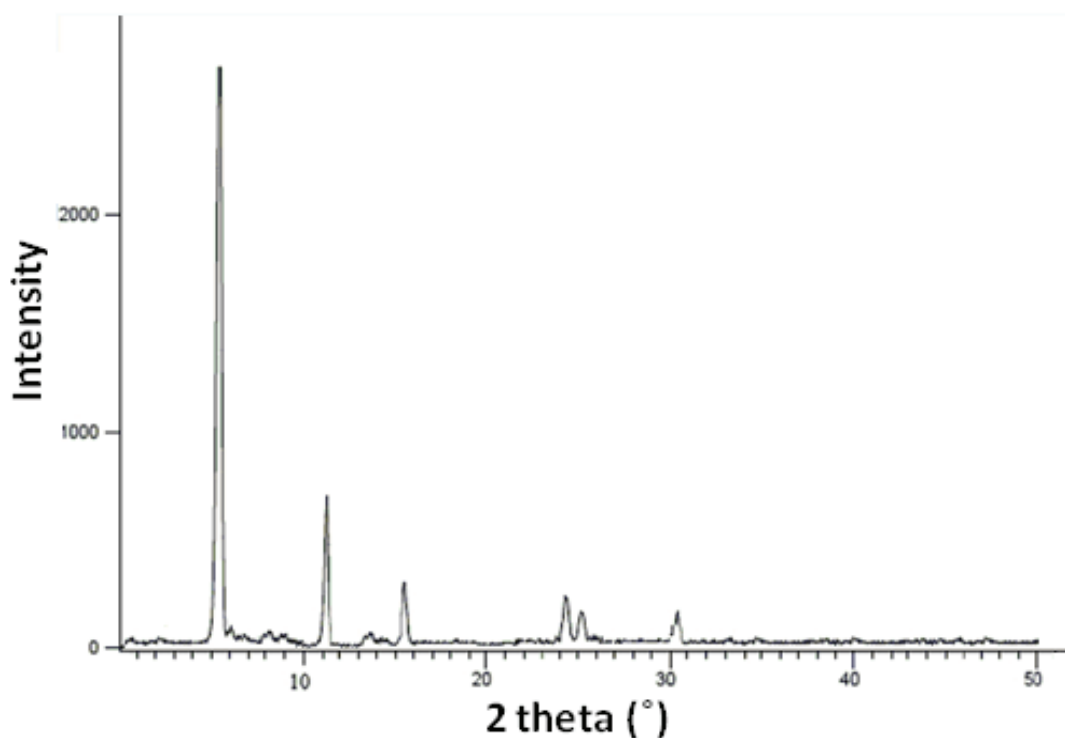


Fig.4. XRD pattern of the synthesized $Zn_2(BDC)_2(DABCO)$ MOF

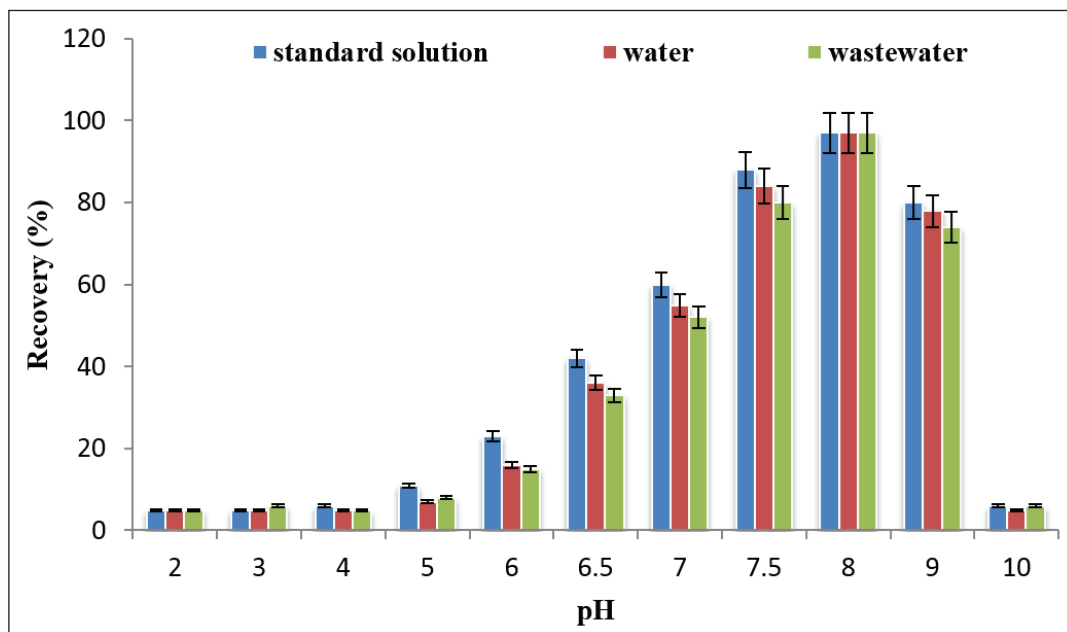


Fig. 5. The effect of pH on nickel extraction in water samples based on $Zn_2(BDC)_2(DABCO)$ MOF by USA-D- μ -SPE procedure

3.5. The effect of sample volume

The influence of sample volume for Ni extraction based on $Zn_2(BDC)_2(DABCO)$ MOF was studied between 5-50 mL in water and wastewater samples with LLOQ and ULLOQ ranges ($0.1-2.88 \mu g L^{-1}$). The results showed us the high recoveries were

achieved for 25 mL of water samples and wastewater samples. So, 25 mL of sample was selected as optimum volume for nickel extraction in water and wastewater samples at pH=8. By increasing the sample volume more than 25 mL, the extraction recoveries were reduced between 43-52% (**Fig. 6**).

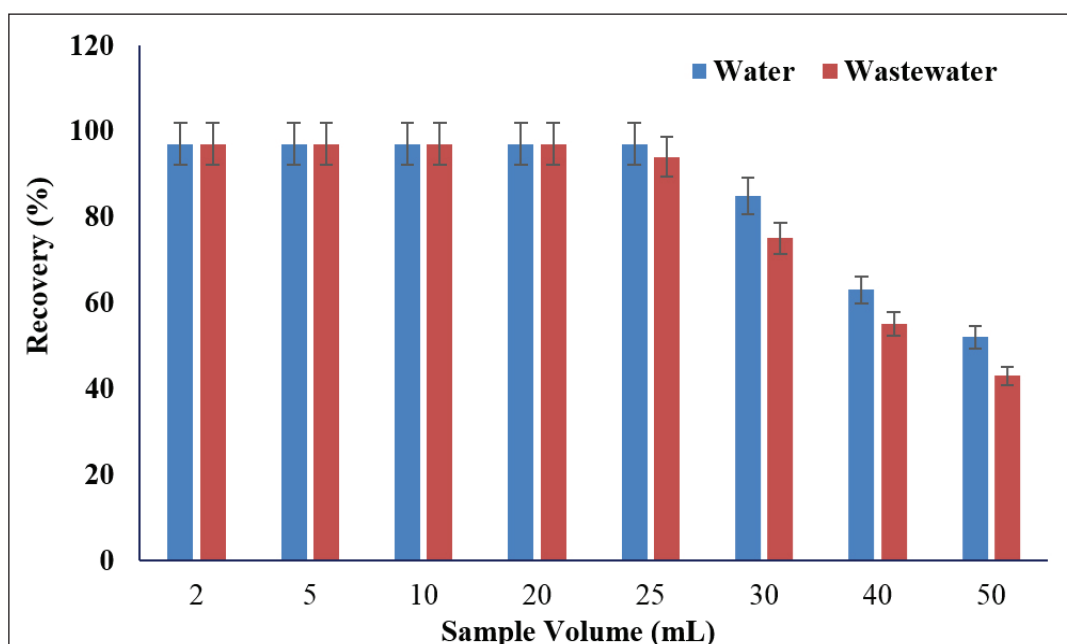


Fig. 6. The effect of sample volume on nickel extraction in water samples based on $Zn_2(BDC)_2(DABCO)$ MOF by USA-D- μ -SPE procedure

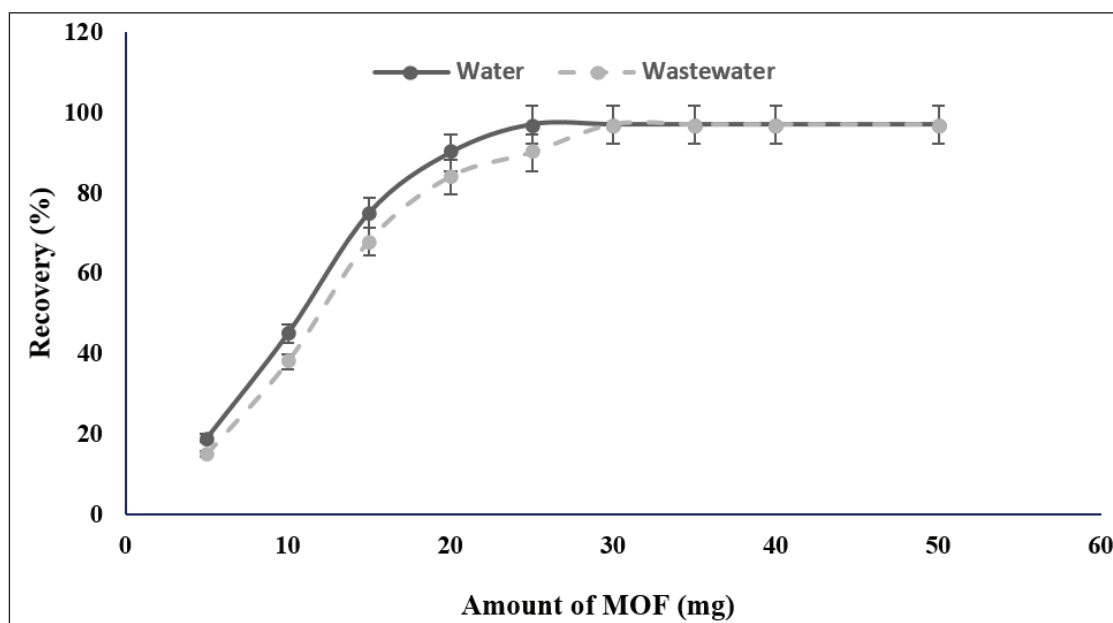


Fig. 7. The effect of MOF mass for nickel extraction in water samples based on $Zn_2(BDC)_2(DABCO)$ MOF by USA-D- μ -SPE procedure

3.6. The effect of $Zn_2(BDC)_2(DABCO)$ MOF

For efficient recovery, the amount of $Zn_2(BDC)_2(DABCO)$ MOF must be evaluated and optimized. Therefore, the amounts of $Zn_2(BDC)_2(DABCO)$ MOF between 5-50 mg were examined for Ni(II) adsorption/extraction by the USA-D- μ -SPE procedure. The results showed that the quantitative recoveries in water samples were obtained with 22 mg of $Zn_2(BDC)_2(DABCO)$ MOF for nickel extraction at pH=8. So, 25 mg of $Zn_2(BDC)_2(DABCO)$ MOF was used as optimum of MOF mass for further process (Fig. 7). The results showed us the extra dosage of MOF had no effect on the extraction value in water samples.

3.7. The effect of eluent

The eluents with different volume and concentration was used for back-extraction of nickel ions from $Zn_2(BDC)_2(DABCO)$ MOF. Acidic pH cause to breakdown the dative bond between nitrogen group in MOF and nickel ions (MOF-N: Ni) and then, the Ni (II) ions release into the eluent phase. Therefore, a different volume of acid solution such as HCl, HNO_3 , H_2SO_4 and H_2CO_3 with various concentration was examined for back extraction

Ni(II) in water samples ($0.1-1 \text{ mol L}^{-1}$, $0.1-0.5 \text{ mL}$) by syringe cellulose acetate filters (SCAF, $0.2 \mu\text{m}$). The results showed that $0.2 \text{ mol L}^{-1} HNO_3$ as elution phase can efficient released the Ni (II) ions from $Zn_2(BDC)_2(DABCO)$ MOF to liquid phase. So, 0.2 mol L^{-1} of HNO_3 (0.1 mL) was selected as the optimum concentration and volume of HNO_3 eluent in this study. As a result, the elution of solid phase ($Zn_2(BDC)_2(DABCO)$ MOF) with nitric acid (0.2 M , 0.1 mL) was simply back extracted nickel ions from MOF (Fig.8).

3.8. Validation

By USA-D- μ -SPE procedure, the nickel extraction based on $Zn_2(BDC)_2(DABCO)$ MOF was obtained in water and wastewater samples. The experimental results showed a validated data for Ni (II) in tab water, drinking water, river water and wastewater samples at pH=8 (Table 1). The accuracy of the data were confirmed by spiking of nickel standard solution to water samples based on $Zn_2(BDC)_2(DABCO)$ MOF adsorbent. Due to results the efficient recovery for extraction Ni ions in wastewater and water samples was achieved by nanoparticles of $Zn_2(BDC)_2(DABCO)$ MOF.

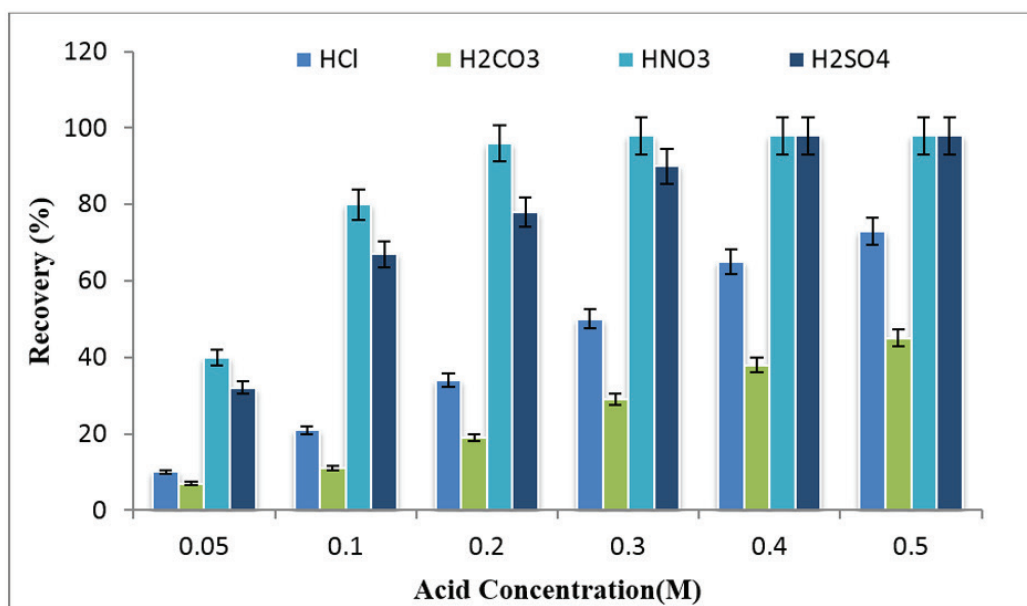


Fig. 8. The effect of eluents on nickel extraction based on $Zn_2(BDC)_2(DABCO)$ MOF

The perfect extraction demonstrated that the USA-D- μ -SPE technique had satisfactory results for nickel in real samples at pH=8. In addition,

the standard reference materials (SRM) were used for validating of DIL-S- μ -SPE procedure (**Table 2**).

Table 1. Validation of methodology for nickel extraction and determination in water samples by spiking of samples by USA-D- μ -SPE procedure coupled to ET-AAS

Sample	Added ($\mu\text{g L}^{-1}$)	*Found ($\mu\text{g L}^{-1}$)	Recovery (%)
Tab Water	---	0.454 ± 0.022	---
	0.5	0.948 ± 0.045	98.80
Drinking Water	---	1.641 ± 0.072	---
	1.5	3.103 ± 0.147	97.46
^a Wastewater	---	1.723 ± 0.084	---
	1.0	2.745 ± 0.133	102.22
Well water	---	0.832 ± 0.042	---
	0.5	1.311 ± 0.058	95.81
River water	---	1.074 ± 0.053	---
	1.0	2.108 ± 0.105	103.42
^b Sea Water	---	1.824 ± 0.092	---
	1.0	2.787 ± 0.128	96.30

*Mean of three determinations of samples \pm confidence interval (P = 0.95, n = 10)

^a wastewater dilution with DW (1:10)

^b Sea water dilution with DW (1:5)

Table 2. Determination of nickel in water samples based on Zn₂(BDC)₂(DABCO) MOF by standard reference materials (SRM)

Sample	Added ($\mu\text{g L}^{-1}$)	SRM Value ($\mu\text{g L}^{-1}$)	*Found ($\mu\text{g L}^{-1}$)	Recovery(%)
^a 1643f	-----	1.5	1.49 \pm 0.06	-----
	1.5	-----	2.91 \pm 0.13	94.6
^a 1643e	-----	1.5	1.59 \pm 0.07	-----
	1.5	-----	3.15 \pm 0.15	104.1
^a 1640a	-----	0.6	0.63 \pm 0.03	-----
	0.5	-----	1.12 \pm 0.05	98.0
^b 3136	-----	1.0	1.02 \pm 0.05	-----
	1.0	-----	1.98 \pm 0.08	96.0

* Mean of three determinations of samples \pm SD (P = 0.95, n = 10)

^a Standard Reference Material 1643f (1.50), 1643e (1.50) and 1640a (0.6), trace elements in water, after dilution with DW (1:40)

^b NIST, SRM 3136, Sigma, after dilution with DW the concentration of 1.0 $\mu\text{g L}^{-1}$ daily prepared

3.9. Comparing with other methods

The USA-D- μ -SPE procedure was compared to other published articles for extraction and determination of Ni ions in water samples (Table 3). Due to table 3, the different methodology and adsorbents compared for nickel extraction in water samples. Many parameters such as LOD,

PF, RSD%, sample volume, capacity adsorption and etc. compared together. The results showed us, the USA-D- μ -SPE procedure was comparable to other presented works in Table 3. Therefore, the Zn₂(BDC)₂(DABCO) MOF with favorite properties can be used for extraction of nickel in water samples in optimized conditions.

Table 3. Comparing of USA-D- μ -SPE procedure with other published method for nickel extraction in different matrixes

Methods	Instrument	Metal	Matrix	LOD($\mu\text{g L}^{-1}$)	EF/PF	%RSD	Ref
SPE	F-AAS	Ni/Cu	Water and biological samples	0.6	200	3.1	[31]
IIPSPE	UV-VIS	NI	Water	1.0	125	2.4	[32]
SPE	F-AAS	Ni, Ca, Co, Cu	Tea, Water	1.0	10	2.0	[33]
ISSADSPE	F-AAS	Ni	Water	0.7	50	2.5	[34]
NH-IS-SPE	μ S-FAAS	Ni,Cr,Co	Water and Food	2.74	205	3.5	[35]
SPE	ICP-OES	Ni	Water	0.025	80	2.6	[36]
PPT-SPE	F-AAS	Ni	Water	2.7	120	4.4	[37]
USA-D- μ -SPE	ET-AAS	Ni	Water	0.03	48.7	1.26	This week

SPE: solid phase extraction

IIPSPE: Ion imprinted polymer- solid phase extraction

ISSADSPE: In-syringe solvent-assisted dispersive solid phase extraction

NH-IS-SPE: Needle hub in-syringe solid phase extraction

μ S-FAAS: micro-sampling flame atomic absorption spectrometry

PPT-SPE: Pipette tip Solid phase extraction

4. Conclusions

In this study, the $Zn_2(BDC)_2(DABCO)$ MOF adsorbent was synthesized by solvothermal method at 90 °C via the self-assembly metal centers and linkers using DMF solvent. Based on the results, the MOF was propped as a good candidate for nickel adsorption/extraction from water samples by USA-D- μ -SPE procedure at pH=8. The syringe cellulose acetate filters (SCAF, 0.2 μ m) was used for separation of $Zn_2(BDC)_2(DABCO)$ MOF from liquid phase and back-extraction of Ni ions from adsorbent before determined by ET-AAS. The $Zn_2(BDC)_2(DABCO)$ MOF had the high recovery between 94.6-104.1 for Ni extraction from water samples. The proposed USA-D- μ -SPE method had low LOD and RSD% with good reusability about 21 times for water samples. Therefore, the $Zn_2(BDC)_2(DABCO)$ MOF caused to create the efficient extraction of Ni ions in water samples based on chemical adsorption. The nickel concentration in remain solution has simply determined by ET-AAS after back-extraction and dilution with DW.

5. Acknowledgement

The authors wish to thank from Department of Medical Nanotechnology, Tehran Medical Sciences, Islamic Azad University (IAUMS), Iranian Research Institute of Petroleum Industry (RIPI) and Iranian Petroleum Industry Health Research Institute (IPIHRI) for supporting this work.

6. References

- [1] M.R. Mehmandoust, N. Motakef-Kazemi, F. Ashouri, Nitrate adsorption from aqueous solution by metal-organic framework MOF-5, Iran. J. Sci. Technol. Trans. A-Sci., 43 (2019) 443-449.
- [2] N. Kazemi, M. Yaqoubi, Synthesis of bismuth oxide: removal of benzene from waters by bismuth oxide nanostructures, Anal. methods Environ. Chem. J., 2 (2019) 5-14.
- [3] M. Odar, N. Kazemi, Nanohydroxyapatite and its polycaprolactone nanocomposite for lead sorbent from aqueous solution, Nanomed. Res. J., 5 (2020) 143-151.
- [4] N. Motakef-Kazemi, A novel sorbent based on metal-organic framework for mercury separation from human serum samples by ultrasound assisted-ionic liquid-solid phase microextraction. Anal. methods Environ. Chem. J., 2 (2019) 67-78.
- [5] E. Mosafayian Jahromy, N. Kazemi, Speciation of selenium (IV, VI) in urine and serum of thyroid patients by ultrasound-assisted dispersive liquid-liquid microextraction, Anal. methods Environ. Chem. J., 3 (2020) 5-17.
- [6] P.B. Tchounwou, C.G. Yedjou, A.K. Patlolla, D.J. Sutton, Heavy metal toxicity and the environment, Mol. Clin. Environ. Toxicol., 101 (2012) 133-164.
- [7] S.K. Seilkop, A.R. Oller, Respiratory cancer risks associated with low-level nickel exposure: An integrated assessment based on animal, epidemiological, and mechanistic data, Regul. Toxicol. Pharm., 37 (2003) 173-190.
- [8] Agency for Toxic Substances and Disease Registry (ATSDR), Toxicological profile for Nickel. Atlanta, GA: U.S. Department of Health and Human Services, Public Health Service, 2005.
- [9] A.A. Satti, D.I. Temuge, S. Bektas, A.C. Sahin, An application of coacervate-based extraction for the separation and preconcentration of cadmium, lead, and nickel ions prior to their determination by flame atomic absorption spectrometry in various water samples, Turk. J. Chem., 40 (2016) 979-987.
- [10] E.M. Sedykh, L.N. Bannykh, G.S. Korobeinik, N.P. Starshinova, Determination of nickel and vanadium in crude oils by electrothermal atomic absorption spectrometry and inductively coupled plasma atomic emission spectroscopy after mineralization in an

- autoclave, *Inorg. Mater.*, 47 (2011) 1539–1543.
- [11] Q. Zhang, J. Gao, Y.R. Qiu, Removal of Ni (II) and Cr (III) by complexation-ultrafiltration using rotating disk membrane and the selective separation by shear induced dissociation, *Chem. Eng. Process.*, 135 (2019) 236-244.
- [12] A. Dabrowski, Z. Hubicki, P. Podkościelny, E. Robens, Selective removal of the heavy metal ions from waters and industrial wastewaters by ion-exchange method, *Chemosphere*, 56 (2004) 91-106.
- [13] M.M Matlock, B.S Howerton, D.A Atwood, Chemical precipitation of heavy metals from acid mine drainage, *Water Res.*, 36 (2002) 4757-4764.
- [14] T. Mohammadi, A. Moheb, M. Sadrzadeh, A. Razmi, Modelling of metal ion removal from wastewater by electrodialysis, *Sep. Purif. Technol.*, 41 (2005) 73-82.
- [15] V. Srivastava, C.H. Weng, V.K. Singh, Y.C. Sharma, Adsorption of nickel ions from aqueous solutions by nano alumina: kinetic, mass transfer, and equilibrium studies, *J. Chem. Eng. Data*, 56 (2011) 4.
- [16] R. Acharya, S. Kolay, A.V.R. Reddy, Determination of nickel in finished product alloys by instrumental neutron activation analysis and spectrophotometry, *J. Radioanal. Nucl. Chem.*, 294 (2012) 309–313.
- [17] D.P.C. De Quadros, D.L.G. Borges, Direct analysis of alcoholic beverages for the determination of cobalt, nickel and tellurium by inductively coupled plasma mass spectrometry following photochemical vapor generation, *Microchem. J.*, 116 (2014) 244–248.
- [18] S.Z. Mohammadi, H. Hamidian, L. Karimzadeh, Z. Moeinadini, Simultaneous extraction of trace amounts of cobalt, nickel and copper ions using magnetic iron oxide nanoparticles without chelating agent, *J. Anal. Chem.*, 68 (2013) 953–958.
- [19] M. Nassiri, R. Gharanjik, H. Hashemi, Spectrophotometric determination of copper and nickel in marine brown Algae after preconcentration with surfactant assisted dispersive liquid-liquid microextraction, *Iran. J. Chem. Chem. Eng.*, 39 (2020) 117-126.
- [20] M. Behbahani, V. Zarezade, A. Veisi, F. Omidi, S. Bagheri, Modification of magnetized MCM-41 by pyridine groups for ultrasonic-assisted dispersive micro-solid-phase extraction of nickel ions, *Int. J. Environ. Sci. Technol.*, 16 (2019) 6431–6440.
- [21] M. Rajabi, M. Abolhosseini, Magnetic dispersive micro-solid phase extraction merged with micro-sampling flame atomic absorption spectrometry using (Zn-Al LDH)-(PTh/DBSNa)-Fe₃O₄ nanosorbent for effective trace determination of nickel(II) and cadmium(II) in food samples, *Microchem. J.*, 159 (2020) 105450.
- [22] S. Hajiashrafi, N. M. Kazemi, Green synthesis of zinc oxide nanoparticles using parsley extract, *Nanomed. Res. J.*, 3 (2018) 44-50.
- [23] N. M. Kazemi, A.A. Salimi, Chitosan nanoparticle for loading and release of nitrogen, potassium, and phosphorus nutrients, *Iran. J. Sci. Technol. Trans A-Sci.*, 43 (2019) 2781–2786.
- [24] N. Motakef-Kazemi, M. Sandalnia, In situ production and deposition of bismuth oxide nanoparticles on cotton fabric, *Iran. J. Sci. Technol. Trans. A-Sci.*, 44 (2020) 1217–1223.
- [25] S. Hajiashrafi, Preparation and evaluation of ZnO nanoparticles by thermal decomposition of MOF-5, *Heliyon*, 5 (2019) e02152.

- [26] B. Miri, S.A. Shojaosadati, A. Morsali, Application of a nanoporous metal organic framework based on iron carboxylate as drug delivery system, *Iran. J. Pharm. Res.*, 17 (2018) 1164-1171.
- [27] N. Motakef-Kazemi, S.A. Shojaosadati, A. Morsali, Evaluation of the effect of nanoporous nanorods $Zn_2(bdc)_2(dabco)$ dimension on ibuprofen loading and release, *J. Iran. Chem. Soc.*, 13 (2016) 1205-1212.
- [28] F. Ataei, D. Dorrnian, N. Motakef-Kazemi, Bismuth-based metal-organic framework prepared by pulsed laser ablation method in liquid, *J. Theor. Appl. Phys.*, (2020). [http://doi: 10.1007/s40094-020-00397-y](http://doi:10.1007/s40094-020-00397-y).
- [29] N. Motakef-Kazemi, S.A. Shojaosadati, A. Morsali, In situ synthesis of a drug-loaded MOF at room temperature, *Micropor. Mesopor. Mat.*, 186 (2014) 73-79.
- [30] H. Shirkhanloo, Z. Karamzadeh, J. Rakhtshah, N. Motakef-Kazemi, A novel biostructure sorbent based on CysSB/MetSB@MWCNTs for separation of nickel and cobalt in biological samples by ultrasound assisted-dispersive ionic liquid-suspension solid phase micro extraction, *J. Pharm. Biomed. Anal.*, 172 (2019) 285-294.
- [31] M. Karimi, Sh. Dadfarnia, A.M. Haji Shabani, Application of deep eutectic solvent modified cotton as a sorbent for online solid-phase extraction and determination of trace amounts of copper and nickel in water and biological samples, *Biol. Trace Elem. Res.*, 176 (2017) 207-215.
- [32] H.R. Rajabi, S. Razmpour, Synthesis, characterization and application of ion imprinted polymeric nanobeads for highly selective preconcentration and spectrophotometric determination of Ni^{2+} ion in water samples, *Spectrochim. Acta A*, 153 (2016) 45-52.
- [33] S.Z. Mohammadi, H. Hamidian, Tween 80 coated alumina: an alternative support for solid phase extraction of copper, nickel, cobalt and cadmium prior to flame atomic absorption spectrometric determination, *A. J. Chem.*, 9 (2016) S1290-S1296.
- [34] Jamshid Mofid Nakhaeia, Mohammad Reza Jamali, In-syringe solvent-assisted dispersive solid phase extraction followed by flame atomic absorption spectrometry for determination of nickel in water and food samples, *Microchem. J.*, 144 (2019) 88-92.
- [35] M. Shirania, F. Salaria, Needle hub in-syringe solid phase extraction based a novel functionalized biopolyamide for simultaneous green separation/preconcentration and determination of cobalt, nickel, and chromium (III) in food and environmental samples with micro sampling flame atomic absorption spectrometry, *Microchem. J.* 152 (2020) 104340.
- [36] M.S. Yalcin, S. Ozdemir, E. Kılinc, Preconcentrations of Ni(II) and Co(II) by using immobilized thermophilic geobacillus stearothermophilus SO-20 before ICP-OES determinations, *Food Chem.*, 266 (2018) 126-132.
- [37] M.A. Habila, Z.A. Alothman, E. Yilmaz, M. Soylak, Activated carbon cloth filled pipette tip for solid phase extraction of nickel(II), lead(II), cadmium(II), copper(II) and cobalt(II) as 1,3,4-thiadiazole-2,5-dithiol chelates for ultra-trace detection by FAAS, *Int. J. Environ. Anal. Chem.*, 98 (2018) 171-181.



Sulfamethizole functionalized graphene oxide for in-vitro separation and determination lead in blood serum of battery manufactories workers by syringe filter-dispersive-micro solid phase extraction

Abhijit De^{a,*} and S. Mojtaba Mostafavi^b

^a HITech institute of theoretical and computational chemistry, Shivakote, Hesaraghatta Hobli, Bengaluru, India

^b Department of Chemistry, Iranian-Australian Community of Science, Hobart, University of Tasmania, Australia

ARTICLE INFO:

Received 18 Aug 2020

Revised form 24 Oct 2020

Accepted 14 Nov 2020

Available online 29 Dec 2020

Keywords:

Lead,
Human blood/serum,
Sulfamethizole,
Nano graphene oxide,
Syringe filter,
Dispersive-micro solid phase extraction procedure

ABSTRACT

The toxic effect of lead (Pb) causes to anemia and iron deficiency in human body. So, the lead determination in blood/serum samples is very important. In this study, a novel adsorbent based on sulfamethizole functionalized on nanographene oxide (C₃H₁₀N₄O₂S₂-NGO; SM-NGO) was used for extraction of Pb(II) from human blood, serum and plasma samples in battery manufactories workers by syringe filter-dispersive-micro solid phase extraction procedure (SF-D- μ -SPE). By procedure, 25 mg of SM-NGO mixed with 10 mL of human blood/serum or plasma samples and aspirated by 10 mL of syringe tube. After sonication of samples for 5 min, the Pb ions adsorbed based on sulfur of SM-NGO adsorbent at pH=6 and the solid phase separated by syringe coupled to Millex-FG hydrophobic PTFE membrane (0.2 μ m). Then, the lead ions were back-extracted from SM-NGO/PTFE by elution phase with 0.5 mL of nitric acid solution (0.5 M). Finally, the concentrations of Pb(II) ions were determined by atom trap flame atomic absorption spectrometry (AT-FAAS) after dilution with DW up to 1 mL. After optimization, the linear range (LR), LOD and enrichment factor (EF) for Pb ions was obtained, 10-500 μ g L⁻¹, 2.5 μ g L⁻¹ and 9.86, respectively. The validation of procedure was confirmed by electothermal atomic absorption spectrophotometer (ET-AAS) and certified reference material (NIST, CRM) in human samples.

1. Introduction

Heavy metals intakes to human body from air, water and foods. Heavy metals such as lead (Pb), chromium (Cr_{vI}) and mercury (Hg) cause to serious problem in humans and depended on way entrance

(Skin, lungs and gastrointestinal system) and concentrations [1-3]. The battery manufactories, gasoline, wastewater, x-ray protection and paint are main source of lead in environment [4,5]. The battery factories are a main source of lead toxicity in workers and cause to dysfunction in blood red cells, the central nervous system tissues (CNST), bones and renal tissues [6]. Also, the lead poisoning can

*Corresponding Author: Abhijit De

Email: abhijit@iitcc.org, ade@actrec.gov.in

<https://doi.org/10.24200/amecj.v3.i04.124>

be effected on human organs such as braine, renal, liver and bone [7,8]. The lead complexes in human body create by interaction of lead with proteins/ amino acids and cause anemia [9,10]. On the other hand the lead exposure causes to decrease the erythrocytes cells (RBC) and reducing biosynthesis of hemoglobin. The occupational safety and health administration (OSHA) has reported that the exposure lead (Pb) more than $600 \mu\text{g L}^{-1}$ is toxic and workers must be offline from work and return to work when the BLL is below $300 \mu\text{g L}^{-1}$. Also, the food and drug administration (FDA) has announced the normal range of Pb in human blood is below $250\text{-}300 \mu\text{g L}^{-1}$ [11]. The limit exposure of lead (Pb) in air is considered about $50 \mu\text{g m}^{-3}$ by NIOSH [12]. Due to lead toxicity in human, the accurate technology need to use for determination of lead ions in the human blood/ serum samples. Recently, the various methods were reported for lead determination in human biological samples. The instrumental techniques such as the electrothermal atomic absorption spectrometry (ET-AAS) [13,14], the inductively coupled plasma - atomic emission spectroscopy or mass spectrometry (ICP-AES/MS) [16], the high-performance liquid chromatographic (HPLC) and the isotope dilution inductively coupled plasma mass spectrometry (ID-ICP-MS) were used for lead determination in different matrixes[17]. Moreover, the sample preparation method is required for extracting of lead ions in different biological samples before determination by spectrometry techniques. Various sample preparation method such as liquid-phase microextraction or dispersive liquid-liquid microextraction (DLLME) [18,19], hydrophobic deep eutectic solvents based on microextraction techniques[20], the headspace solid-phase microextraction [21], the carrier-mediated hollow fiber liquid phase microextraction [22], the dispersive solid-phase extraction (DSPE) combined with ultrasound-assisted emulsification microextraction based on the solidification of floating organic drop (UAEME-SFO)[23], the microextraction based on precipitation[24], the magnetic solid-phase extraction (MSPE) [25], and dispersive-micro solid phase extraction procedure

(D- μ -SPE) [26], were used for lead determination in different human matrixes. Between them, D- μ -SPE procedure is used in different matrixes by researchers. In addition, the characterizations of sorbents are important factor for lead extraction by the SPE method. For examples, the adsorbents such as, the silica aerogel nanoadsorbent [27], the magnetic phosphorus-containing polymer [28], the magnetic metal organic frameworks MMOF[29], the carboxylated graphene [30], the graphene Oxide Sheets [31], and modified-carbon nanotubes with NiFe_2O_4 [32] were reported by chemistry and nanochemistry scientists. The previously works showed that the different pretreatment techniques based on metal nanoparticles, the drugs, the functionalization of CNTs or GO, the magnetic nanoparticles can be increased the efficient extraction of heavy metals in human samples. Recently, some drugs use for in-vitro and in-vivo extraction of heavy metal in human samples and depend on structure and function groups. The antibiotic of sulfamethizole (SM) is a drug and use as an insistent inhibitor of bacterial enzyme. The SM can be complexed with metals in human body and depended on pH and covalence bonding.

In this study, a new SM-NGO adsorbent was used for determination lead in blood/serum samples by syringe filter-dispersive-micro solid phase extraction procedure (SF-D- μ -SPE) at $\text{pH}=6.0$. The high recovery and absorption capacity for lead extraction was obtained in optimized conditions. The lead concentrations in blood/serum samples were determined by AT-FAAS after sample pretreatment.

2. Experimental

2.1. Instrumental

Lead in human blood and serum samples determined by the GBC906 atom trap flame atomic absorption spectrophotometer (AT-FAAS, AUS) after sample preparation. The atom trap accessory put on burner and the fuel gas (air-acetylene), lamp position, slit and light line were manually tuned. Other parameters such as current and silt adjusted by Avanta Software. The minimum sample volume

(0.5-1 mL) vacuumed by nebulizer of AT-FAAS after adjusting flow rate of sample (mL min^{-1}). The LOD for Pb determination with AT-FAAS and F-AAS in standard solutions was obtained 0.025 mg L^{-1} and 0.07 mg L^{-1} , respectively. The linear ranges of $0.08\text{-}6.0 \text{ mg L}^{-1}$ and $0.25\text{-}6.0 \text{ mg L}^{-1}$ were obtained for AT-FAAS and F-AAS at wavelength of 283.3 nm (5 mA). All samples were injected with an auto-sampler injector from $100 \mu\text{L}$ to $1000 \mu\text{L}$. The Inductively coupled plasma mass spectrometry (ICP-MS, Perkin Elmer, Main Plasma Gas: Ar flow $\sim 15 \text{ L min}^{-1}$, 1.2 s/m , USA) as high sensitive analyzer was used for determining of Pb in real human samples after microwave digestion. ICP-MS atomizes the liquid sample and generate atomic ions ($\text{M} \rightarrow \text{M}^+ + \text{e}^-$), which are then detected by quadrupole-based mass analyzer system (mass-to-charge ratio (m/z), ICP-Q-MS). Before mass separation, a beam of positive ions has to be extracted from the plasma and focused into the mass-analyzer. The pH meter was used for determining of pH in liquid samples (Metrohm E-744). The vortex mixer (Thermo, USA) with $100\text{-}500 \text{ rpm}$, ultrasonic heating (Iran) and Falcon centrifuging ($1000\text{-}4500 \text{ rpm}$) prepared for this study.

2.2. Reagents and Materials

The lead standard solution (Pb; 1000 mg L^{-1} in 2 % nitric acid) was purchased from Sigma (Germany). All standard of lead ($0.08, 0.1, 0.2, 0.5, 1, 2, 5 \text{ mg L}^{-1}$) prepared by dilution of the stock lead solution (1000 mg L^{-1}) with ultrapure water (UPW, Millipore, USA). Also, the sub-ppb concentration ($10\text{-}500 \mu\text{g L}^{-1}$) prepared by dilution of stock lead standard solution (1 mg L^{-1}). The pure reagents such as, the polyoxyethylene octyl phenyl ether (TX-100), nitric acid (HNO_3), HCl, acetone, and ethanol were purchased from Sigma Aldrich, Germany. Sulfamethizole (4-Amino-*N*-(5-methyl-1,3,4-thiadiazol-2-yl) enzenesulfonamide; $\text{C}_9\text{H}_{10}\text{N}_4\text{O}_2\text{S}_2$; CASN:144-82-1) and the hydrophobic ionic liquid of 1-methyl-3-octylimidazolium hexafluorophosphate. ([OMIM] PF₆; $\text{C}_{12}\text{H}_{23}\text{F}_6\text{N}_2\text{P}$; CASN: 304680-36-2) was purchased from Sigma

Aldrich, Germany. The GO and GO-COOH was prepared from chemistry department, India. The pH was adjusted to 6 by sodium phosphate buffer solution ($\text{Na}_2\text{HPO}_4/\text{NaH}_2\text{PO}_4$) from Merck (Germany).

2.3. Sample preparations

All glasses such as vials, volumetric, dishes and beakers cleaned with HNO_3 and H_2SO_4 solution (1:1, 2 M) for at least 12 h. After cleaning, all of glasses washed for 10 times with DW. The normal Pb values in blood samples have less than $250 \mu\text{g L}^{-1}$ or $>25 \mu\text{g dL}^{-1}$ and more than $500 \mu\text{g L}^{-1}$ is toxic. By procedure, 10 mL of the blood or serum samples were prepared from 50 workers of lead-acid batteries factories in India (Men, 20-55 age). The sterilized syringes were used for blood samples. The pure heparin based on free of Pb was prepared and injected to blood. The blood samples were maintained at $-5 \text{ }^\circ\text{C}$. In this work, all blood samples prepared based on the world medical association declaration of Helsinki for physicians in human and all blood samples prepared from worker with agreement forms.

2.4. Synthesis of GO@ Sulfamethizole

2.4.1. Preparation of GO

The graphene oxide (GO) was prepared with pure graphite (G) by modified hummers procedure [33]. The 0.2 g of graphite powder was added into mixing solution ($\text{H}_2\text{SO}_4/\text{H}_3\text{PO}_4$; 9:1) and then potassium permanganate (KMnO_4 , 1.3 g) was slowly added by stirring solution up to became black green. The H_2O_2 slowly added to solution and stirred for removal of excess of KMnO_4 . After cooling, the hydrochloric acid (HCl:10 mL in 30 mL DW) was added and centrifuged. Then, the powder product of GO was washed with HCl and DW for 5 times and dried at $90 \text{ }^\circ\text{C}$ for 1 day.

2.4.2. Synthesis of GO@Cl

Chlorinated graphene oxide was prepared due to the Liu procedure [34]. First, 1.0 g of GO, 20 ml of benzene, and 100 ml of SOCl_2 were added in a 100-ml round flask and stirred ($60\text{-}70 \text{ }^\circ\text{C}$). Then,

the excess of SOCl_2 was exit out from mixture by distillation process based on vacuum condition. The solid product put in acetone and the suspension in acetone was filtered with Watman filter (200 nm). Finally, the product washed with acetone for 3 times and dried at 60 °C.

2.4.3. Synthesis of Sulfamethizole functionalized on nanographene oxide (SM@NGO)

1 g of sulfamethizole (SM) solved in 20 mL H_2O with 5 mL of NaOH and then 1 mL of SM solution were mixed in 60 mL ethanol (99%) by an ultrasonic bath (25 min) in a 100 mL round bottom flask. Then, 0.1 mL of triethylamine was added to mixture, and the mixture was refluxed at 70 °C for 5 hours. The obtained product was separated from the mixture by a hydrophobic PTFE Membrane Filters (polytetrafluoroethylene) for filtering SM@NGO. The SM@NGO product washed with ethanol for many times and finally dried under vacuum at 95 °C.

2.5. Extraction Procedure

By the SF-D- μ -SPE procedure, 10 mL of serum and plasma samples were used for determination of lead ions. Firstly, 25 mg of SM@NGO added to human blood/serum and lead standard solution (10-500 $\mu\text{g L}^{-1}$) at pH=6.0 and aspirated by 10 mL of syringe

tube. The syringe tube placed on shaking tube for 5.0 min, after shaking, the lead was extracted by the sulfur group of SM@NGO in optimized pH ($\text{Pb}^{2+} \rightarrow \text{SR@GO}$). The SM@NGO separated from liquid phase by syringe hydrophobic PTFE membrane. Then, the pb^{2+} ions back-extracted from SM@NGO-PTFE membrane with elution of nitric acidic (0.5 mL, 0.5 M) and remain solution was determined by AT-FAAS after dilution with DW up to 1 mL (Fig.1). The procedure run for 10 blank solutions without any lead. The calibration curve of lead based on SF-D- μ -SPE/AT-FAAS procedure (10-500 $\mu\text{g L}^{-1}$) and standard method by AT-FAAS (0.1- 5 mg L^{-1}) were done. The enrichment factor (EF) calculated by curve fitting rules ($Tga = m_1/m_2$).

3. Results and discussion

3.1. Mechanism of Extraction by SM@NGO

The pure sulfamethizole drug was solved in H_2O /NaOH solutions and then mixed with ethanol (99%) by an ultrasonic bath. Then, the triethylamine were added to mixture. After reflux, the SM@NGO product was separated from the mixture by PTFE membrane by washing and drying. Finally, the sulfamethizole functionalized on nanographene oxide caused to make favorite adsorbent based on sulfur group (dative bond) for lead extraction in blood, serum and plasma samples

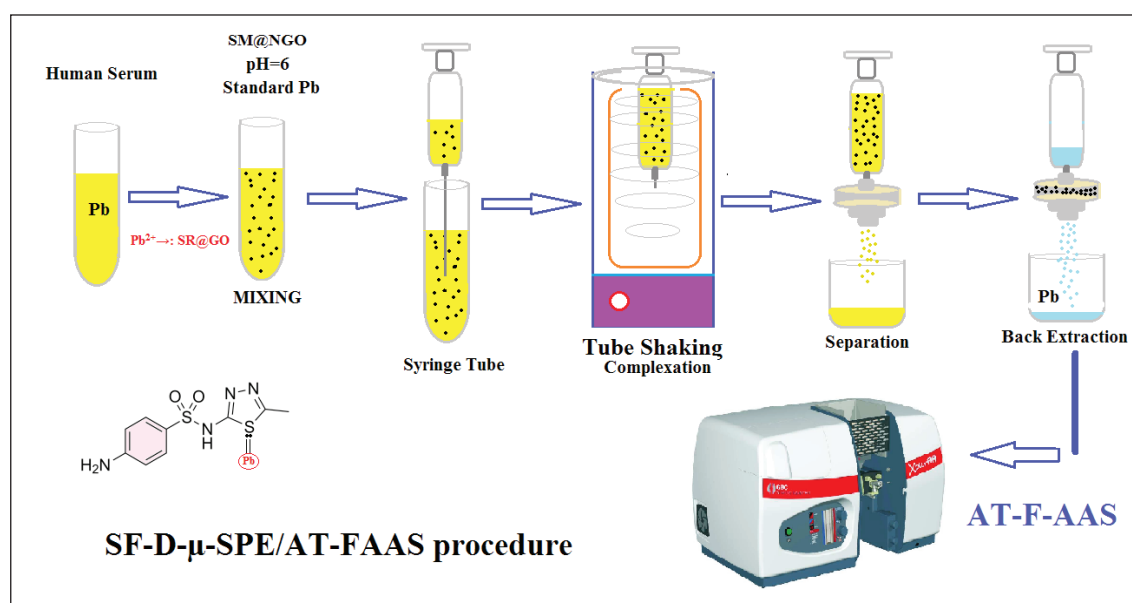


Fig. 1. The SF-D- μ -SPE procedure for extraction of lead in human samples

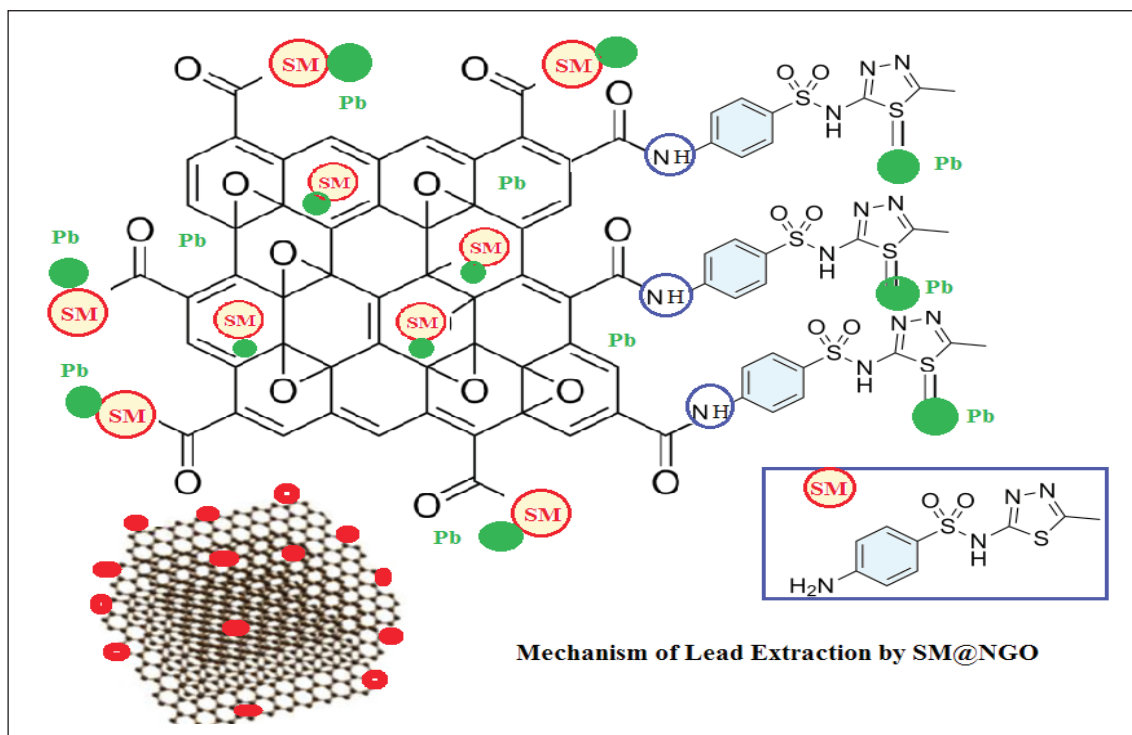


Fig.2. The mechanism of lead extraction in blood/serum samples based on SM@NGO by the SF-D- μ -SPE procedure

with high recovery. Therefore, the lead adsorption/extraction with SM@NGO nanostructure caused to increase the recovery up to 98.5 % as compared to NGO adsorbent (26.4 %). The results showed, the mechanism of lead extraction in serum, blood and plasma samples depended on sulfur group of sulfamethizole in SM@NGO adsorbent at optimized pH (Fig.2).

3.2. SEM, TEM and FTIR of SM@NGO

The NGO adsorbent was synthesized from graphite powder according to the modified Hummer's method from RIPI Company (Iran) [33] and used for synthesis of SM@NGO. The TEM and SEM of SM@NGO showed the minimum size between 30-100 nm which were shown in Figures 3 and 4, respectively. The FT-IR spectrum of NGO-COOH

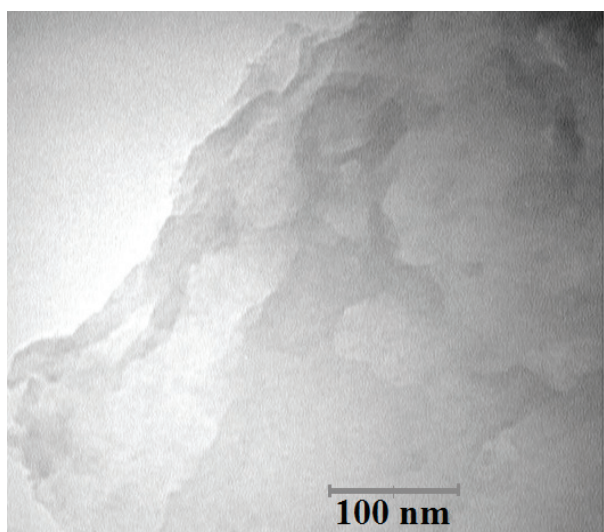


Fig.3. The TEM of SM@NGO adsorbent

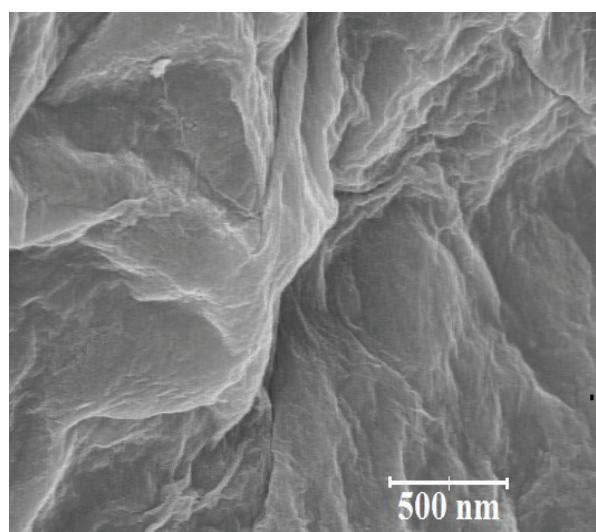


Fig.4. The SEM of SM@NGO adsorbent

and SM@NGO adsorbent was shown in **Figure 5**. Based on FT-IR spectrum, the C=N double bond is about twice as strong as a C-N single bond, and the C≡N triple bond is similarly stronger than double bond. The infrared stretching frequencies of these groups vary in the same order, ranging from 1100 cm⁻¹ for C-N, to 1660 cm⁻¹ for C=N. Also,

symmetric and a symmetric traction for sulfur bond (S-C) ranging from 1135-1165 cm⁻¹ and 1310-1360 cm⁻¹ were seen. The O-H bond is about 3600 cm⁻¹, S-H bond in 2570 cm⁻¹, C-H bond in 3000 cm⁻¹ and N-H bond in 3400 cm⁻¹ observed.

The X-ray diffraction (XRD) of NGO and SM@NGO were shown in **Figure 6**. XRD of graphene

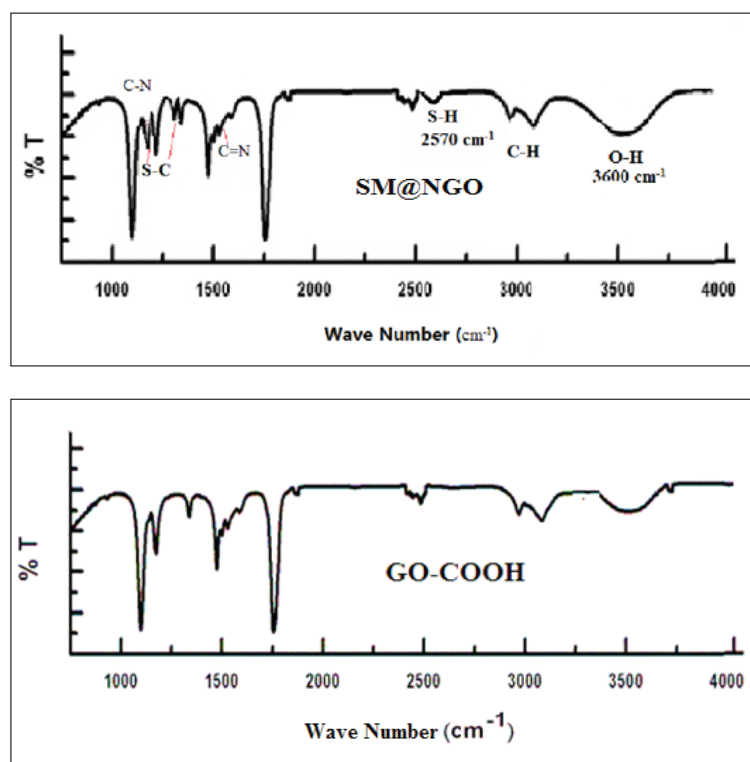


Fig.5. The FT-IR spectrum of NGO-COOH and SM@NGO adsorbent

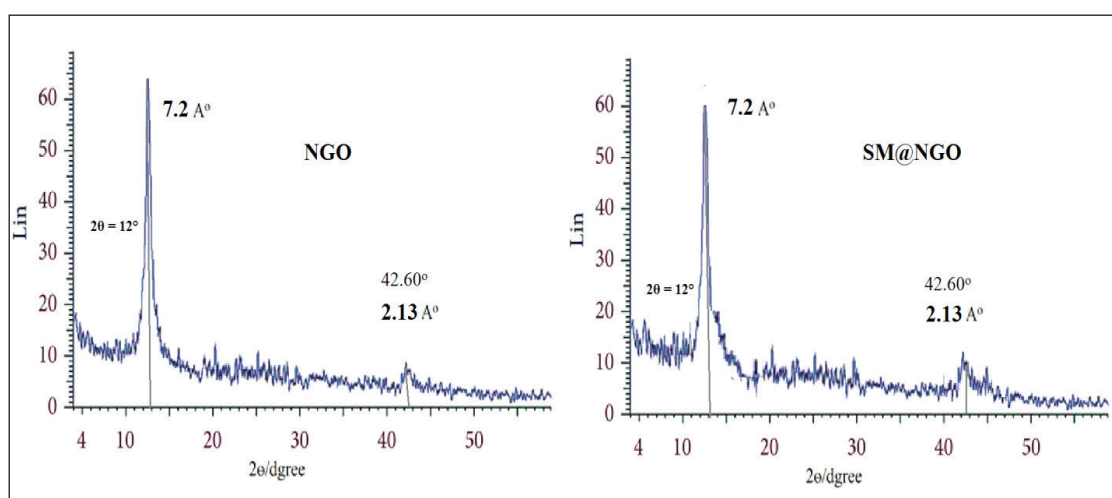


Fig.6. The X-ray diffraction (XRD) for NGO and SM@NGO adsorbents

oxide shows the one main diffraction peak at $2\theta=12^\circ$ related to the oxygen groups which are intercalated between graphene sheets. The peaks at $2\theta=12^\circ$ and 42.60° are related to the diffraction planes of (002) and (100) respectively, which can be showed in both of the XRD of GO and SM@NGO.

3.3. Optimization of extraction parameters

The SF-D- μ -SPE procedure based on new SM@NGO adsorbent was used for the extraction and determination Pb(II) ions in serum and plasma samples. For efficient lead extraction, the analytical parameters such as pH, sample volume and amount of SM@NGO adsorbent were optimized.

3.3.1. Influence of pH

The efficient extraction of lead in blood serum of battery workers was depended to pH. So, the pH of samples must be examined and optimized. The pH can be affected on increasing /decreasing extraction processes of lead in serum samples. The buffer solutions help us to improved extraction recovery by adjusting pH. Therefore, the different value of pH between 2-10 was evaluated by lead concentration from 10 to 500 $\mu\text{g L}^{-1}$. The results showed, the high extraction of lead ions in human biological samples was obtained at pH of 6.0 by SM@NGO adsorbent. On the other hand, the recoveries can be

decreased at acidic or basic pH. So, the pH point of 6 was used for extraction Pb in real samples (Fig.7). Based on extraction mechanism, the coordination of dative bond of sulfur as negative charge in SM@NGO with the positively charged of Pb^{2+} were happened in optimized pH. At low pH (less than 5.5), the SM@NGO adsorbent protonated and surface of adsorbent got the positively charged. Due to the electrostatic repulsion, the recoveries of lead extraction were decreased. Moreover, in optimized pH(6), the surface of SM@NGO have negatively charged and high recovery was obtained for Pb^{2+} ions by the SF-D- μ -SPE procedure (more than 96%).

3.3.2. Influence of SM@NGO amount

The amount of SM@NGO nanoparticles for lead extraction in human samples has studied with lead concentration between 10-500 $\mu\text{g L}^{-1}$ as a low and high LOQ ranges. For this proposed, 1-50 mg of SM@NGO adsorbent were used for lead extraction in serum, blood, plasma and standard solutions by the SF-D- μ -SPE method. The obtained results showed that the maximum of lead extraction in human samples was achieved for 22 mg of SM@NGO nanostructure. So, 25 mg of SM@NGO adsorbent was used for further work (Fig. 8). The extra mass of 25 mg had no effect on recovery of lead extraction in human samples.

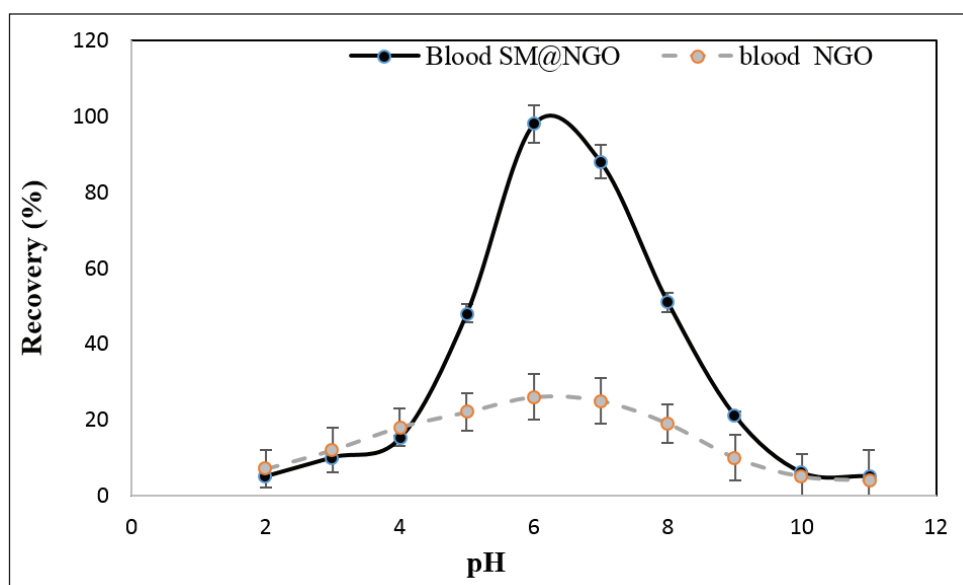


Fig.7. The influence of pH on lead extraction based on SM@NGO adsorbent by the SF-D- μ -SPE procedure

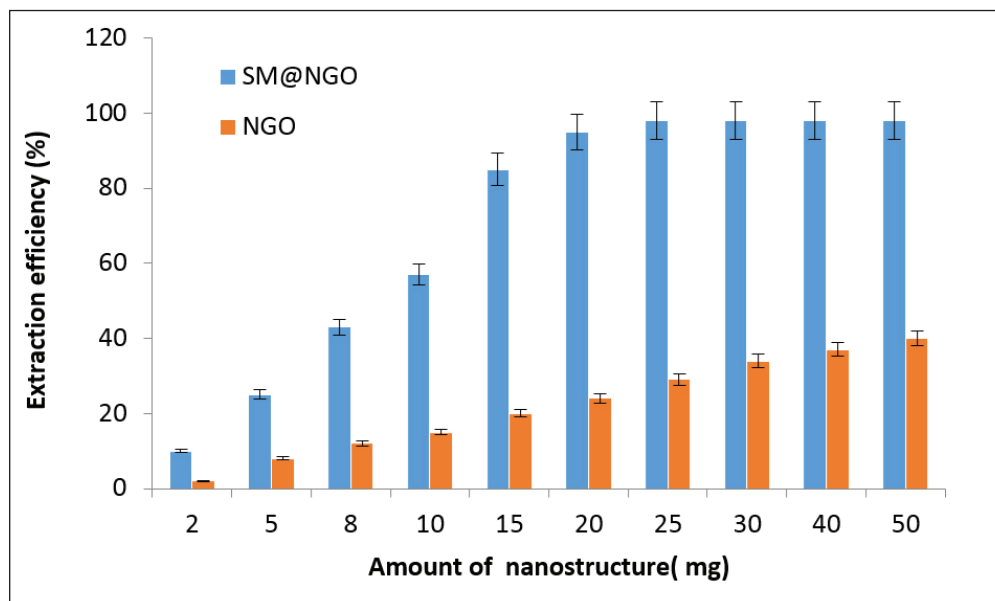


Fig.8. The influence of amount of SM@NGO on lead extraction by the SF-D- μ -SPE procedure

3.3.3. Influence of sample volume

Sample volume is an effective parameter for extraction lead ions in human biological samples such as serum, blood and plasma. So, the lead extraction for sample volume between 1-30 mL was studied and optimized with the low and high LOQ concentration ranges ($10\text{-}500\ \mu\text{g L}^{-1}$) by the SF-D-

μ -SPE method (**Fig. 9**). The experimental results confirmed that the best extraction was obtained for less than 15 mL of human samples. Therefore, 10 mL was selected as optimum volume of human samples for lead extraction with 25 mg of SM@NGO adsorbent at pH=6. The recovery was decreased by adding sample volume in optimized conditions.

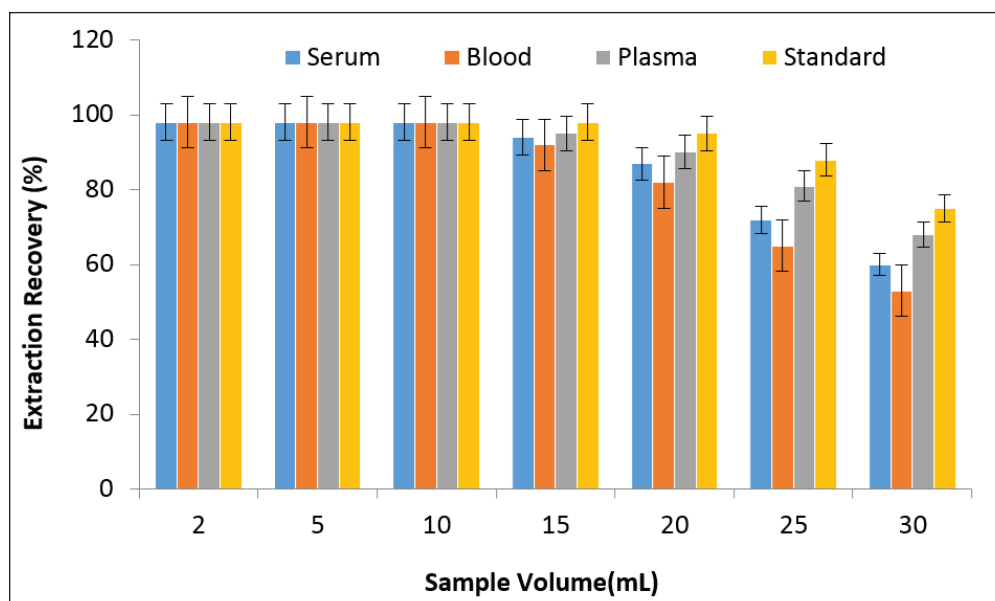


Fig.9. The influence of sample volume on lead extraction based on SM@NGO adsorbent by the SF-D- μ -SPE procedure

3.3.4. Influence of volume and concentration of eluents

The influence of volume and concentration of eluents such as HCl, HNO₃, NaOH and CH₃COOH for back-extraction of lead ions from solid phase were studied and optimized by SF-D- μ -SPE procedure. The syringe coupled to Millex-FG hydrophobic PTFE membrane (0.2 μ m) was used for back-extraction lead from adsorbent by different volume of eluents between 0.5-2 mL (0.2-1 M). After pushing the plunger of syringe, the elution of SM@NGO/hydrophobic PTFE membrane was performed by different eluents. In acidic or basic pH, the lead (Pb) released from SM@NGO/PTFF to elution phase and due to participate of lead hydroxyl in basic pH, the acidic pH was selected. Therefore, the acid solution can be used for back-extraction of lead from solid phase. The results demonstrated that the lead ions were simply back-extracted from SM@NGO adsorbent by nitric acid solution more than 0.4 mol L⁻¹. Therefore, 0.5 mol L⁻¹ of nitric acid (HNO₃) was used as optimum concentration of eluent for this study. Also, The results showed, the lead was efficiently back-extracted from SM@NGO by 0.5 mL of HNO₃. Finally, the lead concentration in remained solution was determined with AT-FAAS after dilution with DW up to 1 mL.

3.3.5. Membrane filter reusing

The reusability of the SM@NGO packed Millex-FG hydrophobic PTFE membrane was evaluated by several extraction and elution cycles under optimized conditions. It was found that the membrane filter could be reused after back-extraction processes and then rinsed by 5 mL of DW. The membrane filter was used for over 14 adsorption–elution cycles without significant decrease in extraction recoveries of lead ions. As collection adsorbent on membrane, the flow rate of eluent or samples through membrane filter was hardly done and so, the extraction recovery decreased more than 18 adsorption–elution cycles.

3.3.6. Adsorption capacity

The main parameter for evaluating of lead extraction with the SM@NGO packed Millex-FG hydrophobic PTFE membrane is adsorption capacity. So, the adsorption capacity of 25 mg of SM@NGO adsorbent for Pb (II) in 10 mL of human sample containing 5 mg L⁻¹ Pb (II) ions was investigated at pH 6 in static system. After adjusting pH with favorite buffer solution, the mixture was shaken for 15 min and filtered with Millex-FG hydrophobic PTFE membrane (0.2 μ m). Finally the residual concentrations of lead in the Millex-FG hydrophobic PTFE membrane were determined using AT-FAAS. The adsorption capacities of GO and SM@NGO for Pb (II) ions were found to be 57.5 mg g⁻¹ and 162.1 mg g⁻¹, respectively.

3.3.7. influence of Interference ions

The influence of some coexisting ions for lead extraction in human samples was examined by the SF-D- μ -SPE procedure. For investigation of the effect of different interference ions on lead extraction, the various ions (0.5-2 mg L⁻¹) added to 10 mL of lead samples with 500 μ g L⁻¹ at pH 6.0. So, the most of the concomitant ions in human blood such as Cu, Zn, Mn, Mg, Se, Li, F, NO₃, HCO₃, Ca, Na an K were considered for lead extraction by SM@NGO adsorbent. The experimental results showed, the interference coexisting ions had no effect on lead extraction by proposed method. (Table1). Therefore, the SM@NGO adsorbent was efficiently extracted lead ions from human biological samples in the present of the interference coexisting ions.

3.3.8. Determination of lead in real samples

The SM@NGO adsorbent was used for extraction and determination of lead ions in human samples by the SF-D- μ -SPE procedure. For validation of the results, the human blood, serum and plasma samples were spiked with lead standard solution based on SM@NGO nanostructure before determination by AT-FAAS. The high extraction of spiked samples demonstrated that the SM@NGO adsorbent had satisfactory results for lead

Table 1. The influence of interferences coexisting ions on lead extraction in human blood samples by the SF-D- μ -SPE procedure

Interfering Ions	Mean ratio ($C_I/C_{Pb(II)}$)	Recovery (%)
	Pb(II)	Pb(II)
Cr ³⁺ , Se ²⁺ , Mn ²⁺ ,	600	97.4
Zn ²⁺ , Cu ²⁺	700	98.6
I ⁻ , Br ⁻ , F ⁻ , Cl ⁻	1200	97.2
Na ⁺ , K ⁺ , Li ⁺	1000	99.2
Ca ²⁺ , Mg ²⁺	800	97.7
Ni ²⁺ , Co ²⁺	450	98.4
CO ₃ ²⁻ , PO ₄ ³⁻ , HCO ₃ ⁻ , NO ₃ ⁻	950	96.6

extraction and determination in human samples at pH=6.0 (Table 2). Also, 10 mL of the blood or serum samples were prepared from 50 workers of lead-acid batteries factories in India (Men, 20-55 age) by the SF-D- μ -SPE procedure

and compared to healthy peoples (Table 3). Moreover, the certified reference materials (NIST; CRM) and lead analysis with ICP-MS were used for validating of methodology based on SM@NGO by the proposed procedure (Table 4)

Table 2. Determination of lead based on SM@NGO adsorbent and spiking samples by the SF-D- μ -SPE procedure coupled to AT-FAAS

*Sample	Added ($\mu\text{g L}^{-1}$)	*Found ($\mu\text{g L}^{-1}$)	Extraction efficiency (%)
Blood	---	9.7 \pm 224.2	---
	200	17.8 \pm 418.6	97.2
Plasma	---	2.8 \pm 55.4	---
	50	4.8 \pm 106.7	102.6
Serum	---	7.6 \pm 168.9	---
	150	14.3 \pm 311.6	95.1
Blood	---	8.2 \pm 178.8	---
	150	13.8 \pm 322.3	95.6
Serum	---	9.4 \pm 192.3	---
	200	19.3 \pm 399.5	103.6
Plasma	---	4.2 \pm 88.5	---
	100	8.4 \pm 186.8	98.3

*Mean of three determinations of samples \pm SD (P = 0.95, n = 10)

Table 3. Determination of lead in serum, blood and plasma by the SF-D- μ -SPE procedure coupled to AT-FAAS (intra –day and inter day, n=50, μgL^{-1})

* Sample	^b Workers (n=50)		^b Healthy peoples (n=50)		^a Workers	
	Intra-day	Inter day	Intra-day	Inter day	r	P value
Blood	352.8 \pm 15.7	360.2 \pm 16.2	33.1 \pm 1.4	29.5 \pm 1.3	0.092	<0.001
Serum	276.7 \pm 12.6	281.2 \pm 13.9	24.6 \pm 1.1	28.2 \pm 1.2	0.112	<0.001
Plasma	147.5 \pm 6.8	152.4 \pm 7.3	12.8 \pm 0.6	14.6 \pm 0.7	0.086	<0.001

^a Correlations are based on Pearson coefficients (r). Statistical significance will be observed if $P < 0.05$

^b Mean of three determinations of samples \pm confidence interval ($P = 0.95$, $n = 10$)

* 50 workers of lead–acid batteries factories in India (Men, 20-55 age)

Table 4. Validation of methodology for lead determination by certified reference materials(CRM, NIST)

Sample	CRM*($\mu\text{g L}^{-1}$)	Added	Found*($\mu\text{g L}^{-1}$)	Recovery (%)
Caprine blood, level 2	139.5 \pm 0.8	-----	135.8 \pm 6.5	-----
		100	233.6 \pm 11.4	97.8
Caprine blood, level 3	277.6 \pm 1.6	-----	272.6 \pm 13.1	-----
		200	465.7 \pm 21.8	96.5
Serum by ICP-MS	86.4 \pm 2.1	-----	84.2 \pm 4.4	-----
		50	131.5 \pm 4.4	94.6

*Mean of three determinations of samples \pm SD ($P = 0.95$, $n = 10$)

CRM955c, caprine blood, level 2, 139.5 \pm 0.8 $\mu\text{g L}^{-1}$

CRM955c, caprine blood, level 3, 277.6 \pm 1.6 $\mu\text{g L}^{-1}$

4. Conclusions

A novel SM@NGO adsorbent was used for lead separation/extraction in human blood, serum and plasma samples by the SF-D- μ -SPE coupled to AT-FAAS. The Millex-FG hydrophobic PTFE membrane (0.2 μm) was used as a filter for separating solid phased from liquid phase. By the SF-D- μ -SPE method, the high extraction, the low cost, the fast separation and simple method in short time was obtained in optimized pH. The trace amount of SM@NGO as a solid-phase caused to extract the lead ions from the human biological samples without any ligand. The developed SF-D- μ -

SPE method presented a analytical nanotechnology for lead separation/extraction/preconcentration in human blood samples with low interference ions, good reusability and simple sample preparation in difficulty matrixes. Therefore, the SM@NGO nanostructure was used as a perfect adsorbent for determination and extraction of lead in blood, serum and plasma samples by AT-FAAS.

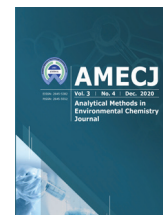
5. Acknowledgments

The authors wish to thank from Department of Chemistry, Hi Tech institute of theoretical and computational chemistry, India

6. References

- [1] S. Morais, F.G. Costa, M.L. Pereira, Heavy metals and human health, Intech publisher, pp. 227–246, 2012.
- [2] K. Rehman, F. Fatima, I. Waheed, Prevalence of exposure of heavy metals and their impact on health consequences, *J. Cell. Biochem.*, 119 (2018) 157–184.
- [3] F. Zhushan, X. Shuhua, The effects of heavy metals on human metabolism, *Toxicol. Mech. Meth.*, 30 (2020) 167–176.
- [4] W. Liu, J.P. Tian, L.J. Chen, Y. Guo, Temporal and spatial characteristics of lead emissions from the leadacid battery manufacturing industry in China, *Environ. Pollut.*, 220 (2017) 696–703.
- [5] P.V. Bossche, F. Vergels, J.V. Mierlo, J. Matheys, W.V. Autenboer, An assessment of sustainable battery technology, *J. Power Sources*, 162 (2006) 913–919.
- [6] A.I. Wani, A. Ara, J.A. Usmani, Lead toxicity: A review, *Int. Toxicol.*, 8 (2015) 55–64.
- [7] J.w. Lee, H. Choi, U.K. Hwank, J.C. Kang, Y.J. Kang, K.I. Kim, J.H. Kim, Toxic effects of lead exposure on bioaccumulation, oxidative stress, neurotoxicity, and immune responses in fish: A review, *Environ. Toxicol. Pharmacol.*, 68 (2019) 101–108. [
- [8] Lead toxicity, what Is the biological fate of lead in the body, environmental health and medicine education, Agency for toxic substances and disease registry (ATSDR), 2017. <https://www.atsdr.cdc.gov/csem/csem.aspx?sem=34&po=9>
- [9] M. Giel-Pietraszuk, K. Hybza, M. Chelchowska, J. Barciszewski, Mechanisms of lead toxicity, *Adv. Cell Biol.*, 39 (2012) 17–248.
- [10] M. Irberger, J.J. Yang, Structural differences between Pb^{2+} - and Ca^{2+} -binding sites in proteins: implications with respect to toxicity, *J. Inorg. Biochem.*, 102 (2008) 1901–1909.
- [11] Elemental impurities guidance for industry, department of health and human services, food and drug administration (FDA), 2017.
- [12] Atlanta centers for disease control (ACDC), US department of health and human services, national institute for occupational safety and health (NIOSH), Adult blood lead epidemiology and surveillance (ABLES), 2017.
- [13] R.A. Zounr, M. Tuzen, M.Y. Khuhawar, A simple and green deep eutectic solvent based air assisted liquid phase microextraction for separation, preconcentration and determination of lead in water and food samples by graphite furnace atomic absorption spectrometry, *J. Mol. Liq.*, 259 (2018) 220–226.
- [14] J.S. Mandlate, B.M. Soares, T.S. Seeger, P.D. Vecchia, P.A. Mello, E.M.M. Flores, F.A. Duarte, Determination of cadmium and lead at sub-ppt level in soft drinks: An efficient combination between dispersive liquid-liquid microextraction and graphite furnace atomic absorption spectrometry, *Food Chem.*, 221 (2017) 907–912
- [15] M.A. Habila, Z.A. AlOthman, M. Soylak, Fe_3O_4 nanoparticles and ultrasound assisted dispersive liquid-liquid microextraction of lead(ii) for its microsampling flame atomic absorption spectrometric determination in food and environmental samples, *RSC Adv.*, 4 (2014) 55610–55614.
- [16] M.A. Habila, Z.A. AlOthman, A.M. El-Toni, J.P. Labis, X. Li, F. Zhang, M. Soylak, Mercaptobenzothiazole-functionalized magnetic carbon nanospheres of type $Fe_3O_4@SiO_2@C$ for the preconcentration of nickel, copper and lead prior to their determination by ICP-MS, *Microchim. Acta*, 183 (2016) 2377–2384.
- [17] M. García, M. Ángel Aguirre, A multinebulization technique for the determination of trace metals in a marine biota sample by on-line isotope dilution inductively coupled plasma mass spectrometry (OID-ICP-MS), *J. Anal. At. Spectrom.*, 35 (2020) 2509–2516.
- [18] Y. Yamini, M. Rezazadeh, S. Seidi, Liquid-phase microextraction–The different principles and configurations, *Trends Analyt Chem.*, 112 (2019) 264–272.
- [19] S.Z. Mohammadi, T. Shamspur, Y.M. Baghelani, Combination of flame atomic absorption spectrometry with ligandless-dispersive liquid-liquid microextraction for preconcentration and determination of trace

- amount of lead in water samples, *Bull. Chem. Soc. Ethiop.*, 27 (2013) 161–168.
- [20] P. Makoś, E. Słupek, J. Gębicki, Hydrophobic deep eutectic solvents in microextraction techniques—A review, *Microchem. J.*, 152 (2020) 104384.
- [21] C. Zheng, L. Hu, X. Hou, B. He, G. Jiang, Headspace solid-phase microextraction coupled to miniaturized microplasma optical emission spectrometry for detection of mercury and lead, *Anal. Chem.*, 90 (2018) 3683–3691.
- [22] L. Alavi, S. Seidi, A. Jabbari, T. Baheri, Deep eutectic liquid organic salt as a new solvent for carrier-mediated hollow fiber liquid phase microextraction of lead from whole blood followed by electrothermal atomic absorption spectrometry, *New J. Chem.*, 41 (2017) 7038–7044.
- [23] M. Sadeghi, E. Rostami, D. Kordestani, H. Veisi, M. Shamsipur, Simultaneous determination of ultra-low traces of lead and cadmium in food and environmental samples using dispersive solid-phase extraction (DSPE) combined with ultrasound-assisted emulsification microextraction based on the solidification of floating organic drop (UAEME-SFO) followed by GFAAS, *RSC Adv.*, 7 (2017) 27656–27667.
- [24] E. Koosha, M. Shamsipur, F. Salimi, M. Ramezani, A microextraction method based on precipitation for the simultaneous separation and preconcentration of cadmium and lead before their determination by FAAS: Experimental design methodology, *Sep. Sci. Technol.*, 56 (2020) 1–9.
- [25] E. Zolfonoun, Solid phase extraction and determination of indium using multiwalled carbon nanotubes modified with magnetic nanoparticles, *Anal. Methods Environ. Chem. J.*, 1 (2018) 5-10.
- [26] H.R. Sobhi, A. Mohammadzadeh, M. Behbahani, A Implementation of an ultrasonic assisted dispersive μ -solid phase extraction method for trace analysis of lead in aqueous and urine samples, *Microchem. J.*, 146 (2019) 782-788.
- [27] M. Falahnejad, H.Z. Mousavi, H. Shir Khanloo, A. Rashidi, Preconcentration and separation of ultra-trace amounts of lead using ultrasound-assisted cloud point-micro solid phase extraction based on amine functionalized silica aerogel nanoadsorbent, *Microchem. J.*, 125 (2016) 236-241.
- [28] E. Yilmaz, R.M. Alosmanov, M. Soylak, Magnetic solid phase extraction of lead(ii) and cadmium(ii) on a magnetic phosphorus-containing polymer (M-PhCP) for their microsampling flame atomic absorption spectrometric determinations, *RSC Adv.*, 5 (2015) 33801–33808.
- [29] Y. Wang, H. Chen, J. Tang, G. Ye, H. Ge, X. Hu, Preparation of magnetic metal organic frameworks adsorbent modified with mercapto groups for the extraction and analysis of lead in food samples by flame atomic absorption spectrometry, *Food Chem.*, 181 (2015) 191–197.
- [30] M. Rosillo-Lopez, C. Salzmman, Highly efficient heavy-metal extraction from water with carboxylated graphene nanoflakes, *RSC Adv.*, 8 (2018) 11043–11050.
- [31] A. slam, H. Ahmad, N. Zaidi, S. Kumar, Graphene oxide sheets immobilized polystyrene for column preconcentration and sensitive determination of lead by flame atomic absorption spectrometry, *ACS Appl. Mater. Interfaces*, 6 (2014) 13257–13265.
- [32] A. Ensafi, S. Rabiei, B. Rezaei, A. Allafchian, Magnetic solid-phase extraction to preconcentrate ultra trace amounts of lead(ii) using modified-carbon nanotubes decorated with NiFe₂O₄ magnetic nanoparticles, *Anal. Methods*, 5 (2013) 3903–3908.
- [33] C. Botas, P. Ivarez, P. Blanco, M. Granda, C. Blanco, R. Santamar, L. J. Romasanta, R. Verdejo, M. A. L. pez-Manchado, R. Menndez, Graphene materials with different structures prepared from the same graphite by the Hummers and Brodie methods, *Carbon*, 65 (2013) 156–164.
- [34] Z.B. Liu, Y.F. Xu, X.Y. Zhang, X.L. Zhang, Y.S. Chen, J.G. Tian, Porphyrin and fullerene covalently functionalized graphene hybrid materials with large nonlinear optical properties, *J. Phys. Chem. B*, 113 (2009) 9681–9686



Adsorption methodology: Synthesis of Nano-structured nitrogen-doped porous carbon adsorbents for perchloroethylene vapor adsorption

Mohammad Ghasemi Kahangi^{a,b}, Alimorad Rashidi^{b*} and Mohammad Samipoorgiri^a

^aChemical Engineering Department, Islamic Azad University, North Tehran Branch, Tehran, Iran

^bCarbon and Nanotechnology Research Center, Research Institute of Petroleum Industry, Tehran, Iran

ARTICLE INFO:

Received 12 Aug 2020

Revised form 5 Oct 2020

Accepted 12 Nov 2020

Available online 30 Dec 2020

Keywords:

Perchloroethylene,
Adsorption procedure,
Gas chromatography mass spectrometry,
Porous Nano carbon,
Nitrogen-doped adsorbent.

ABSTRACT

The perchloroethylene (PCE, tetrachloroethylene), as a representative of chlorinated ethylenes and volatile organic compounds (VOCs), can be easily transported and remain in the atmosphere due to its volatility and stability properties. As a result, there is a crucial need to reduce this pollution to the extent permitted by international standards. The concentration of PCE determined with Gas chromatography–mass spectrometry analyzer (GC-MS). Activated nanocarbons (ACs) doped with nitrogen functional groups were prepared using the walnut shell as a precursor to evaluate their adsorption capacity for PCE vapors. Several techniques, including scanning electron microscopy (SEM), N₂ adsorption-desorption, and the Fourier transforms infrared spectrometry (FTIR), were applied to characterize the physical-chemical properties of the ACs. It is found that the PCE adsorption considerably increased on the nitrogen-doped ACs (KNCWS) due to their structural and surface charge properties. By conducting kinetic study, the pseudo-first-order model matched well with experimental data that could indicate reversible adsorption of the PCE on heteroatom doped ACs. The sips model agreed well with the equilibrium adsorption of PCE on the nitrogen-doped ACs, and the maximum adsorption capacities for PCE reached 166, 285, and 95 mg/g for KNCWS-11, KNCWS-21, and KNCWS-31, respectively. Also, the concentration of PCE were online measured based on nitrogen-doped ACs as solid-phase extraction (SPE) by the GC-MS as analytical procedure. Therefore, the nitrogen-doped ACs was good choices for the removal of PCE vapors.

1. Introduction

Atmospheric air, as an important topic of the environment that ensures the lives on Earth, not only contains natural and vital compounds, but also a set of undesirable and unnatural materials [1].

Since the existence of volatile organic compounds (VOCs) in the atmosphere can cause severe health problems. They have attracted a lot of attention and many efforts have been made to removal them in recent years [2]. In addition, numerous VOCs contribute to the degradation of the stratospheric ozone layer, which is part of climate change. VOCs are also considered a precursor to the secondary formation of PM2.5 particulate

* Corresponding Author: [A.M. Rashidi](mailto:A.M.Rashidi)

E-mail addresses: rashidiam@ripi.ir

<https://doi.org/10.24200/amecj.v3.i04.125>

matter [3]. According to various sources, volatile organic compounds in atmospheric air are divided into several main groups of alkanes, alkenes, alkynes, aromatics, volatile organic compounds of chlorine, and volatile organic compounds of sulfur. Chlorine volatile organic compounds are much more environmentally toxic than other VOCs. Specifically, Cl-VOCs are primarily known as stable, biogenic, and biodegradable compounds in the environment. Most of them are toxic, and carcinogenic. Therefore, today we need to research effective techniques for managing currents contaminated with Cl-VOCs that are economically viable [4]. Perchloroethylene (PCE, tetrachloroethylene) as a representative of chlorine ethylenes is a synthetic chlorine hydrocarbon known for its exceptional solubility and low inflammability. PCE is a colorless and sweet-smelling liquid with highly solubility in water that is widely utilized as a solvent in industrial processes like metal degreasing, drying, and drug, pesticides, adhesives, and antifreeze production [5]. Due to the prevalence of leakage and its inappropriate disposal, large amounts of PCE enter the environment in industrial sites [6]. PCE with a vapor pressure of 18.5 mm Hg at 25 °C is predicted to exist only as vapor in the ambient atmosphere [7]. According to OSHA, PCE levels above 100 ppm can cause neurological effects that can damage to the central nervous system in humans [8]. Many methods have been reported to control environmental pollution, such as adsorption, advanced oxidation, electrochemical and photocatalytic method. Because of low cost, simplicity in design, and operation, the adsorption method is widely used among the various methods to remove the Cl-VOCs. Cost-effective, efficient, and sustainable methods for removing VOCs are still a challenge and need more attention in this regard. Zeng et al. (2015) found that activated carbon aganite-nanocomposite (β -FeOOH-AC) has outstanding capacity for PCE adsorption. It is shown that PCE removal with an adsorbent dose of 8 g/L and an initial concentration of 100 mg/L can reach 97.83%. Adsorption kinetics indicates that the quasi-second-order model fits well with the

experimental data. The Langmuir and Freundlich isotherm models were reasonably fitted to describe the PCE adsorption behavior on β -FeOOH-AC from water. The thermodynamic results of adsorption show that the PCE adsorption process on β -FeOOH-AC is a spontaneous, endothermic, monolayer, and multilayer adsorption process joint with a physical process that occurs through an ion-exchange surface adsorption mechanism [9]. In the adsorption process, the price of the adsorbent is one of the most important factors in the economics of the process, so most researchers try to build and select a cheap adsorbent in this process [10]. Lignocellulose wastes are a good option for cheap adsorbents, as the existing wastes enter efficient cycles. Activated carbon used to prevent normal landfilling in landfills is recyclable and economically competitive with other methods. In addition, the solid phase extraction as analytical techniques, such as the needle trap extraction, the tube extraction, the sorption trap, solid-phase microextraction (SPME), the thin-film extraction, dynamic SPE, and stir bar SPE were used for determination PCE and VOCs in air by GC-MS.

This method has the dual advantage of reducing waste production and greenhouse gas emissions. Accordingly, In this research, by using the walnut shell as a precursor, a series of urea modified carbons were activated by KOH and the effect of in situ N-doping on the textural properties as well as PCE adsorption performance were investigated. In addition the proposed procedure based on nitrogen-doped ACs coupled to GC-MS analyzer. Moreover, Different analysis (BET, FE-SEM, and FT-IR) were employed to characterize the as-prepared ACs.

2. Experimental

2.1. Apparatus and Reagents

The gas chromatography (GC) equipped with loop injector was used for tetrachloroethylene analysis in air (Agilent GC, 7890A, GC-MS, Netherland). The detector of triple quadrupole (MS) have used in Agilent GC. Due to injection process, the slide of plunger carrier down and tighten the plunger thumb screw until finger-tight. The sampling

valves introduce a sample into the carrier gas stream and valves were used to inject a sample gas in gas streams. Iranian walnut shell was used as the precursor of nanocarbons. Moreover, KOH, urea, and HCl with analytical grade were purchased from Merck. The tetrachloroethylene (perchloroethylene, PCE) was purchased from Sigma Aldrich ([HOCH₂CH₂N(CH₂COOH)]; CAS Number: 93-62-9). Acetone and ethanol prepared from Sigma, Germany.

2.2. Preparation of N-doped nanocarbons

Walnut shell was respectively crushed, washed, and dried at 100 °C for 24 hours. The precursor was powdered and sieved into 150 μm. The carbonization of powdered WS was carried out under nitrogen gas stream by a heating rate of 5 °C/min to 600 °C for about 1 hour (CWS). Then urea—as a source of nitrogen—was mixed with different ratios of carbonized samples (1:1, 2:1, and 3:1) and heated at 400 °C for 1 hour through a heating rate of 3.33 °C/min (NCWS). Next, the nitrogen-doped carbon was mixed with KOH with the ratio of 1:4 and activated under N₂ using a heating rate of 7.5 °C per minute up to 900 °C for 1 hour. The as-prepared samples were washed with 1 M HCl and hot distilled water until neutral pH and finally were dried in the vacuum oven at 80 °C for 5h. The as-prepared samples were denoted as KNCWS-xy in which xy represents the ratio of urea to CWS.

2.3. Characterization

To investigate the specific surface area, pore diameter, and total pore volume, adsorption/desorption isotherm of nitrogen was performed using a Micromeritics ASAP 2020 Plus device. Each sample was degassed at vacuum at 250 °C and nitrogen uptake was performed at 196 °C. To provide the morphology of as-prepared ACs, a TESCAN MIRA3 field emission scanning electron microscope (FE-SEM) was used. Reflectance fourier transform infrared (FT-IR) spectra were collected from the absorbance intensities of functional groups of as-prepared ACs by Thermo Nicolet AVATAR 360 within the 4000-400 cm⁻¹ wave number range.

2.4. Procedure

Figure 1 shows a schematic of a PCE adsorption laboratory system operating according to the law of thermodynamic equilibrium between the liquid and gas phases. This device is used to absorb PCE in the range of 0-1000 ppm, 25 °C, and atmospheric pressure.

Continuous N₂-PCE flow is produced by the flow of N₂ through a liquid PCE tank to obtain a certain concentration of PCE in the gas stream by changing the ratio of concentrated and dilute N₂ flow. Concentrated N₂ flows out of the bubble tank and flows continuously onto the activated carbon sample located in the adsorbent bed. Contaminated N₂ passed through the adsorbent and the process

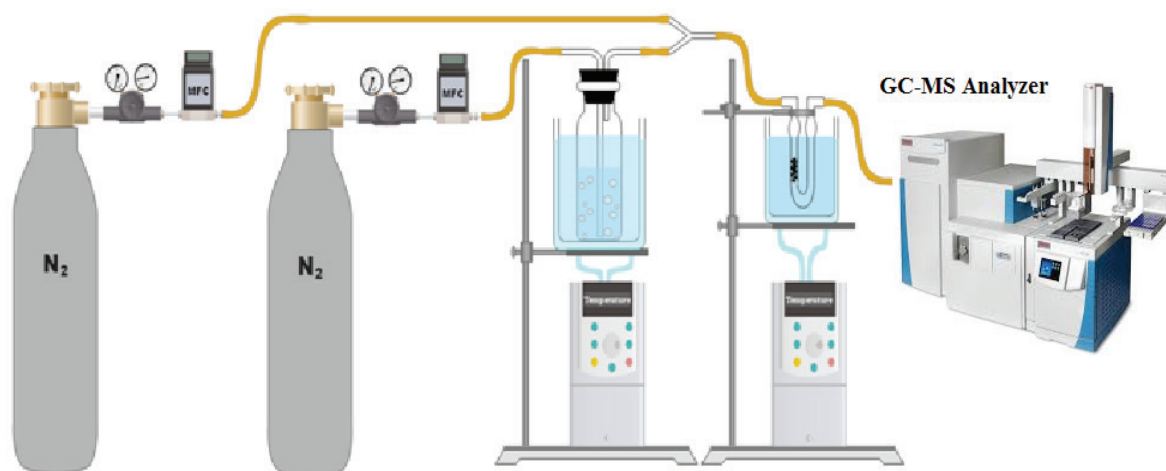


Fig. 1. Schematic of the PCE adsorption laboratory system

continued until the adsorbent saturated with PCE and the gas flow at the inlet and outlet of the column was analyzed online with GC-MS analyzer. Using the refractive index, the time required for saturation can be achieved [11].

3. Results and Discussion

3.1. FE-SEM

SEM micrographs of the carbonized walnut shell (Fig. 2a) has a smooth, pore-free surface in which, after nitrogen doping (Fig. 2b), a number of macropores are seen on the sample. Figure 2c shows a spongy structure containing uniform, very fine cavities of micro and nano size, showing that severe morphological changes have occurred during the activation process and that the active

nano carbons bear no resemblance to the carbonized sample. To better understand the textural properties of activated nano carbons, the surface was analyzed by physical adsorption of N_2 .

3.2. Physical Properties

N_2 adsorption/desorption isotherms were measured to evaluate the textural properties of the samples. The adsorption isotherms of Figure 3a are of type I according to the IUPAC classification, and its desorption is of type H4. According to research, H4 type hysteresis rings are related to the narrow slit of the specimen [12]. The isotherms have a soft curvature in the relative pressure between 0 and 0.4 owing to the presence of cavities larger than the average adsorbed diameter. On the other hand,

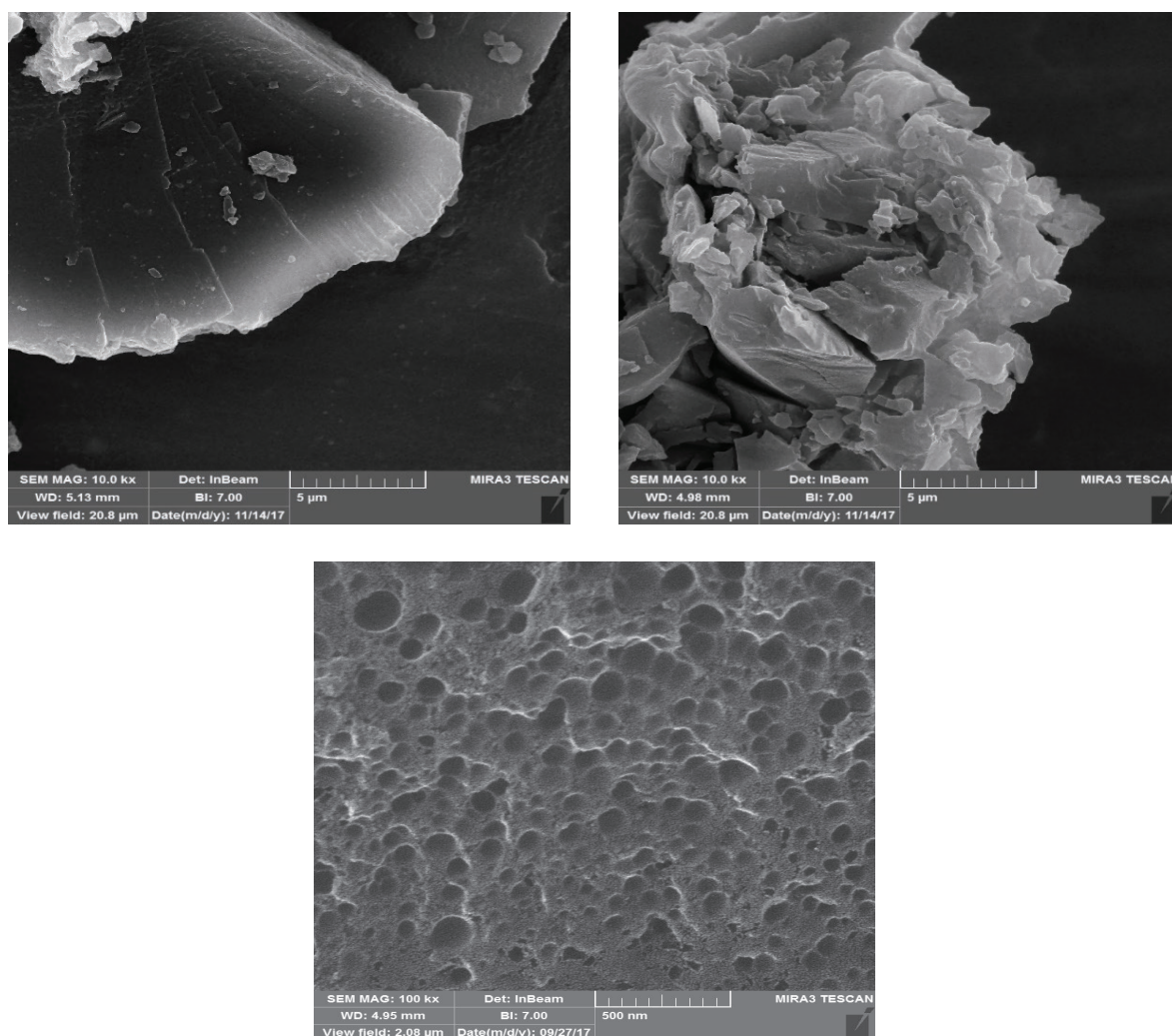
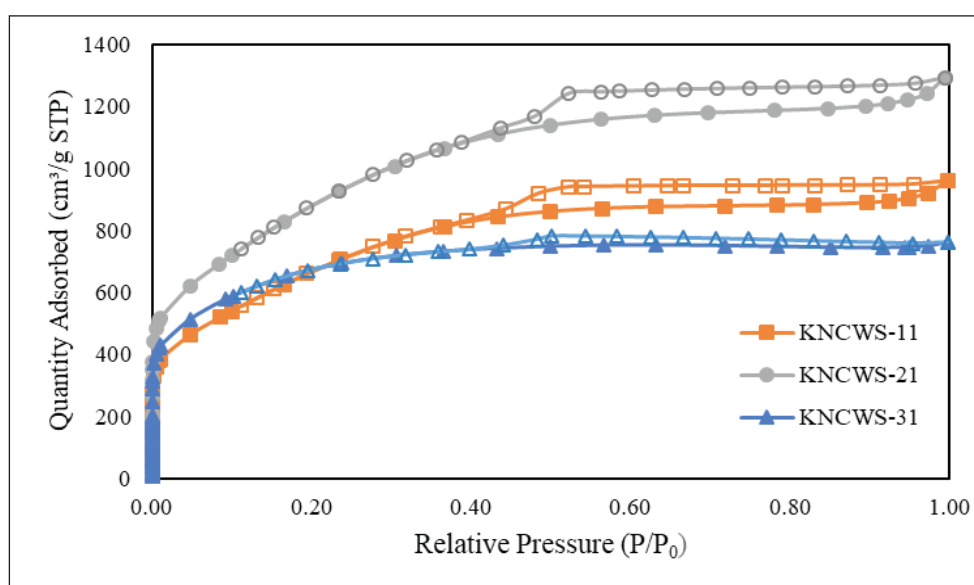


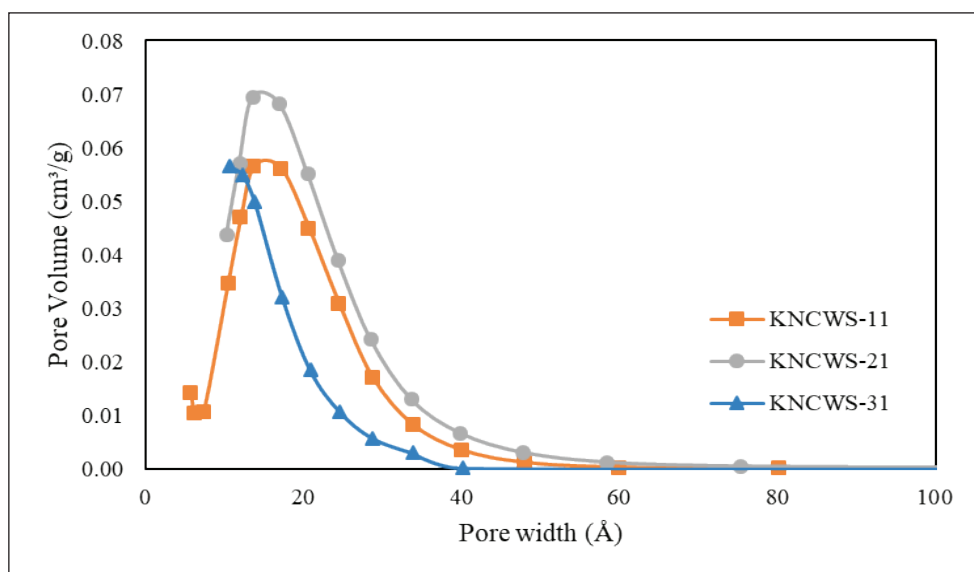
Fig. 2. FE-SEM images of a) CWS, b) NCWS-21, c) KNCWS-21

more curvature of the isotherm knee at low relative pressure and a slight increase in N_2 adsorbed with increasing pressure indicate expansion (enlargement) of the micropore structure. The hysteresis ring exhibited at a relative pressure of about 0.5 indicates the definite presence of meso-cavities in the samples ($P/P_0 > 0.4$) [13]. As can be seen from the wider circle of KNCWS-21 and KNCWS-11 hysteresis, the participation of mesopores is greater. This is in line with our findings, which show a maximum average pore width of 2.48 nm for KNCWS-21 and 2.41 nm for

KNCWS-33 [14]. Based on the distribution shown in Figure 3b, the cavities mainly contain sizes less than 10 nm, which indicates the presence of both micropores and mesopores. With increasing the urea to carbon ratio from 1:1 to 2:1, the peak intensity in the pore distribution curves of the samples increased and then decreased to a ratio of 3:1. The degradation of the structural parameters of the KNCWS-31 sample compared to KNCWS-21 and occurred due to the destruction of the walls between the cavities or the blockage of the cavities with excessive nitrogen [15] (Table 1).



(a)



(b)

Fig. 3. N_2 adsorption/desorption isotherms(a) and BJH pore size distribution of KNCWSs(b).

Table 1. Textural properties of the KNCWSs

Specimens	S_{BET}	D	V_{tot}	$V_{\text{mic}}/V_{\text{tot}}$
	(m^2/g)	(nm)	(cm^3/g)	(%)
KNCWS-11	2461	2.41	1.48	8.78
KNCWS-21	3225	2.48	1.99	10.05
KNCWS-31	2319	2.03	1.17	20.5

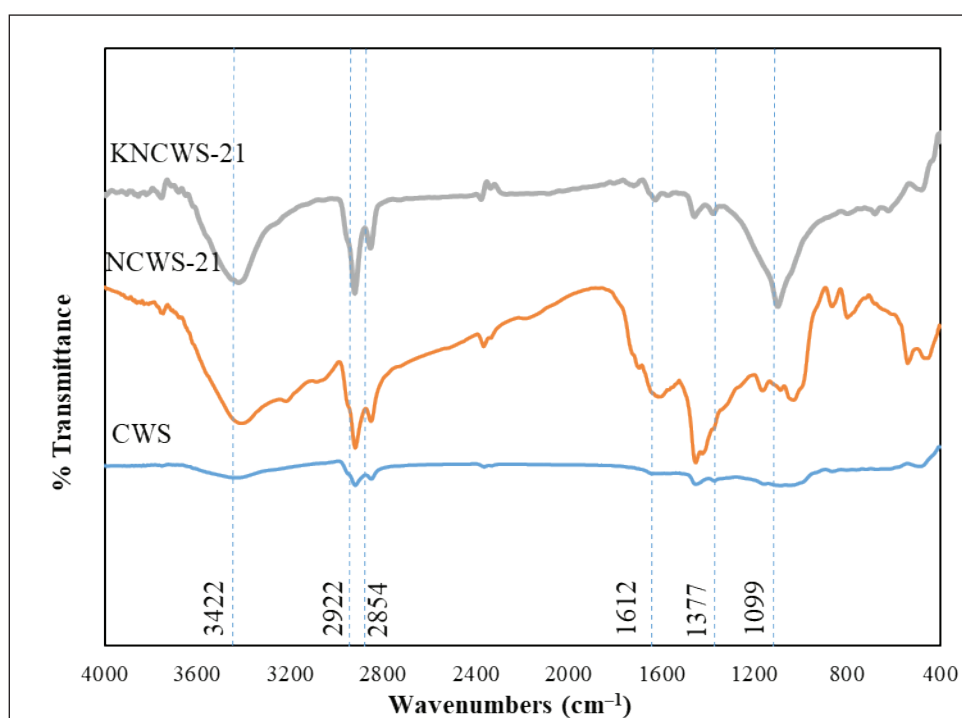
3.3. FT-IR

The diagrams in Figure 4 are the results of the FT-IR tests (a) CWS, (b) NCWS-21, and (c) KNCWS-21. The samples show almost the same spectrum, however, some of the weak/strong functional groups have disappeared. Nitrogen doping as well as different activation conditions have resulted in changes in the carbon sample spectrum. 3426 ~ 3409 cm^{-1} bandwidth is seen for all samples, indicating tensile vibration of N-H groups or tensile vibration of O-H hydroxyl groups of phenol, alcohol, and carboxylic acid [16]. The broadband in the range of 2922 ~ 12851 cm^{-1} is related to the asymmetric tensile vibration of CH_2 , which can be attributed to the -CH- bond on the carbon surface. -CH- bonds may belong to alkyl groups such as methyl, methylene groups, or aldehyde groups [17]. The bandwidth at 1612 ~

11376 cm^{-1} is due to amides, pyridine, and $\text{C}=\text{N}$, indicates nitrogen functional groups at temperatures higher than crude carbon [18]. The peak range of 1030 ~ 1099 cm^{-1} is also attributed to the C-N tensile vibration [19]. Therefore, analysis of FT-IR spectra confirms the presence of N-containing groups in the synthesized samples.

3.4. Equilibrium adsorption

Figure 5 shows the performance of both chemical adsorption processes (nitrogen doping) and physical adsorption (increasing surface area and pore volume). Due to the trend of PCE adsorption isotherms, intensification of carbon activation has improved the adsorption process. Also, increasing the adsorption of PCE by adding nitrogen plays an important role for functional groups, because the

**Fig. 4.** FT-IR spectra of the as-synthesized KNCWSs

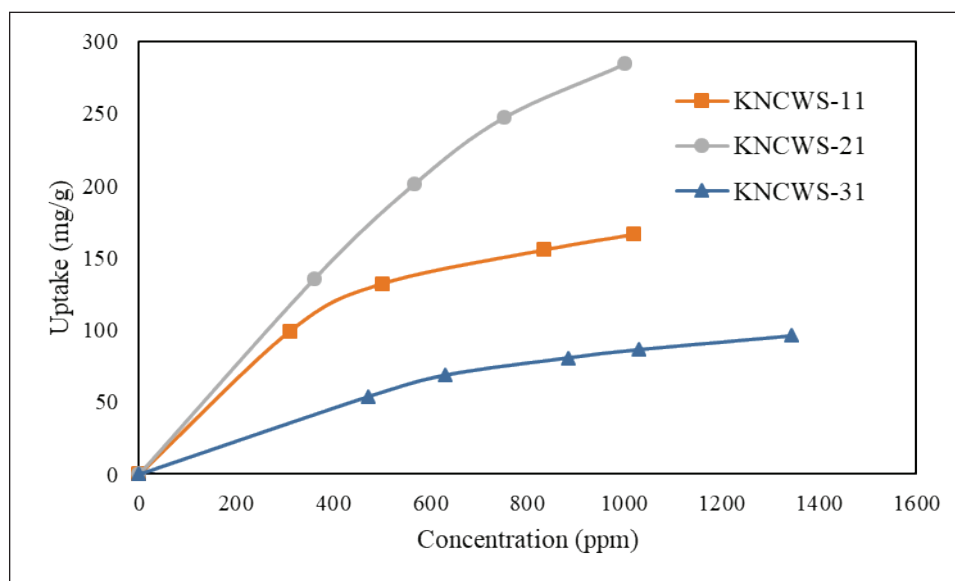


Fig. 5. Isotherm of PCE adsorption on KNCWs

nature of PCE is electron-accepting, and nitrogen groups are electron-giving and cause chemical adsorption. It should be noted that the high share of mesopores also facilitates the transfer of PCE mass and increases adsorption. According to the results of PCE adsorption, it can be acknowledged that the reason for the significant decrease in the adsorption rate of the KNCWS-31 sample is the decrease in its physical characteristics, which occurred due to the destruction of the walls between cavities or blockage of cavities with excessive nitrogen.

According to Table 2, the modulus of adsorption equilibrium data for the adsorption of PCE on doped activated nano carbons was consistent with the Langmuir, Freundlich, and Sips models [20]. However, the Sips model showed higher values of R^2 than the Langmuir and Freundlich models for all samples studied. In this experiment, the b-constant of the Sips model was approximately zero, indicating that the Sips model was reduced to the Freundlich model. This means that multilayer adsorption occurs with a non-uniform distribution of heat and tensile adsorption across the surface of doped activated nano table 2.

3.5. Kinetic adsorption

In order to evaluate the speed of the adsorption

process and to determine the process speed control stage, kinetic modeling is performed. Kinetic data were evaluated using pseudo-first-order [21] and pseudo-second-order [22] models to provide a suitable model for the kinetic behavior of the studied gravity (Fig. 6).

The adsorption kinetics and correlation coefficients of PCE on doped and non-doped activated nano carbons are shown in Table 3. Both pseudo-first-order and pseudo-second-order equations can predict the adsorption process under experimental conditions. Given the calculated values of q_e and R^2 , the pseudo-first-order equation better describes the adsorption of PCE. The values of R^2 in the pseudo-first-order equation have higher values than the pseudo-second-order equation. The results show that the adsorption of PCE in doped activated nano carbons belongs to the pseudo-first-order equation, which indicates the reversible adsorption between PCE and the adsorbent table 3.

4. Conclusion

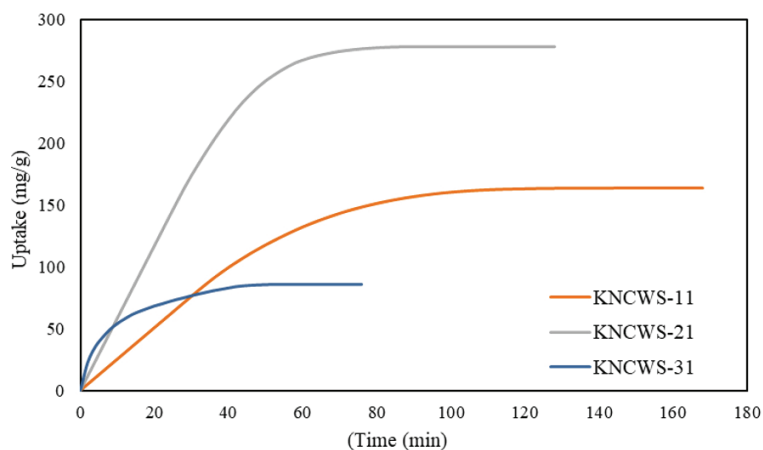
In this study, a series of nitrogen-doped activated nano carbons were synthesized using walnut shell and evaluated to adsorb perchloroethylene (PCE) vapor. In practice, the vapor adsorption capacity of PCE using nitrogen-doped activated carbon

Table 2. The parameters of Langmuir, Freundlich, and Sips isotherms of PCE adsorption on doped activated nano carbons

Isotherms		Adsorbents		
		KNCWS-11	KNCWS-21	KNCWS-31
Langmuir $q_e = q_m \frac{bP}{1 + bP}$	q_m	348.3383	703.6625	168.2004
	b	0.00065812	0.00069629	0.0010431
	R-squared	0.99962	0.99824	0.99847
Freundlich $q_e = q_m (bP)^{1/n}$	q_m	50.3955	179.2698	23.3665
	b	0.0042402	0.0020152	0.009701
	n	1.4203	1.4426	1.7413
	R-squared	0.99839	0.99586	0.99721
Sips $q_e = q_m \frac{(bP)^{1/n}}{1 + (bP)^{1/n}}$	q_m	232.0382	399.4676	100.7033
	b	0.0013378	0.0018034	0.0022754
	n	0.78099	0.64366	0.48246
	R-squared	1.00000	0.99989	0.99979

Table 3. Pseudo-first and second-order kinetics parameters of PCE adsorption on doped activated nano carbons

Isotherms		Adsorbents		
		KNCWS-11	KNCWS-21	KNCWS-31
pseudo-first-order $q_t = q_e (1 - \exp(-K_1 t))$	q_e		140.582	295.911
	K_1		0.0309	0.031
	R-squared		0.990	0.982
pseudo-second-order $q_t = \frac{K_2 q_e^2 t}{1 + K_2 q_e t}$	q_e		176.946	382.646
	K_2		0.0001	7.603
	R-squared		0.970	0.960

**Fig. 6.** Kinetics of PCE adsorption on KNCWs

varies considerably due to their structural and surface properties. Nitrogen plays an important role in the adsorption of PCE. Samples of KNCWS-11, KNCWS-21, and KNCWS-31 at initial concentrations of 1000 ppm have adsorption rates of 166, 285, and 95 mg g⁻¹, respectively. Therefore, the use of nitrogen-doped activated nano carbons as a green adsorbent provides a cost-effective means of combating biomass waste and can partially reduce the climate change caused by PCE vapor. Contaminated PCE/ N₂ at the inlet and outlet of the column was analyzed online with GC-MS analyzer.

5. Acknowledgments

The authors wish to thank the Chemical Engineering Department, Islamic Azad University, North Tehran Branch, Tehran, Iran

6. References

- [1] M. Słomińska, P. Konieczka, J. Namieśnik, The fate of BTEX compounds in ambient air, *Crit. Rev. Environ. Sci. Technol.*, 44 (2014) 455–472.
- [2] L. Yu, L. Wang, W. Xu, L. Chen, M. Fu, J. Wu, D. Ye, Adsorption of VOCs on reduced graphene oxide, *J. Environ. Sci.*, 67 (2018) 171–178.
- [3] S. Jafari, F. Ghorbani-Shahna, A. Bahrami, H. Kazemian, Adsorptive removal of toluene and carbon tetrachloride from gas phase using zeolitic imidazolate framework-8: Effects of synthesis method, particle size, and pretreatment of the adsorbent, *Microporous Mesoporous Mater.*, 268 (2018) 58–68.
- [4] C. Dai, Y. Zhou, H. Peng, S. Huang, P. Qin, J. Zhang, Y. Yang, L. Luo, X. Zhang, Current progress in remediation of chlorinated volatile organic compounds: A review, *J. Ind. Eng. Chem.*, 62 (2018) 106–119.
- [5] R.E. Doherty, A history of the production and use of carbon tetrachloride, tetrachloroethylene, trichloroethylene and 1,1,1-trichloroethane in the United States: Part 1--historical background; carbon tetrachloride and tetrachloroethylene, *Environ. Forensics.*, 1 (2000) 69–81.
- [6] B. Huang, C. Lei, C. Wei, G. Zeng, Chlorinated volatile organic compounds (Cl-VOCs) in environment sources, potential human health impacts, and current remediation technologies, *Environ. Int.*, 71 (2014) 118–138.
- [7] C. Barton, Tetrachloroethylene, in: P. Wexler (Ed.), *Encycl. Toxicol.* (Third Ed., Third Edition, Academic Press, Oxford, pp. 498–502, 2014. <https://doi.org/10.1016/B978-0-12-386454-3.00436-X>.
- [8] J.D. Tucker, K.J. Sorensen, A.M. Ruder, L.T. McKernan, C.L. Forrester, M.A. Butler, Cytogenetic analysis of an exposed-referent study: perchloroethylene-exposed dry cleaners compared to unexposed laundry workers, *Environ. Heal.*, 10 (2011) 16.
- [9] Y. Zeng, Z. Zeng, T. Ju, F. Zhang, Adsorption performance and mechanism of perchloroethylene on a novel nano composite β-FeOOH-AC, *Micropor. Mesopor. Mater.*, 210 (2015) 60–68.
- [10] Z. Rouzitalab, D.M. Maklavany, S. Jafarinejad, A. Rashidi, Lignocellulose-based adsorbents: A spotlight review of the effective parameters on carbon dioxide capture process, *Chemosphere*, 246 (2020). <https://doi.org/10.1016/j.chemosphere.2019.125756>.
- [11] E. Jangodaz, E. Alaie, A.A. Safekordi, S. Tasharrofi, Adsorption of ethylbenzene from air on metal–organic frameworks MIL-101(Cr) and MIL-53(Fe) at room temperature, *J. Inorg. Organomet. Polym. Mater.*, 28 (2018) 2090–2099.
- [12] M. Thommes, K. Kaneko, A. V Neimark, J.P. Olivier, F. Rodriguez-Reinoso, J. Rouquerol, K.S.W. Sing, Physisorption of gases, with special reference to the evaluation of surface area and pore size distribution (IUPAC Technical Report), *Pure Appl. Chem.*, 87 (2015) 1051–1069.
- [13] M.S. Shafeeyan, W.M.A.W. Daud, A. Houshmand, A. Arami-Niya, Ammonia modification of activated carbon to enhance

- carbon dioxide adsorption: Effect of pre-oxidation, *Appl. Surf. Sci.*, 257 (2011) 3936–3942.
- [14] Z. Rouzitalab, D. Mohammady Maklavany, A. Rashidi, S. Jafarinejad, Synthesis of N-doped nanoporous carbon from walnut shell for enhancing CO₂ adsorption capacity and separation, *J. Environ. Chem. Eng.*, 6 (2018) 6653–6663.
- [15] J. Chen, J. Yang, G. Hu, X. Hu, Z. Li, S. Shen, M. Radosz, M. Fan, Enhanced CO₂ capture capacity of nitrogen-doped biomass-derived porous carbons, *ACS Sustain. Chem. Eng.*, 4 (2016) 1439–1445.
- [16] A. Heidari, H. Younesi, A. Rashidi, A.A. Ghoreyshi, Evaluation of CO₂ adsorption with eucalyptus wood based activated carbon modified by ammonia solution through heat treatment, *Chem. Eng., J.* 254 (2014) 503–513.
- [17] A. Kongnoo, P. Intharapat, P. Worathanakul, C. Phalakornkule, Diethanolamine impregnated palm shell activated carbon for CO₂ adsorption at elevated temperatures, *J. Environ. Chem. Eng.*, 4 (2016) 73–81.
- [18] Z. Xiong, Z. Shihong, Y. Haiping, S. Tao, C. Yingquan, C. Hanping, Influence of NH₃/CO₂ modification on the characteristic of biochar and the CO₂ capture, *Bioenergy Res.*, 6 (2013) 1147–1153.
- [19] Z. Geng, Q. Xiao, H. Lv, B. Li, H. Wu, Y. Lu, C. Zhang, One-step synthesis of microporous carbon monoliths derived from biomass with high nitrogen doping content for highly selective CO₂ capture, *Sci. Rep.*, 6 (2016) 4–11.
- [20] N.S. Nasri, U.D. Hamza, S.N. Ismail, M.M. Ahmed, R. Mohsin, Assessment of porous carbons derived from sustainable palm solid waste for carbon dioxide capture, *J. Clean. Prod.*, 71 (2014) 148–157.
- [21] N. Álvarez-Gutiérrez, M. V. Gil, F. Rubiera, C. Pevida, Kinetics of CO₂ adsorption on cherry stone-based carbons in CO₂/CH₄ separations, *Chem. Eng. J.*, 307 (2017) 249–257.
- [22] Y.S. Ho, G. McKay, Pseudo-second order model for sorption processes, *Process Biochem.*, 34 (1999) 451–465.



Solid phase microextraction for organochlorine pesticides in water samples using MWCNTs-doped polypyrrole coated on steel fiber before determination by gas chromatography electron capture detector

Hamideh Assadollahzadeh^{a,*} and Ebrahim Noroozian^b

^a Department of Chemistry, Kerman Branch, Islamic Azad University, Kerman, Iran, P. O. Box 7635131167.

^b Department of Chemistry, Shahid Bahonar University of Kerman, P.O. Box 133-76175, Kerman, Iran

ARTICLE INFO:

Received 18 Aug 2020

Revised form 15 Oct 2020

Accepted 23 Nov 2020

Available online 29 Dec 2020

Keywords:

Organochlorine pesticides,
Multiwalled carbon nanotubes,
Polypyrrole composite,
Solid phase microextraction,
Gas chromatography

ABSTRACT

The analysis of organochlorine pesticides (OCPs) residues has received an increasing attention in the last decades. The solid-phase microextraction (SPME) is a convenient and fast analytical method, which has been widely used for the determination of volatile and semivolatile organic compounds in aqueous samples. In this study, the multiwalled carbon nanotubes/polypyrrole composite (MWCNTs-PPy) coated on steel fiber was used for extraction OCPs from water samples by the SPME technique. The effects of various parameters on the efficiency of SPME process such as extraction time, extraction temperature, ionic strength, desorption time, and desorption temperature were studied. Under optimized conditions, the detection limits for the OCPs varied between 0.051 and 0.39 $\mu\text{g mL}^{-1}$, the inter-day and intra-day relative standard deviations for various OCPs using a single fiber were 6.5-11.5% and 3.6-11.5, respectively. The linear ranges varied between 0.001 and 1 ng mL^{-1} . The proposed method was successfully applied to the analysis of ground water samples with the recoveries from 86 to 110%

1. Introduction

Determination of OCPs has received great attention in recent decades. These compounds have been widely used worldwide in order to increase crops output and enhance quality of products. But most of these compounds have been eliminated or restricted in use after evidence of their toxicity and persistence in the environment [1-4]. For determination of trace pesticides/OCPs in complex matrices which contain a high number of interfering compounds, usually

require both efficient sample preparation techniques and high performance analytical instruments. Sample preparation before chromatographic analysis is one of the most important steps in analytical processes. The main conventional methods of sample preparation are liquid-liquid extraction (LLE) [5] and solid-phase extraction (SPE) [6]. Although these methods offer efficient and precise results but they have drawbacks. For example, LLE requires the use of a large amount of expensive and toxic solvents that can damage the environment. This method is also time-consuming, tedious, and very often requires solvent evaporation prior to introduction

*Corresponding author: [Hamideh Assadollahzadeh](mailto:Hamideh.Assadollahzadeh@iaukerman.ac.ir)

E-mail: asadollahzadeh90@yahoo.com

<https://doi.org/10.24200/amecj.v3.i04.117>

of the sample into the analytical instrument. Solid-phase extraction also has certain drawbacks, such as plugging of cartridges, solvent consumption for conditioning and elution steps and lack of elution selectivity. Alternative methods, such as dispersive liquid-liquid microextraction (DLLME) [7], single-drop microextraction (SDME) [8], membrane-protected micro-solid-phase extraction (μ -SPE) [9], dispersive solid-phase microextraction (DSPME) [10], stir bar sorptive extraction (SBSE) [11] have been developed to improve extraction efficiencies and reduce solvent consumption, etc. However, solid-phase microextraction (SPME) developed by Pawliszyn and coworkers [12] is a practical solvent-free alternative for the extraction of organic compounds. This method is easily automated, it simplifies the extraction process and meaningfully decreases the analysis time. In this method, analytes are generally extracted and concentrated by a thin layer of a sorbent coated on a silica fiber. The fiber is then introduced into a chromatographic system for separation and measurement. SPME integrates sampling, extraction, concentration and sample introduction into a single solvent-free step. Various sorbents have been used as SPME coating materials. Currently, the improvement in the applications of SPME is focused on the development of novel coatings to enhance the extraction efficiency. Some coatings include polyaniline [13], polythiophene [14], polypyrrole [15, 16], metalorganic frameworks (MOFs) [17], layered double hydroxide (LDH) [18], metal and metal oxide [19, 20], molecularly imprinted polymer (MIP) [21], carbon nanotubes [22, 23]. A multiwalled carbon nanotube-polypyrrole (MWCNTs/PPy) composite coated SPME fiber was first introduced in our laboratories for the extraction of phthalate esters from water [24]. In the present work, we present an application of MWCNTs/PPy composite polymer in direct immersion SPME/GC-ECD for the analysis of twelve OCPs residues in water.

2. Experimental

2.1. Chemicals

The twelve organochlorine pesticides namely

lindane, heptachlor, aldrin, p,p'-DDE, dieldrin, endrin, endosulfan I, endosulfan II, p,p'-DDD, o,p'-DDD, p,p'-DDT and methoxychlor were of standard grade and obtained from PolyScience (IL, USA, <http://www.polysciences.com>). Pyrrole ($\geq 97\%$ pure) was obtained from Merck (Darmstadt, Germany, <http://www.merck.com>) and was distilled and stored in a dark bottle under nitrogen atmosphere in a refrigerator. Multiwalled carbon nanotubes (MWCNTs) purchased from PlasmaChem GmbH (Berlin, Germany, <http://www.plasmachem.com>) was 20-40 nm in diameter and 1-10 μm in length. Stainless Steel wire (type 100-014, 350 μm O.D.) was obtained from Ortho Organizers (Carlsbad, USA, <http://www.orthoorganizers.com>) and used as the SPME fiber. A 200 $\mu\text{g mL}^{-1}$ stock solution of the mixture of OCPs was prepared in acetone. Working solutions were prepared by appropriate dilution of the stock solution in distilled water. Highly pure helium and nitrogen gases ($\geq 99.999\%$) were obtained from Sabalan Co. (Tehran, Iran). They were used as GC carrier gas and make-up gas, respectively. Other reagents used were of highest purity available. Double distilled water was used in all experiments.

2.2. Apparatus

The SPME device was home made. It consisted of a 23 gauge, 9.0-cm stainless steel spinal needle Dr. Japan Co., (Tokyo, Japan, <http://www.drjapan-jp.com>), housed in a 6.0-cm hollow cylinder of Al with two nuts and two pieces of rubber septum. A 17-cm piece of the stainless steel wire passing through the septum acted as the SPME fiber. One end of the fiber was attached to a cap and 3 cm of the other end was coated with MWCNTs/PPy coating. Electrochemical polymerization of pyrrole was carried out with a Behpajuh potentiostat/galvanostat, model BHP 2061-C (Esfahan, Iran, <http://www.behpajoooh.com>). The Pt counter electrode and the Ag/AgCl reference electrode used in the electrochemical process were from Azar Electrode (Urmieh, Iran). For stirring and heating the samples during the SPME procedure, a Corning model PC-351 hot plate-stirrer (MA, USA) was used.

The chromatographic analysis of OCPs was performed by a Shimadzu model 16A gas chromatograph (Kyoto, Japan, <http://www.Shimadzu.com>), equipped with a split-splitless injector, electron capture detector (ECD) and a BP-10 (25 m × 0.33 mm. I.D. and 0.5- μ m film thickness) capillary column. The flow rates of helium carrier gas and nitrogen make-up gas were adjusted at 1 mL min⁻¹ and 30 mL min⁻¹, respectively. The column temperature was initially kept at 50 °C for 1 min, then increased at 25 °C min⁻¹ to 170 °C, ramped at 4 °C min⁻¹ to 250 °C, and was kept for 3 min. Injector and detector temperatures were adjusted at 250°C and 300 °C, respectively. A Shimadzu QP 2000 GC-MS instrument (Kyoto, Japan, <http://www.Shimadzu.com>) equipped with quadrupole analyzer and electron impact ion-source (EI) was used for the identification of pesticides in real samples. A Bandelin Sonorex ultrasonic bath (Berlin, Germany, <http://www.bandelin.com>) was use for sonication.

2.3. Preparation of composite coating

Briefly MWCNTs was refluxed in concentrated nitric acid. The resultant MWCNTs-COOH was collected on a filter paper and washed with distilled water until neutralized and was dried at room temperature. The composite coating of MWCNTs and polypyrrole was synthesized electrochemically via in-situ polymerization from a solution containing both the acid oxidized-MWCNTs and the pyrrole monomer. The deposition was carried out at room temperature. Stainless steel wire, platinum electrode and Ag/AgCl electrode were used as working, counter and reference electrodes, respectively. The coating procedure was as follow. The oxidized-MWCNTs was ultrasonically dispersed in water for 1h at 28 °C and then pyrrole was added and sonicated for 15 min. The composite polymer coating was directly deposited on the steel wire from this solution by applying a constant potential. To make the coating adhere firmly to the surface of the wire, the wire surface was first roughened by a smooth sand paper and then washed in acetone while sonicating. Thermal conditioning of the coated fiber was carried out by heating at 100 °C for 30 min in an oven, and

then at 250 °C for 2h in the GC injector port under a helium atmosphere. This removes the volatile compounds remaining in the fiber and a smooth chromatographic baseline is obtained.

2.4. SPME procedure

A 0.1 ng mL⁻¹ working solution of the mixture of OCPs in distilled water was prepared from the stock solution on a daily basis. SPME extractions were performed by placing 10.0 mL samples into a 12.0 mL sample vial capped with a septum. Magnetic stirring with a 1-cm long Teflon-coated stirring bar was used to agitate the samples at the highest but constant possible rate. Extractions were carried out by exposing a 3.0 cm length of the composite coated fiber to the sample solution. The extraction temperature was adjusted by placing the extraction vial in a water bath placed on the magnetic stirrer. After the extraction, the fiber was withdrawn into the needle, removed from the sample vial and immediately introduced into the GC injector port for thermal desorption.

3. Results and discussion

3.1. SPME optimization

In this study, the effect of various parameters on the efficiency of SPME process, such as desorption time and temperature, salting out effect, pH, extraction time and extraction temperature were studied on a one-at-a-time strategy. Stirring the sample during the extraction is also an important parameter. This is to generate a continuously fresh layer of the sample solution near the surface of the fiber coating in order to improve the extraction efficiency. In addition, efficient agitation reduces the depth of the boundary layer and thus improves the speed of extraction. Therefore, all the experiments were performed under maximum but constant stirring rate.

3.1.1. Desorption time and desorption temperature

Study of desorption processes can provide useful information on the absorbent and the absorption processes. Desorption of extracted analytes was carried out in the GC injection port at temperatures between 160 and 280 °C. **Figure 1** shows that at the desorption temperature of 250 °C, nearly all

of OCPs were fully desorbed from the fiber and no carryover effect was observed. Therefore in subsequent experiments a desorption temperature of 250 °C was used.

The time necessary for desorbing analytes from the SPME fiber in the injection part of GC was also

studied. For this purpose, desorption times between 1 and 20 min were used. After a desorption time of 5.0 min at 250 °C, analytes were almost fully desorbed from the fiber, but to avoid memory effect or carry over an extra 5.0 min was considered in the desorption step. Therefore all desorptions were

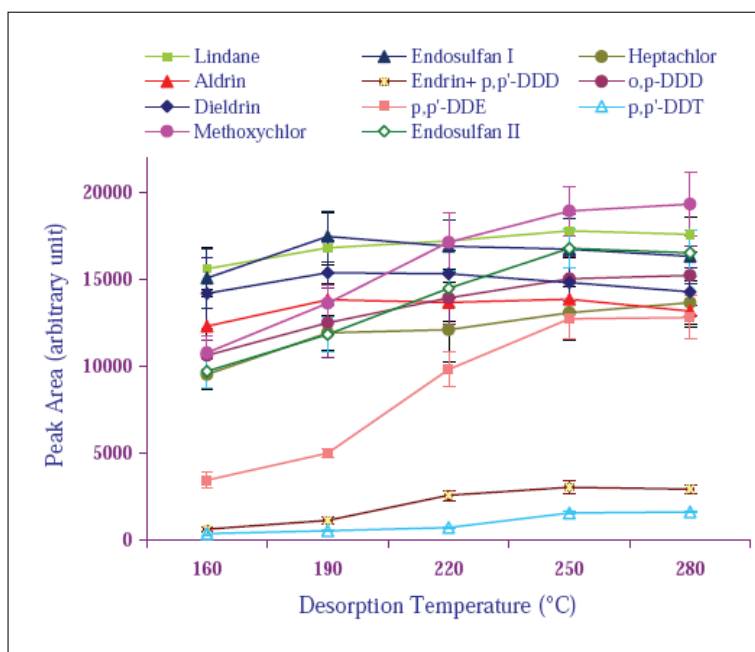


Fig. 1. Effect of desorption temperature on extraction efficiency. Extraction conditions: [OCPs] = 0.1 ng mL⁻¹ each; extraction time = 40 min; extraction temperature = 25 °C, no sample pH and salt was adjusted or added.

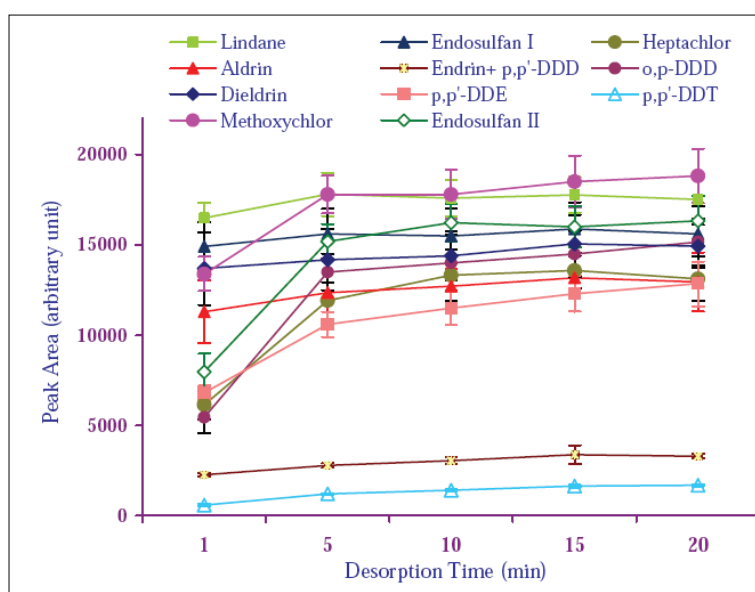


Fig. 2. Effect of desorption time on extraction efficiency. Extraction conditions: [OCPs]=0.1 ng mL⁻¹ each; extraction time=40 min; extraction temperature=25 °C and desorption temperature=250 °C, no sample pH and salt was adjusted or added.

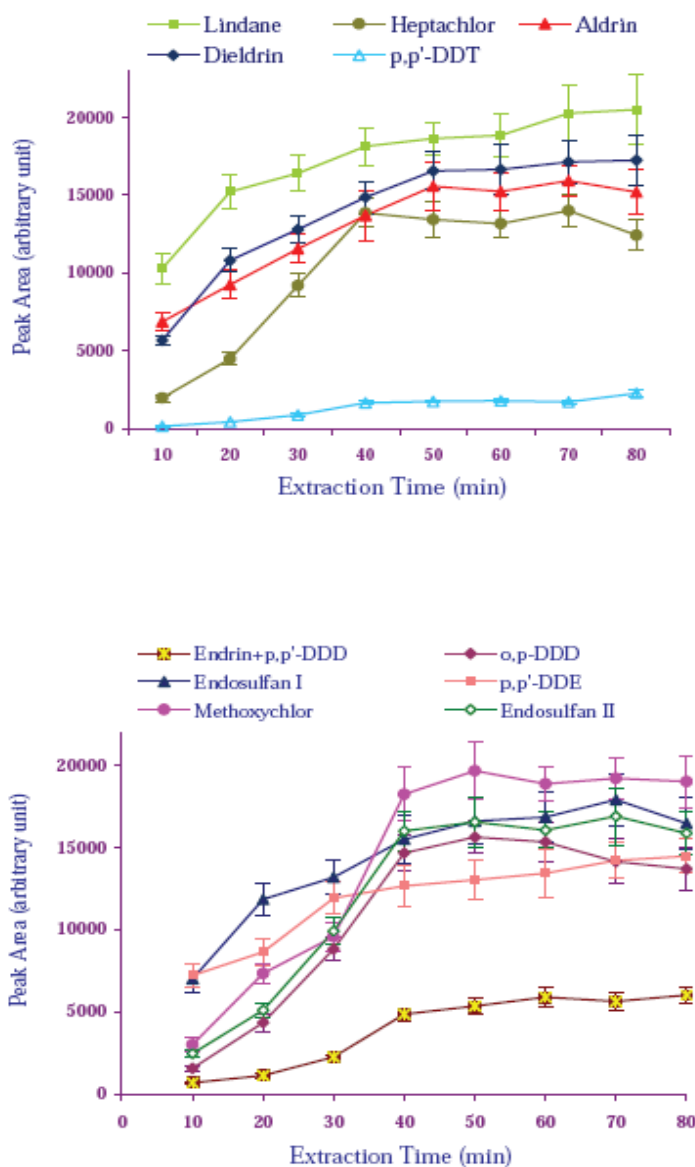


Fig. 3. The effect of extraction time on extraction efficiency. Extraction conditions: [OCPs]=0.1 ng mL⁻¹ each; extraction temperature=25 °C; desorption temperature=250 °C; desorption time=10 min; no sample pH and salt was adjusted or added.

carried out for a period of 10 min (Fig. 2).

3.1.2. Extraction time

The SPME process depends on the equilibrium involving partitioning of the analytes from the sample liquid phase to the sorbent phase on the fiber. Therefore, the resistance to the mass transfer of analytes should be overcome to reach equilibrium between the aqueous phase and the fiber. For this reason, the fiber was exposed to a mixed aqueous solution of the OCPs under study (0.1 ng mL⁻¹ each)

for a period of 10 to 80 min. The results found are shown in Figure 3. As this figure shows, the peak areas sharply increase with increases in the extraction time until 50 min, after which no significant improvement in the extraction efficiency was observed. Therefore, in all subsequent experiments, 50 min was selected as the extraction time.

3.1.3. Extraction temperature

Extraction temperature is a very important

parameter. An increase in the extraction temperature leads to an increase in diffusion coefficient and at the same time a decrease in distribution constant, leading to faster extraction, but reduced extraction efficiency. After optimizing the extraction time, the extraction temperature was varied between 20 and 70 °C. **Figure 4** shows, the extraction efficiencies for most OCPs increase by increasing extraction temperature up to 40 °C, after which it levels off. This may be due to more favorable mass transfer for these analytes. In some cases, at temperatures above 40 °C, the extraction efficiency decreased, because the distribution constant at these temperatures

decreased. This may be due to exothermic nature of the absorption process. Therefore, 40 °C was chosen as the optimum extraction temperature for all subsequent analyses.

3.1.4. Ionic strength

Ionic strength can vary the mechanism of mass transfer of analytes in SPME, depending on the structure, analyte properties and matrix [25]. In addition, the solubility of the non-polar organic solutes in water decreases in the presence of salts. Thus, it is expected that the addition of salts should modify the sorption of analytes by the fiber. For this

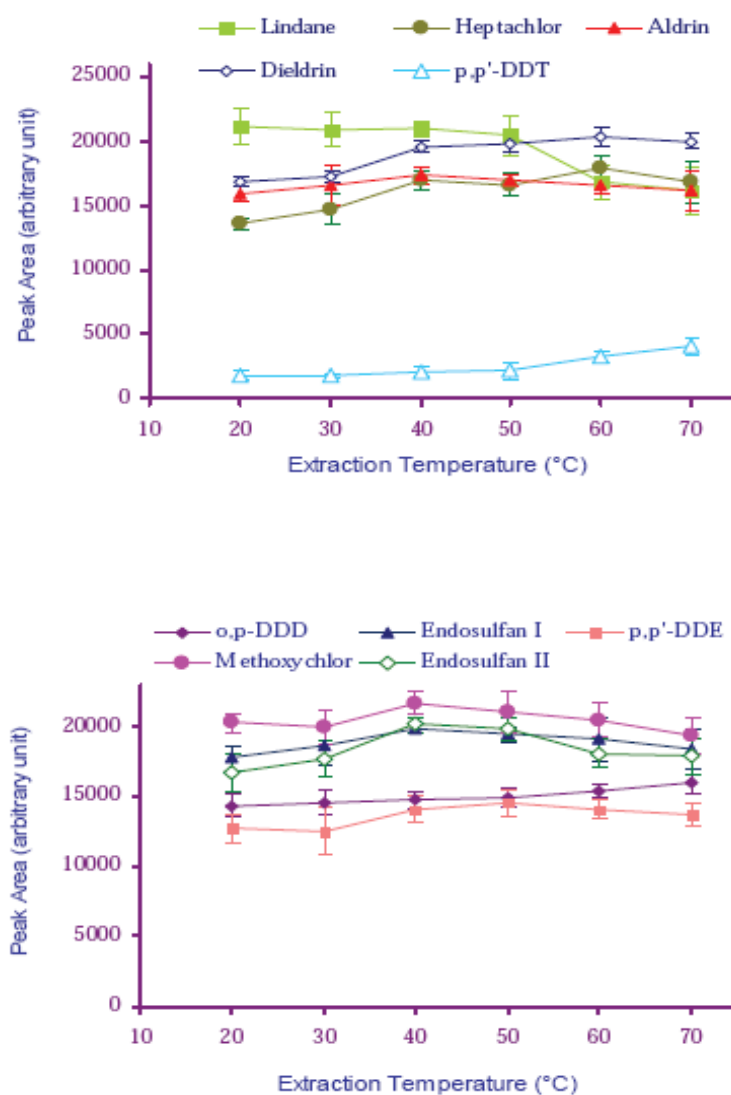


Fig. 4. The effect of extraction temperature on extraction efficiency. Extraction conditions: [OCPs]=0.1 ng mL⁻¹ each; desorption temperature=250 °C; extraction time=50 min; desorption time=10 min; no sample pH and salt was adjusted or added.

reason, the effect of this parameter on extraction efficiency was investigated. Here, extractions were carried out from solutions in the presence of NaCl from 0 to 20% (w/v). **Figure 5** shows that for most analytes no significant improvement in the extraction efficiency is observed up 10% NaCl. However, a decrease in the extraction efficiency is observed at higher NaCl concentrations. This can be explained

by the fact that the present composite coating is a solid porous sorbent, and the extraction occurs on the surface of pores. It seems that large amounts of NaCl in the sample solution occupies the surface of the coating material and have a negative effect on the extraction efficiency. Based on the results obtained, it was decided to carry out all subsequent extractions without adding any salt to sample solutions.

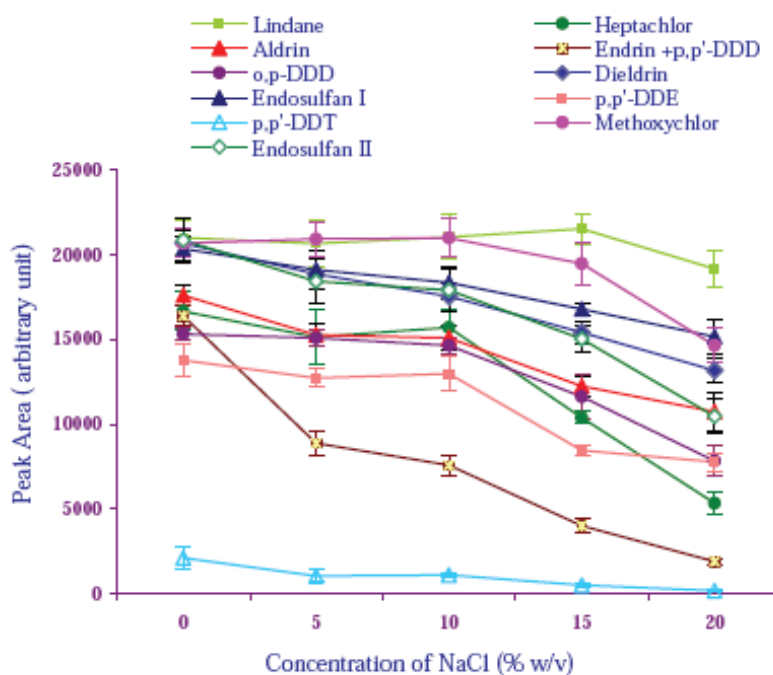


Fig. 5. The effect of NaCl concentration on extraction efficiency.

Extraction conditions: [OCPs]=0.1 ng mL⁻¹ each; desorption time=10 min; desorption temperature=250 °C; extraction time=50 min; extraction temperature=40 °C; no sample pH adjusted.

3.1.5. pH optimization

Further investigations were carried out on pH value of sample solution. The effect of sample pH on the extraction efficiency was experimented in the range from 4 to 9. For the group of OCPs studied, no significant changes were found in the pH values tested. The OCPs are little affected by pH because they are nonionizable compounds in aqueous solution. Therefore, extraction of OCPs was carried out using the original solution.

3.2. Method Validation

Figures of merit including linear range (LR), precision (RSD %) and limit of detection (LOD) were evaluated for the method developed in this work. The linear range was determined by extracting a series of aqueous solutions of the mixture of OCPs in the range between 0.001 and 1.0 ng mL⁻¹ for lindane and heptachlor, 0.01 to 1 ng mL⁻¹ for p,p'-DDT, and 0.005 to 1 ng mL⁻¹ for aldrin, endosulfan I, p,p'-DDE, dieldrin, endrin + p,p'-DDD, endosulfan II, o,p'-DDD and

methoxychlor. As shown in Table 1, the coefficient of determination (r^2) obtained for different OCPs varied from 0.9871 to 0.9979. The repeatability of the method was determined by seven replicate analyses from mixed aqueous solutions containing 0.02 ng mL⁻¹ of each OCP. As Table 1 shows, the intra-day relative standard deviations (RSD%) varied from 3.6 % for lindane to 11.5 % for endosulfan II, while the inter-day RSD% varied from 6.5% for methoxychlor to 11.5% for dieldrin. The limits of detection based on S/N = 3 in this DI-SPME/GC/ECD method varied between 0.051 and 0.39 pg mL⁻¹ (Table 1). To evaluate the accuracy

of the method, a water sample was collected from the university campus and subjected to the present SPME and GC analysis without any pretreatment. No pesticide was detected in this sample using both ECD and MS detection. Therefore, this water sample was used as blank and spiked at 0.01 and 0.075 ng mL⁻¹ of each OCP. The percent recoveries found were reasonable and between 86 and 110% (Table 1). The validation parameters obtained here were compared with results obtained by other methods which show that they are comparable or better than the values reported by other groups (Table 2).

Table 1. Analytical performance of OCPs residues in water: Limit of detection (LOD), percent recovery, linear range (LR), coefficient of determination (r^2) and RSD%.

Compound	LOD (pg mL ⁻¹)	Recovery (%)		LR (ng mL ⁻¹)	Coeff. Det r^2	RSD%	
		0.01 ng mL ⁻¹	0.075 ng mL ⁻¹			Intra-day (N=7)	Inter-day (N=7)
Lindane	0.08	91	103	0.001 - 1	0.9958	3.6	6.8
Heptachlor	0.17	89	94	0.001 - 1	0.9926	8.6	8.1
Aldrin	0.11	89	93	0.005 - 1	0.9879	8.8	10.1
Endosulfan I	0.18	95	93	0.005 - 1	0.9954	5.2	7.1
Endrin+p,p'-DDD	0.16	86	89	0.005 - 1	0.9938	8.6	9.5
p,p'-DDE	0.17	105	101	0.005 - 1	0.9894	7.3	9.8
Dieldrin	0.095	95	88	0.005 - 1	0.9871	6.2	11.5
Endosulfan II	0.065	92	94	0.005 - 1	0.9940	11.5	11.1
o,p'-DDD	0.051	106	101	0.005 - 1	0.9932	9.8	9.4
p,p'-DDT	0.39	110	98	0.05 - 1	0.9976	7.5	9.2
Methoxychlor	0.1	102	98	0.005 - 1	0.9979	6.8	6.5

Table 2. Comparison of limit of detection (LOD) and relative standard deviation (RSD%) of the present SPME-GC analysis based on MWCNTs-pPy coating for OCPs with other works.

Compound	References						
	Present work	[13]	[16]	[26]	[27] ^a	[27] ^b	[4] ^c
Lindane	0.08 ^d	0.3	0.25	3.8	5	0.2	0.34
	3.6 ^e	6	5.6	3.7	5.1	7.1	7.1
Heptachlor	0.17	1.6	0.27	2.7	10	-	0.32
	8.6	3	4.7	4.2	12.4	-	6.7
Endrin	0.16	0.6	0.125	3.7	51	-	3.4
	8.6	6	8.7	3.7	14.6	-	10.2
p,p'-DDD	0.16	-	0.095	-	2	-	-
	8.6	-	6.3	-	7.3	-	-
Aldrin	0.11	0.2	0.66	2.6	14	-	0.39
	8.8	3	9.6	3.9	35.3	-	8.1
p,p'-DDE	0.17	0.1	0.015	5.7	1	-	0.33
	7.3	8	9.1	5.7	15.3	-	9.6
Dieldrin	0.095	0.1	0.015	2.8	9	0.5	0.36
	6.2	12	9.1	3.8	11.5	7.7	8.9
Endosulfan II	0.065	0.1	0.051	3.6	18	1	1.41
	11.5	10	6.5	4.3	11.2	7.8	12.1
o,p'-DDD	0.051	-	0.24	-	-	-	-
	9.8	-	9.7	-	-	-	-
p,p'-DDT	0.39	0.1	0.26	3.7	13	-	0.34
	7.5	5	7.3	3.7	14.7	-	8.2
Endosulfan I	0.18	0.1	0.17	2.9	10	0.8	1.29
	5.2	4	8.3	4.3	10.8	5.8	11.2
Methoxychlor	0.1	-	0.048	-	-	-	0.26
	6.8	-	7.3	-	-	-	11.8

^a: Full scan MS^b: MS/MS^c: Membrane-protected micro-solid-phase extraction^d: The first row of figures for each compound indicates detection limit (ng mL⁻¹)^e: The second row of figures for each compound indicates RSD%

3.3. Real samples

To apply the proposed method in real analysis, four water samples were collected and stored in glass containers and stored at 4 °C. They were then subjected to the present SPME/GC method without any pre-treatment. The results found are shown in **Table 3**. None of the organochlorine

pesticides were detected in the samples collected from the campus of Shahid Bahonar University (SBUC) and Saadi village, but the two samples from Noogh and Zarand area were found to be contaminated. The analysis of real samples based on MWCNTs-PPy for determination OCPs by

Table 3. The OCPs analysis in real samples based on MWCNTs-PPy by SPME-GC procedure

Compound	Location			
	Noogh	Saadi	Zarand	SBUC
	Concentration (pg mL ⁻¹)			
Lindane	N.D	N.D	N.D	N.D
Heptachlor	N.D	N.D	N.D	N.D
Aldrin	N.D	N.D	N.D	N.D
Endrin + p,p'-DDD	N.D	N.D	N.D	N.D
o,p'-DDD	8.6	N.D	N.D	N.D
Dieldrin	N.D	N.D	N.D	N.D
Endosulfan I	65	N.D	54	N.D
p,p'-DDE	11	N.D	7.3	N.D
p,p'-DDT	N.D	N.D	N.D	N.D
Methoxychlor	N.D	N.D	N.D	N.D
Endosulfan II	8	N.D	6.1	N.D

N.D: not detected

4. Conclusions

The determination of organochlorine compounds from water samples was successfully performed by SPME-based electrodeposition of MWCNTs/PPy on stainless steel fiber, followed by GC-ECD analysis. The SPME-GC-ECD method is selective, sensitive, precise, reproducible and linear over a wide range. Due to the widespread use of the organochlorine pesticides until 1970's and the high persistence of these pollutants can still be detected some of these in the environment. The proposed method showed good reproducibility, wide linear range, low detection limit and good recovery for the various OCPs studied.

5. Acknowledgement

The authors thank from Department of Chemistry, Kerman Branch, Islamic Azad University, and Shahid Bahonar University of Kerman, Iran

6. References

- [1] R. Jayaraj, P. Megha, P. Sreedev, Review Article, Organochlorine pesticides, their toxic effects on living organisms and their fate in the environment, *Interdiscip.Toxicol.*, 9 (2016) 90-100.
- [2] A. Taghani, N. Goudarzi, G. Bagherian, Application of multiwalled carbon nanotubes for the preconcentration and determination of

- organochlorine pesticides in water samples by gas chromatography with mass spectrometry, *J. Sep. Sci.*, 39 (2016) 4219-4226.
- [3] R. Kumar, S. Mukherji, Threat posed by persistent organochlorine pesticides and their mobility in the environment, *Curr. Org. Chem.*, 22 (2017) 954-972.
- [4] A. A. Hassan, M. Sajid, H. Al Ghafly, Kh. Alhooshani, Ionic liquid-based membrane-protected micro-solid-phase extraction of organochlorine pesticides in environmental water samples, *Microchem. J.*, 158 (2020) 105295.
- [5] J.J. Jiménez, J.L. Bernal, M.J. del Nozal, C. Alonso, Liquid-liquid extraction followed by solid phase extraction for the determination of lipophilic pesticides in beeswax by gas chromatography electron capture detection and matrix matched calibration, *J. Chromatogr. A*, 1048 (2004) 89-97.
- [6] L. Chen, L. Ding, H. Jin, D. Song, H. Zhang, J. Li, K. Zhang, Y. Wang, H. Zhang, The determination of organochlorine pesticides based on dynamic microwave-assisted extraction coupled with on-line solid-phase extraction of high performance liquid chromatography, *Anal. Chim. Acta*, 589 (2007) 239-246.
- [7] X. Zang, G. Zhang, C. Wang, Z. Wang, Recent developments of dispersive liquid liquid microextraction technique, *Chinese J. Chromatogr.*, 33 (2015) 103-111.
- [8] A. Jain, K.K. Verma, Single-drop microextraction, in: *Liq. Extr.*, Elsevier, pp. 439-472, 2019.
- [9] M. Sajid, Porous membrane protected micro-solid-phase extraction: A review of features, advancements and applications, *Anal. Chim. Acta*, 965 (2017) 36-53.
- [10] M. Ghorbani, M. Aghamohammadhassan, M. Chamsaz, H. Akhlaghi, T. Pedramrad, Dispersive solid phase microextraction, *TrAC - Trends Anal. Chem.*, 118 (2019) 793-809.
- [11] N. Ochiai, K. Sasamoto, H. Kanda, S. Nakamura, Fast screening of pesticide multiresidues in aqueous samples by dual stir bar sorptive extraction-thermal desorption-low thermal mass gas chromatography-mass spectrometry, *J. Chromatogr. A*, 1130 (2006) 83-90.
- [12] R.G. Belardi, J. Pawliszyn, Application of chemically modified fused silica fibers in the extraction of organics from water matrix samples and their rapid transfer to capillary columns, *Water. Pollut. Res. J. Can.*, 24 (1989) 179-191.
- [13] X. Li, M. Zhong, J. Chen, Electrodeposited polyaniline as a fiber coating for solid-phase microextraction of organochlorine pesticides from water, *J. Sep. Sci.*, 31 (2008) 2839-2845.
- [14] A. Mehdinia, F. Bashour, F. Roohi, A. Jabbari, A. Saleh, Preparation and evaluation of thermally stable nano-structured self-doped polythiophene coating for analysis of phthalate ester trace levels, *J. Sep. Sci.*, 35 (2012) 563-570
- [15] K.C.D.P. Roux, E.F. Jasinski, J. Merib, M.L. Sartorelli, E. Carasek, Application of a robust solid-phase microextraction fiber consisting of NiTi wires coated with polypyrrole for the determination of haloanisoles in water and wine, *Anal. Methods*, 8 (2016) 5503-5510.
- [16] A. Mollahosseini, E. Noroozian, Polyphosphate-doped polypyrrole coated on steel fiber for the solid-phase microextraction of organochlorine pesticides in water, *Anal. Chim. Acta*, 638 (2009) 169-174.
- [17] Y. Jia, H. Su, Z. Wang, Y.-L.L.E. Wong, X. Chen, M. Wang, T.-W.W.D. Chan, Metal-organic framework@microporous organic network as adsorbent for solid-phase microextraction, *Anal. Chem.*, 88 (2016) 9364-9367.
- [18] A. Gutiérrez-Serpa, P.I. Napolitano-Tabares, V. Pino, F. Jiménez-Moreno, A.I. Jiménez-Abizanda, Silver nanoparticles supported onto a stainless steel wire for direct-immersion solid-phase microextraction of

polycyclic aromatic hydrocarbons prior to their determination by GC-FID, *Microchim. Acta*, 185 (2018) 341.

- [19] A. Gutiérrez-Serpa, P. Rocío-Bautista, V. Pino, F. Jiménez-Moreno, A.I. Jiménez-Abizanda, Gold nanoparticles based solid-phase microextraction coatings for determining organochlorine pesticides in aqueous environmental samples, *J. Sep. Sci.*, 40 (2017) 2009–2021.
- [20] M. Sajid, C. Basheer, Layered double hydroxides: Emerging sorbent materials for analytical extractions, *TrAC, Trends Anal. Chem.*, 75 (2016) 174-182
- [21] B.B. Prasad, A. Srivastava, M.P. Tiwari, Highly sensitive and selective hyphenated technique (molecularly imprinted polymer solid-phase microextraction-molecularly imprinted polymer sensor) for ultra trace analysis of aspartic acid enantiomers, *J. Chromatogr. A*, 1283 (2013) 9-19.
- [22] J. Lu, J. Liu, Y. Wei, K. Jiang, S. Fan, J. Liu, G. Jiang, Preparation of single-walled carbon nanotube fiber coating for solid-phase microextraction of organochlorine pesticides in lake water and wastewater, *J. Sep. Sci.*, 30 (2007) 2138-2143.
- [23] M.M. Abolghasemi, V. Yousefi, M. Piryaeei, Synthesis of carbon nanotube/layered double hydroxide nanocomposite as a novel fiber coating for the headspace solid-phase microextraction of phenols from water samples, *J. Sep. Sci.*, 38 (2015) 1344-1350.
- [24] H. Assadollahzadeh, E. Noroozian, Sh. Maghsoudi, Solid phase microextraction of phthalate esters from aqueous media by electrochemically deposited carbon nanotube/polypyrrole composite on a stainless steel fiber, *Anal. Chim. Acta*, 669 (2010) 32-38.
- [25] J. Pawliszyn, *Solid Phase Microextraction: Theory and Practice*, Wiley-VCH, USA, 1997.
- [26] J.P. Pérez-Trujillo, S. Frías, M.J. Sánchez, J.E. Conde, M.A. Rodríguez-Delgado, Determination of organochlorine pesticides by gas chromatography with solid-phase microextraction, *Chromatographia*, 56 (2002) 191-197.
- [27] C. Gonçalves, M.F. Alpendurada, Solid phase microextraction gas chromatography-(tandem) mass spectrometry as a tool for pesticide residue analysis in water sample at high sensitivity and selectivity with confirmation capabilities, *J. Chromatogr. A*, 1026 (2004) 239-250.



Dispersive solid phase extraction using graphitic carbon nitride microparticles for the determination of trace amounts of lead in water samples

Ehsan Zolfonoun ^{a,*}

^a Nuclear Fuel Cycle Research School, Nuclear Science and Technology Research Institute, Tehran, Iran

ARTICLE INFO:

Received 6 Sep 2020

Revised form 10 Nov 2020

Accepted 28 Nov 2020

Available online 30 Dec 2020

Keywords:

Lead, Graphitic carbon nitride, Water, Ultrasound-assisted dispersive micro-solid phase extraction, Inductively coupled plasma- optical emission spectroscopy

ABSTRACT

In this work, ultrasound-assisted dispersive micro-solid phase extraction (USA-D- μ SPE) technique using graphitized carbon nitride ($g-C_3N_4$) is proposed for the preconcentration of low level of lead in aqueous samples. In this method, microparticles of graphitized carbon nitride sorbent were dispersed in the samples using ultrasonic bath and Pb(II) ions were directly adsorbed on the surface of $g-C_3N_4$ particles. After adsorption and desorption of lead ions from $g-C_3N_4$ particles, the Pb concentration was determined by the inductively coupled plasma- optical emission spectroscopy (ICP-OES). The main advantages of this method are high speed, simplicity and cheapness. The effects of pH, sorbent amount, eluent type and time on the recovery of the analyte were investigated. Under the optimized conditions and preconcentration of 10 mL of sample, the detection limit of $1.24 \mu\text{g L}^{-1}$ was obtained. The results were validated by standard reference materials (NIST, SRM) and spiking of real samples by USA-D- μ SPE procedure.

1. Introduction

With the development of various industries over the past decades and increasing the amount of pollutants entering the environment, the amount of heavy metals in soil and water increased [1]. Most of these heavy metals are not only environmentally destructive but also healthily hazardous even at trace levels. Lead is one of the most hazardous elements to human health. Metabolic poisoning, enzyme inhibition and nervous connection damages are the most important toxic effects of lead on human [2]. The first step in reducing or eliminating this metal is its accurate measurement. For this purpose,

various analytical techniques have been developed [3-5]. In all of the reported analytical techniques, sample preparation (separation and preconcentration) step is needed prior to instrumental analysis. Among different sample preparation methods, solid phase extraction is the most common one due to its unique features such as simplicity, low cost, high recoveries and low consumption of organic solvents [6,7]. Dispersive micro solid phase extraction (D- μ -SPE) is a new version of solid phase extraction (SPE) which simultaneously possesses the advantages of both dispersive liquid-liquid micro-extraction and solid phase extraction [8]. In this method a mixture of sorbent particles and carrier is injected to the aqueous sample. After formation of cloudy solution, extraction can be achieved within a few seconds because of the large surface area

*Corresponding author: [Ehsan Zolfonoun](mailto:Ehsan.Zolfonoun@aeoi.org.ir)

Email: ezolfonoun@aeoi.org.ir

<https://doi.org/10.24200/amecj.v3.i04.118>

between extraction sorbent and aqueous phase [9]. Recently, D- μ -SPE has received much attention in analytical chemistry because it is a simple, fast and inexpensive method [11,12]. One of the most important parameters that affect the performance of this method is the type of sorbent [12]. The advantages of using nanoparticles as sorbent in D- μ -SPE have been demonstrated in recent reports [13-15]. Unique size and desirable physicochemical properties of nanoparticles have made them suitable options for improving DSPE method. Among different nanosorbents, cheaper and more stable ones such as graphene and carbon nanotubes have been used more frequently [16-18]. Graphitic carbon nitride (g-C₃N₄) is a non-toxic analogue of graphene which is very stable and inexpensive and has suitable band structure, easy synthesis method and unique physicochemical properties [19,20]. It has a 2D layered structure (2D sheets of tri-s-triazine connected via tertiary amines) and is synthesized from various simple and green nitrogen rich precursors such as melamine, thiourea, urea, cyanamide [21]. Due to the hydrophobicity, large π -conjugated structure and polar functional groups, g-C₃N₄ can be a suitable and ecofriendly candidate for conventional sorbents in extraction methods [22].

In the current study, we propose a simple, fast and ligandless preconcentration technique based on ultrasound-assisted dispersive micro-solid phase extraction (USA-D- μ SPE) using graphitic carbon nitride for the determination of lead by inductively coupled plasma-optical emission spectrometry.

2. Experimental

2.1. Reagents and materials

All chemicals used in this work were of analytical grade. All aqueous solutions were prepared in double-distilled deionized water (Milli-Q system, Millipore, USA). Pb(II) stock solution was supplied by Merck (Darmstadt, Germany). The standard solution of lead (Pb²⁺) was purchased with a concentration of 1000 mg L⁻¹ in 1 % HNO₃. Another concentration of lead was daily prepared by dilution of the standard lead solution with DW. Ultrapure water was purchased from Millipore Company.

The g-C₃N₄ was synthesized according to the previously reported method. The syntheses of graphitic carbon nitrides (g-C₃N₄) by heating at 300-600 °C of a mixture of melamine with the formula C₃H₆N₆ and uric acid (C₅H₄N₄O₃) in the presence of crystalline form of alumina (Al₂O₃) has been reported. Alumina favored the deposition of the graphitic carbon nitrides layers on the exposed surface [19].

2.2. Instrumentation

A Perkin Elmer inductively coupled plasma optical emission spectroscopy (ICP-OES, Optima 7300 DV) equipped with a charge-coupled device detector (CCD) and a cyclonic spray chamber with a concentric nebulizer was used for the determination of the target element. The detection wavelength for lead was 220.353 nm. A Metrohm model 744 digital pH meter, equipped with a combined glass-calomel electrode, was employed for the pH measurements. An ultrasonic water bath with temperature control (Tecno-Gaz SpA, Italy) was applied to disperse of adsorbent particles in aqueous solution. The centrifuge accessory based on the rotor with high speed (speed 2000-30.000 rpm x g, Sigma 3K30 centrifuge, UK) was used for separation nanoparticles from water samples. For sampling, all glass tubes were cleaned with a 1.0 mol L⁻¹ HNO₃ solution for 24 h and washed 10 times with DW. The water prepared and stored by standard method for sampling from water by adding nitric acid to waters.

2.3. On-line extraction procedure

Due to **Figure 1**, 6.0 mg of g-C₃N₄ was added to 10 mL of water sample or standard solution and sonicated by an ultrasonic bath for 5 min. The chemical and physical adsorption of lead ions carried out by g-C₃N₄ at optimized pH. The covalence bonding between nitrate and Pb cause to increase extraction efficiency in water samples. After extraction of lead ions with g-C₃N₄, the solution was then centrifuged for 5 min at 5,000 rpm, and the aqueous phase was removed. The preconcentrated target analyte was eluted using 1.0 mL of a 1 mol L⁻¹ solution of HNO₃. Finally, the concentration of Pb(II) in acidic aqueous phase was determined by ICP-

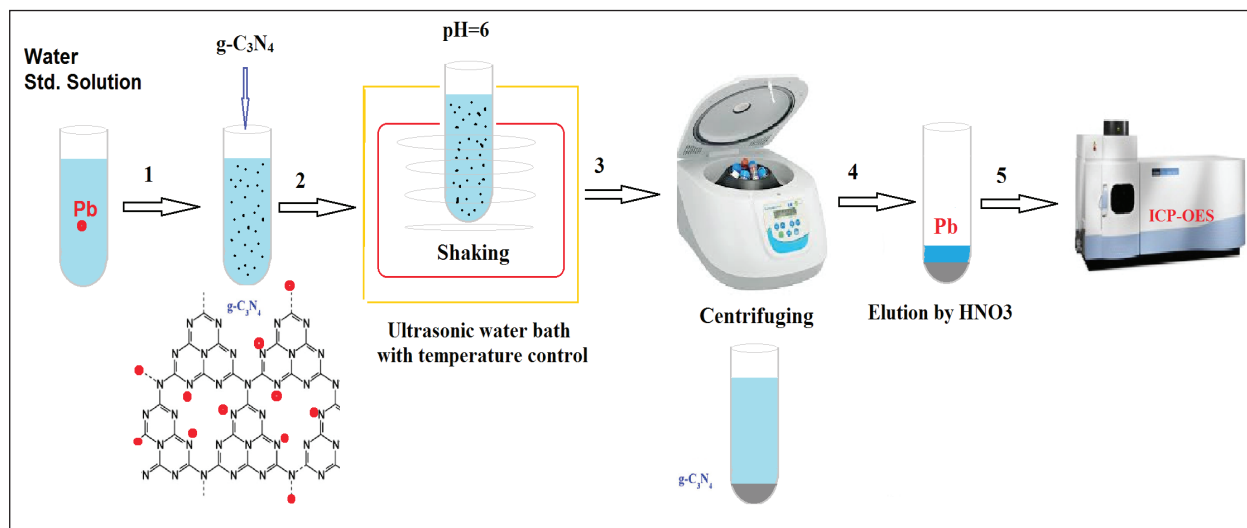


Fig.1. On-line extraction procedure for lead extraction by g-C₃N₄ particles

OES. The proposed procedure developed based on g-C₃N₄ nanostructure with lower and upper limit quantification (5.0–600 µg L⁻¹) for lead analysis in water and standard samples by ultrasound-assisted dispersive micro-solid phase extraction (USA-D-µSPE).

3. Results and discussion

The USA-D-µSPE procedure based on g-C₃N₄ as adsorbent was used for the extraction and separation of lead ions in water samples. In order to obtain the favorite lead speciation with high extraction, the analytical parameters such; pH, the amount of adsorbent, the sonication time, the eluent type and interference ions must be optimized.

3.1. Effect of pH

The pH of the sample solution is one of the most important factors in metal–adsorbent interaction in the SPE procedure. The effect of pH on the extraction of Pb(II) by g-C₃N₄ was studied in the range of 3.0–8.0 using nitric acid or sodium hydroxide. The results in **Figure 2** show that the adsorption of Pb(II) is maximum in the pH range of 6.0 to 7.5. So, pH 6.0 was chosen as the optimum value. The mechanism of extraction of lead achieved based on the coordination of covalent bond of N in g-C₃N₄ with the positively charged inorganic lead (Pb²⁺), which is highly dependent on pH (Pb→:N-C).

3.2. Effect of g-C₃N₄ amount

The effect of amount of g-C₃N₄ on the quantitative extraction of Pb(II) was examined in the range of 1–10 mg by ultrasound-assisted dispersive micro-solid phase extraction (USA-D-µSPE). The results are shown in **Figure 3**. The obtained results revealed that by increasing the sorbent amounts from 1 up to 6 mg, due to increasing accessible sites, the extraction efficiency increased and after that remained constant. Hence, the subsequent extraction experiments were carried out with 6 mg of g-C₃N₄.

3.3. Effect of sonication time

By USA-D-µSPE procedure, the sonication time is one of the main factors influencing the target analytes extraction. By favorite time for solid dispersion in liquid phase, the mass-transference was increased and so, the efficient extraction of lead based on the g-C₃N₄ was obtained in water samples. The effect of the sonication time on the extraction and recovery of Pb(II) was studied in the range of 1–20 min. The obtained results indicated that there was no significant effect on the extraction efficiency when the ultrasonication time increased from 5 to 20 min. So, an ultrasonication time of 5 min was selected for the entire procedure.

3.4. Effect of eluent type

The kind and value of elution for back extraction lead ions from g-C₃N₄ were optimized at pH=6.

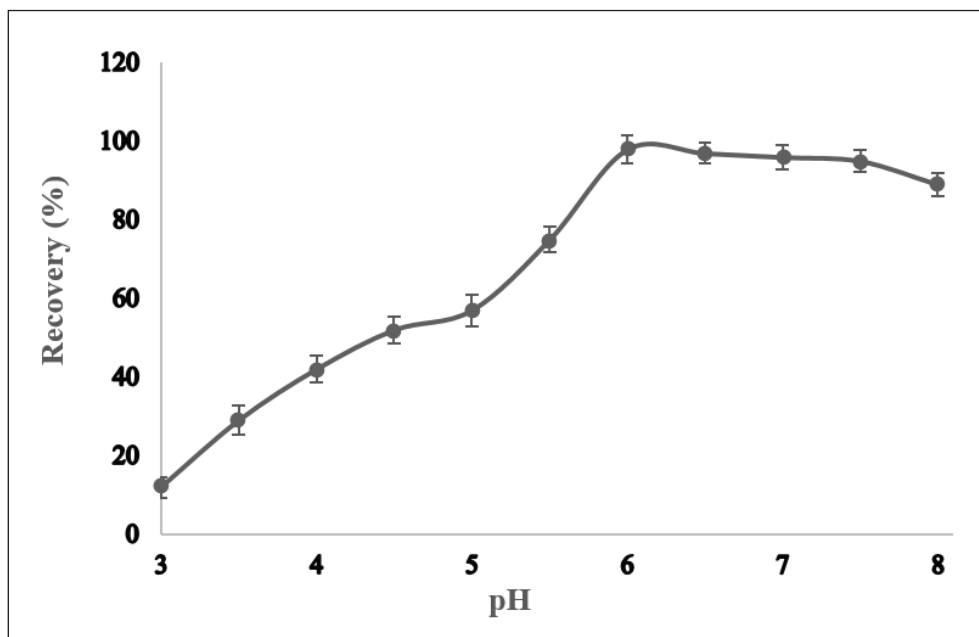


Fig. 2. Effect of pH on the recovery of Pb(II). Conditions: g-C₃N₄ amount, 10 mg; concentration of analyte, 50 $\mu\text{g L}^{-1}$.

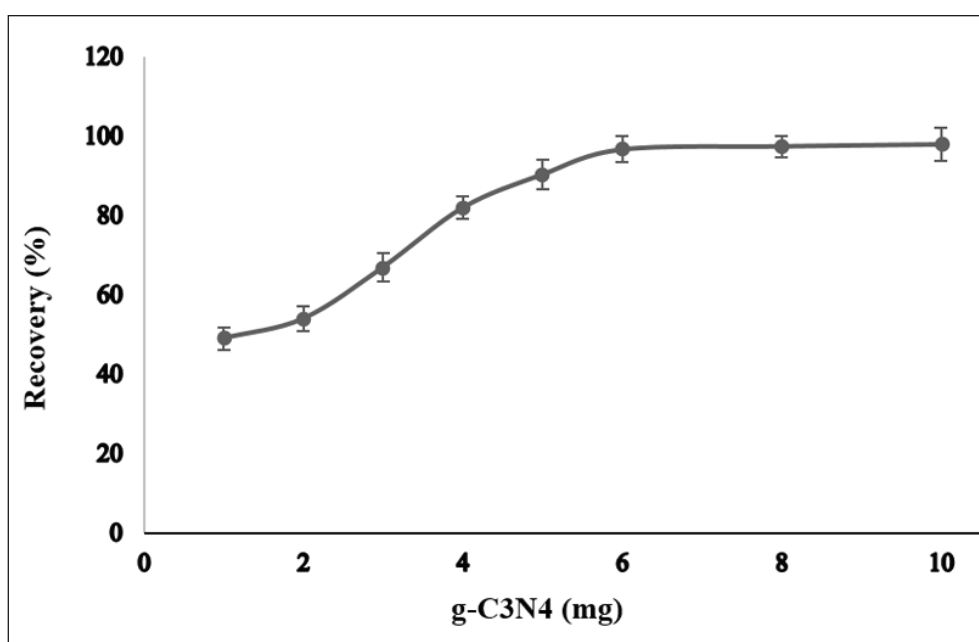


Fig. 3. Effect of the g-C₃N₄ amount on the recovery of Pb(II). Conditions: pH, 6.0; concentration of analyte, 50 $\mu\text{g L}^{-1}$.

Low pH caused to dissociate N-lead bonding and release the Pb (II) into the liquid phase. So, a different acid solution such as HCl, HNO₃, H₂SO₄, and CH₃COOH with different concentration was used for back extraction Pb(II) in blood samples (0.5-3 mol L⁻¹) by USA-D- μ SPE procedure. In order to

find the best eluent, different mineral acids were examined as stripping agents. The results revealed that among the tested eluents, nitric acid was the superior stripping agent for the quantitative elution of Pb(II). Therefore, HNO₃ solution was selected for Pb(II) desorption. The effect of nitric acid con-

centration on the recovery of the adsorbed analyte was studied in the range of 0.1 to 3 mol L⁻¹. Based on the obtained results, 1.0 mol L⁻¹ HNO₃ was sufficient for complete desorption of the target analyte from the sorbent surface (Fig.4).

3.5. Effect of diverse ions on the recovery

In order to evaluate the analytical applicability of the developed method, the effect of commonly occurring ions in natural water samples on the extraction and determination of lead was studied. In these experiments, 10 mL of sample solutions containing 50.0 µg L⁻¹ of Pb(II) and various amounts of interfering ions were treated according to the recommended procedure. Tolerable limit was set as the highest amount of foreign ions which cause an approximately ± 5 % relative error in the determination of the analyte. The results showed that

40,000-fold Li⁺, Na⁺, K⁺, Cl⁻, NO₃⁻; 20,000-fold Ca²⁺, Mg²⁺, Ba²⁺, Sr²⁺, 400-fold Ag⁺, Cd²⁺, Co²⁺, Zn²⁺, Mn²⁺, 200-fold Fe³⁺, Ni²⁺, Cr³⁺, Ce³⁺, and 100-fold Al³⁺, Cu²⁺, Hg²⁺ ions had no significant influence on the extraction and determination of Pb(II).

3.6. Analytical figures of merit

The analytical parameters of the proposed are summarised in Table 1. Linear working range of the method for determination of Pb(II) was found to be 5.0–600 µg L⁻¹. The limit of detection (LOD) of the proposed method was calculated as three times the standard deviation of 10 measurements of the blank solution over the slope of the calibration curve. The LOD for the determination of Pb(II) was found to be 1.24 µg L⁻¹. The relative standard deviation (R.S.D) of the proposed method for determination of 50.0 µg L⁻¹ Pb(II) (n= 10) was 2.3 %.

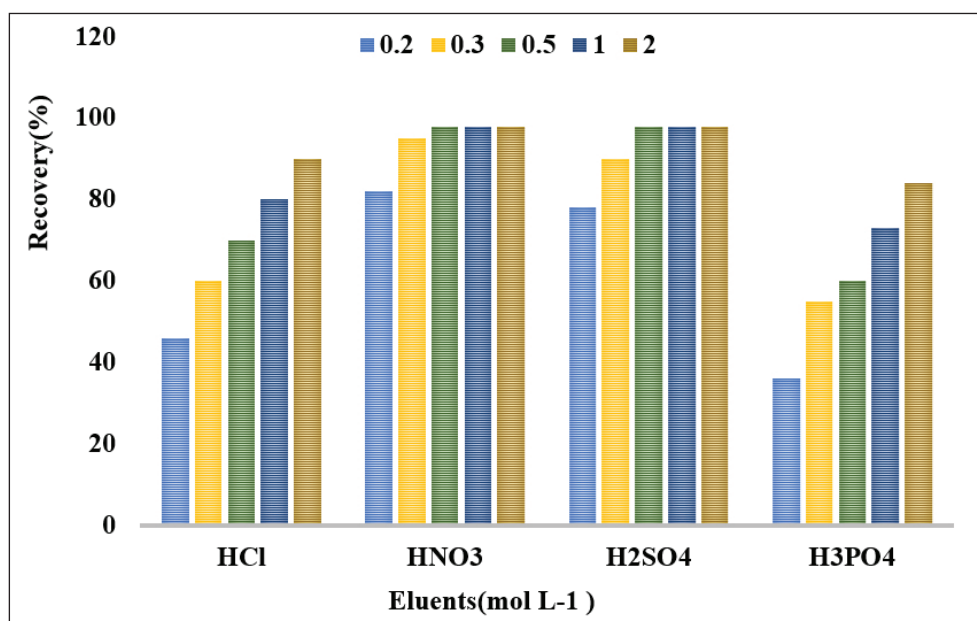


Fig.4. The effect of eluents on lead extraction based on g-C₃N₄ particles by USA-D-µSPE procedure

Table 1. Analytical parameters of the proposed method

Parameter	Analytical feature
Linear range (µg L ⁻¹)	5.0–600
r ²	0.998
LOD (ng L ⁻¹)	1.24
R.S.D. % (n = 10)	2.3
Enrichment factor	10

3.7. Application

The developed method was applied to find the amount of Pb(II) in tap water, well water and river water samples by USA-D- μ SPE procedure. The analytical results, along with the recovery for the spiked samples, are given in **Table 2**. The recovery values calculated for the spiked samples were in the range of 94–105 %. The results demonstrated that the UA-D- μ SPE can be used as a reliable sample treatment technique for extraction and determination of Pb(II) in real samples. Moreover, the standard reference materials (NIST; SRM) were used for validating of proposed procedure by g-C₃N₄ nanostructure in water and urine samples (**Table 3**).

4. Conclusions

Apreconcentration technique based on ultrasound-assisted micro-solid phase extraction using graphitic carbon nitride microparticles was developed for the extraction and preconcentration of Pb(II) from aqueous samples, prior to ICP-OES determination. In the proposed method there is no need to use any chelating agent. The obtained results indicate that the proposed method gives a high enhancement factor and low LOD and can be used for the preconcentration and determination of lead in real water samples.

5. Acknowledgements

The authors wish to thank Nuclear Fuel Cycle Research School, Nuclear Science and Technology Research Institute, Tehran, Iran

Table 2. Recovery of lead from water samples based on g-C₃N₄ particles by USA-D- μ SPE procedure

Sample	Added ($\mu\text{g L}^{-1}$)	Found ($\mu\text{g L}^{-1}$)	Recovery (%)
Tap water	0.0	<LOD	–
	10.0	10.2 (2.5) ^a	102
Well water	0.0	5.1 (3.2)	–
	10.0	14.5 (3.0)	94
River water	0.0	4.3 (2.9)	–
	10.0	14.8 (2.6)	105

^a Values in parentheses are R.S.D.s based on three replicate analyses

Table 3. Validation of USA-D-SPE procedure in water by standard reference materials (SRM, NIST)

Sample	SRM ($\mu\text{g L}^{-1}$)	Added ($\mu\text{g L}^{-1}$)	Found* ($\mu\text{g L}^{-1}$)	Recovery (%)
^a SRM1643d	18.2 \pm 0.6	-----	17.4 \pm 0.9	-----
		15.0	31.9 \pm 1.4	96.6
^b SRM 2668	137.9 \pm 3.6	-----	138.6 \pm 6.5	-----
		150.0	287.7 \pm 11.4	99.4

*Mean of three determinations of samples \pm SD (P = 0.95, n = 10)

^aSRM1643d, trace element in water

^bSRM 2668, Human Freeze-Dried Urine, level (II), $\mu\text{g L}^{-1}$

6. References

- [1] E.L. Silva, P.d.S. Roldan, Simultaneous flow injection preconcentration of lead and cadmium using cloud point extraction and determination by atomic absorption spectrometry, *J. Hazard. Mater.*, 161 (2009) 142-147.
- [2] W.I. Mortada, A.M. Abdelghany, Preconcentration of Lead in Blood and Urine Samples Among Bladder Cancer Patients Using Mesoporous Strontium Titanate Nanoparticles, *Biol. Trace Elem. Res.*, 193 (2020) 100-110.
- [3] P.K. Tewari, A.K. Singh, Preconcentration of lead with Amberlite XAD-2 and Amberlite XAD-7 based chelating resins for its determination by flame atomic absorption spectrometry, *Talanta*, 56 (2002) 735-744.
- [4] F. Shah, T.G. Kazi, Naemullah, H.I. Afridi, M. Soylak, Temperature controlled ionic liquid-dispersive liquid phase microextraction for determination of trace lead level in blood samples prior to analysis by flame atomic absorption spectrometry with multivariate optimization, *Microchem. J.*, 101 (2012) 5-10.
- [5] S.R. Yousefi, F. Shemirani, Development of a robust ionic liquid-based dispersive liquid-liquid microextraction against high concentration of salt for preconcentration of trace metals in saline aqueous samples: Application to the determination of Pb and Cd, *Anal. Chim. Acta*, 669 (2010) 25-31.
- [6] K. Saberyan, E. Zolfonoun, M. Shamsipur, M. Salavati-Niasari, Separation and preconcentration of trace gallium and indium by Amberlite XAD-7 resin impregnated with a new hexadentates naphthol-derivative Schiff base, *Sep. Sci. Technol.*, 44 (2009) 1851-1868.
- [7] V.O. Vasylechko, G.V. Gryshchouk, M.I. Kaminska, B.M. Stel'makhovych, A solid-phase extraction method using acid-modified Transcarpathian clinoptilolite for preconcentration of trace amounts of lead in water samples, *Appl. Nanosci.*, 9 (2019) 1057-1065.
- [8] A. Chisvert, S. Cárdenas, R. Lucen, Dispersive micro-solid phase extraction, *TrAC-Trends Anal. Chem.*, 112 (2019) 226-233.
- [9] S.M. Yousefi, F. Shemirani, S.A. Ghorbanian, Deep eutectic solvent magnetic bucky gels in developing dispersive solid phase extraction: Application for ultra trace analysis of organochlorine pesticides by GC-micro ECD using a large-volume injection technique, *Talanta* 168 (2017) 73-81.
- [10] T. Khezeli, A. Daneshfar, Development of dispersive micro-solid phase extraction based on micro and nano sorbents, *TrAC-Trends Anal. Chem.*, 89 (2017) 99-118.
- [11] M. Krawczyk, M. Jeszka-Skowron, Multiwalled carbon nanotubes as solid sorbent in dispersive micro solid-phase extraction for the sequential determination of cadmium and lead in water samples, *Microchem. J.*, 126 (2016) 296-301.
- [12] A.A. Asgharinezhad, H. Ebrahimzadeh, F. Mirbabaei, N. Mollazadeh, N. Shekari, Dispersive micro-solid-phase extraction of benzodiazepines from biological fluids based on polyaniline/magnetic nanoparticles composite, *Anal. Chim. Acta*, 844 (2014) 80-89.
- [13] J. Wang, Z. Chen, Z. Li, Y. Yang, Magnetic nanoparticles based dispersive micro-solid-phase extraction as a novel technique for the determination of estrogens in pork samples, *Food Chem.*, 204 (2016) 135-140.
- [14] E. Zolfonoun, Solid phase extraction and determination of indium using multiwalled carbon nanotubes modified with magnetic nanoparticles, *Anal. Method Environ. Chem. J.*, 1 (2008) 5-10.
- [15] F. Aydin, E. Yilmaz, E. Ölmez, M. Soylak, Cu₂O-CuO ball like/multiwalled carbon nanotube hybrid for fast and effective ultrasound-assisted solid phase extraction of uranium at ultra-trace level prior to ICP-MS detection, *Talanta*, 207 (2020) 120295.

- [16] E. Zolfonoun, Spectrofluorometric determination of L-tryptophan after preconcentration using multi-walled carbon nanotubes, *Anal. Method Environ. Chem. J.*, 2 (2019) 43-48.
- [17] M. Alvand, F. Shemirani, Fabrication of Fe_3O_4 @graphene oxide core-shell nanospheres for ferrofluid-based dispersive solid phase extraction as exemplified for Cd(II) as a model analyte, *Microchim. Acta*, 183 (2016) 1749-1757.
- [18] S.M. Yousefi, F. Shemirani, Carbon nanotube-based magnetic bucky gels in developing dispersive solid-phase extraction: application in rapid speciation analysis of Cr(VI) and Cr(III) in water samples, *Int. J. Environ. Anal. Chem.*, 97 (2017) 1065-1079.
- [19] N. Xu, Y. Wang, M. Rong, Z. Ye, Z. Deng, X. Chen, Facile preparation and applications of graphitic carbon nitride coating in solid-phase microextraction, *J. Chromatogr. A*, 1364 (2014) 53-58.
- [20] J. Yang, L. Si, S. Cui, W. Bi, Synthesis of a graphitic carbon nitride nanocomposite with magnetite as a sorbent for solid phase extraction of phenolic acids, *Microchim. Acta*, 182 (2015) 737-744.
- [21] J. Liu, T. Zhang, Z. Wang, G. Dawson, W. Chen, Simple pyrolysis of urea into graphitic carbon nitride with recyclable adsorption and photocatalytic activity, *J. Mater. Chem.*, 21 (2011) 14398-14401.
- [22] H.B. Zheng, J. Ding, S.J. Zheng, G.T. Zhu, B.F. Yuan, Y.Q. Feng, Facile synthesis of magnetic carbon nitride nanosheets and its application in magnetic solid phase extraction for polycyclic aromatic hydrocarbons in edible oil samples, *Talanta*, 148 (2016) 46-53.



Determination and investigation of heavy metal concentrations in sediments of the Persian Gulf coasts and evaluation of their potential environmental risk

Hoda Allami^a, Afsaneh Afzali^{a,*} and Rouhollah Mirzaei^a

^aDepartment of Environment, Faculty of Natural Resources and Earth Sciences, University of Kashan, Kashan, Iran

ARTICLE INFO:

Received 22 Aug 2020

Revised form 20 Oct 2020

Accepted 15 Nov 2020

Available online 30 Dec 2020

Keywords:

Heavy metals,
Analysis,
Sediments of the Persian Gulf coasts,
Flame/electrothermal atomic
absorption spectrometry,
Environmental risk

ABSTRACT

The contamination of coastal sediments with toxic heavy metals caused to a serious concern due to their environmental consequences. The aim of this study was to determine the concentration of heavy metals such as lead (Pb), copper (Cu), nickel(Ni) and manganese (Mn) in the sediments of the Persian Gulf coast in Kangan and Siraf ports in Bushehr province. In this regard, the sampling was performed in 10 stations with different uses in two depths of 0-5 and 5-20 cm along the coast of the Persian Gulf. The concentration of heavy metals was measured after drying, acid digestion and microwave by using flame atomic absorption spectrometry (F-AAS). Ecological risk index was used to assess the potential of environmental risk due to heavy metal pollution in the coastal sediments of the study area and the sensitivity of the biological community to toxic substances. Then statistical analysis in SPSS environment was used for analyzing the data. The results showed that the average concentrations of Mn(II), Ni(II), Cu(II) and Pb(II) was measured 121.47, 11.51, 11.59 and 5.30 in surface sediments, and 131.59, 10.81, 12.56 and 4.88 $\mu\text{g g}^{-1}$ in deep sediments. The results of the ecological risk index with the value of less than 150, showed a low environmental risk of heavy metals detected in the region. Also, the results of multivariate statistical analyzes indicated the existence of a correlation and common origin of Cu, Ni and Mn. In general, this study led to a better understanding of the contamination of heavy metals in the region and considered it necessary to try to prevent, control and reduce the amount of pollution in the sediments of the Persian Gulf coast. All analysis validated by electrothermal atomic absorption spectrometry(ET-AAS) after dilution samples with DW.

1. Introduction

Heavy metals as the inorganic pollutants are considered as one of the serious threats in natural ecosystems due to their non-degradability, the

environmental stability, the toxicity to various aquatic species and biological magnification [1]. Heavy metal pollution results from rapid urbanization and human activities including electricity generation, transportation, fossil fuel combustion, use of various chemicals, and other related activities [2, 3]. Heavy metals are metals with a specific density of less than 5 g cm^{-2} [4]. In the

*Corresponding Author: [Afsaneh Afzali](mailto:Afsaneh.Afzali@kashanu.ac.ir)

Email: a.afzali@kashanu.ac.ir

<https://doi.org/10.24200/amecj.v3.i04.122>

aquatic ecosystem, a number of metals such as Zn, Fe, Mn and Ni are required for the activity of biological systems. For example, diseases such as skin diseases are the result of removing essential elements such as zinc from the diet of living beings. However, the high concentrations of heavy metals can be toxic to human organisms. While some heavy metals such as; Cd, Ni, Hg, and Pb are not essential for the activity of biological systems, their presence in aquatic ecosystems causes toxicity to living organisms [5]. Also, some metals such as Pb have caused the most concern due to their toxic and carcinogenic properties. In addition, due to the fact that the amount of Pb that enters the environment through human activities is higher than the Pb that enters the environment from natural sources, the high concentration of this metal in the environment can be considered as an indicator of the level of pollution caused by human activities in the region [6]. Coastal areas are the point of connection between land and ocean, which are more important than other marine habitats due to their ecological sensitivity to pollutants, transmission of contaminants in the food chain and poisoning of living organisms [7]. Since the beginning of the industrial revolution and the subsequent increase in industry growth, the large amounts of toxic pollutants have been discharged into the coastal environment, causing metal pollution of the sediments. Heavy metals in the coastal environment originate from two natural and human sources [1, 3]. Metal contaminants in coastal sediments are precipitated by adsorption, hydrolysis, and co-sedimentation, while a small fraction of free metal ions remain in the water column. However, when environmental conditions such as pH change, the metals in the sediment enter the water, as a result, the sediments can also act as a secondary source of metals [8]. Since more than 90% of heavy metal pollution entering the marine ecosystem originates from terrestrial sources [9], the coastal sediments are often referred to as heavy metal reservoirs or inlets [9]. Some researchers have been performed to investigate and identify the

concentration of heavy metals and evaluation of their potential environmental risk on the coastal area i.e on the coastal sediments of Kerala, India [6], on the surface sediments along the southeast coast of the Caspian Sea [10], on surface sediments of the Sobi Shoal, China [11] and on the coastal sediments of northern part along the Persian Gulf [3]. The results of environmental risk index in the study of Arfaeinia et al. (2019) on coastal sediments of the Persian Gulf showed that the industrial, agricultural, urban and natural areas are in the category of very high, considerable, moderately and low environmental risk levels, respectively. Due to the lack of data on the abundance and distribution of heavy metals in sediments of the coastal areas of the world, especially the Persian Gulf coast, and the possible consequences of these pollutions, especially their negative impact on marine ecosystem and the life of living things, further studies on the extent of heavy metal pollution are necessary. The different techniques such as; flame atomic absorption spectrometry (F-AAS), inductively coupled plasma-atomic emission spectrometry (ICP-AES), inductively coupled plasma spectrometry (ICP), inductively coupled plasma mass spectrometry (ICP-MS), electrothermal atomic absorption spectrometry (ETAAS) and others were used for determination heavy metals in water, industrial wastewater and sediment samples. As difficulty matrixes in biological, industrial wastewater and sediment samples sample preparation based on solid phase extraction(SPE) or liquid-liquid extraction (LLE) and microwave digestion/acid digestion was used before determination of heavy metals by instruments.

The coast of the Persian Gulf in the south of Iran, due to its high biodiversity, rich natural resources, warm climate and natural attractions, attracts millions of tourists annually. Consequently, the discharge of municipal and industrial wastewater has caused the presence of various pollutants, including heavy metals in the sediments of this area the objective of this study is to measure the concentration of heavy metals in the coasts

of the Persian Gulf i.e Kangan and Siraf ports to estimate the extent of heavy metal pollution and evaluation of their potential environmental risk in the region. All heavy metals were determined by microwave digestion/acid digestion coupled to F-AAS.

2. Experimental

2.1. Instrumental

Determination of lead (Pb), copper (Cu), nickel(Ni) and manganese (Mn) was performed with a flame atomic absorption spectrometer (F-AAS), with an air-acetylene flame, was used for determination in surface and deep sediments samples (GBC, model plus 932, Aus). Copper based on wavelength 324.7 nm, slit 0.5 nm, lamp current 3.0 mA (1-5 mg L⁻¹), lead based on wavelength 217.0 nm, slit 1.0 nm, lamp current 5.0 mA (2.5-20 mg L⁻¹), nickel with wavelength 232.0 nm, slit 0.2 nm, lamp current 4.0 mA (1.8-8 mg L⁻¹) and manganese by wavelength 279.8 nm, slit 0.2 nm, lamp current 5.0 mA (1-36 mg L⁻¹) were selected. The spectra GBC electrothermal atomic absorption spectrometer (ET-AAS, Plus 932, Australia) using a graphite furnace module (GF3000, GBC) was used for validation of results. The operating parameters for the metal of interest were set as recommended by the manufacturer book. The

light of hollow cathode lamp (GBC) adjusted on the furnace tube or burner. All samples were performed using sample volumes of 20 µL and 1000-2000 µL by auto-sampler for ET-AAS and F-AAS, respectively. The instrumental conditions and temperature programming for the graphite atomizer are listed in **Table 1a and 1 b**.

2.2. Reagents

All reagents were of analytical grade from Merck Germany. The lead (Pb), copper (Cu), nickel(Ni) and manganese (Mn) stock solution was prepared from an appropriate amount of the nitrate salt of this analyte as 1,000 mg L⁻¹ solution in 0.01 mol L⁻¹ HNO₃ (Merck). Standard solutions were prepared daily by dilution of the stock solution. Ultrapure water (18 MΩ.cm) was obtained from Millipore Continental Water System (Bedford, USA).

2.3. Area of study

Persian Gulf is a border and semi-enclosed sea with an area of about 226,000 square kilometers, which is located at latitude 24° to 30° 30' north latitude and 48° to 56° 25' east longitude surrounded by the land. This sea has a dry and subtropical climate with a minimum water exchange and an average depth of 35-40 meters. Various factors such as limited circulation, shal-

Table 1a. Instrumental conditions for heavy metal determination by F-AAS

Parameters	Cu	Pb	Mn	Ni
Wavelength (nm)	324.7 nm	217.0 nm	279.8 nm	232.0 nm
Slit (nm)	0.5 nm	1.0 nm	0.2 nm	0.2 nm
Lamp current (mA)	3.0 mA	5.0 mA	5.0 mA	4.0 mA
Injection mode	Automatic	Automatic	Automatic	Automatic
Working range (mg L ⁻¹)	1-5	2.5-20	1-36	1.8-8
Mode	Peak integration	Peak integration	Peak integration	Peak integration

Table 1b. Temperature programming for heavy metal determination by ET-AAS

Step	Temperature Cu (°C)	Temperature Pb (°C)	Temperature Mn (°C)	Temperature Ni (°C)	Ramp time (s)	Hold time (s)	Ar flow rate (mL min ⁻¹)
Drying	120	120	130	130	20	10	300
Ashing	800	400	700	900	40	10	300
Atomization	2300	2000	2400	2400	1	2	0.0
Cleaning	2500	2200	2600	2600	1	3	300

low depth, high water temperature and salinity have caused the Contaminants remain stable in this area for a long time. Kangan port with a population of 60187 people is located in the south of Bushehr province and on the coast of the Persian Gulf. Kangan city is the place implementation of a large part of South Pars refinery projects. The economic background of its people has been agriculture, fishing and marine trade. Also, Siraf port with a population of 6992 people

is in the central part of Kangan city in Bushehr province. This port is located between Kangan and Assaluyeh ports and has a special characteristic due to its location between the two regions of South Pars energy and Kangan energy region. Also, the its historical area and the beautiful sea of Siraf has attracted many tourists. The name of each station and the geographical coordinates of the sampling points are presented in **Table 2** and shown in **Figure 1**.

Table 2. Geographical coordinates of sampling stations

Station name	Station location	Geographical coordinates	
		X	Y
S ₁	Siraf port	635084	3059458
S ₂		634398	3059481
S ₃		632126	3060955
K ₁	Kangan port	607211	3075796
K ₂		603885	3079199
K ₃		603295	3079640
K ₄		602444	3080053
K ₅		601383	3080147
K ₆		600489	3080150
K ₇		599667	3080196

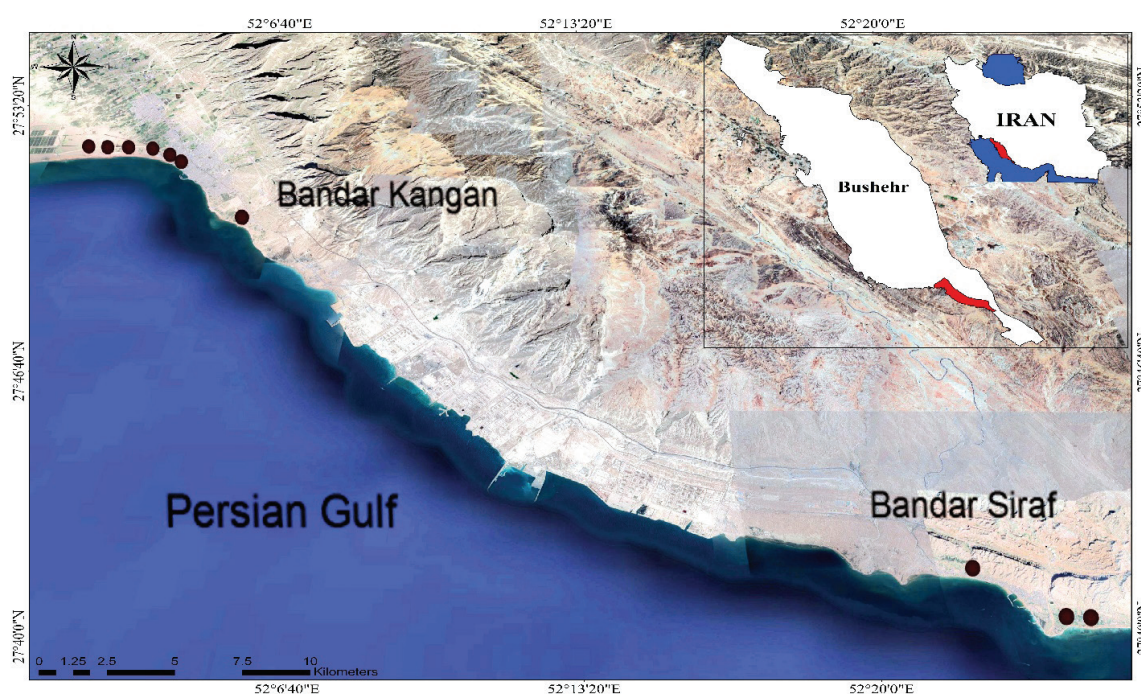


Fig. 1. Location of the study area and sampling stations

2.4. Sampling method

In order to determine the concentration of heavy metals, sampling was performed in January 2018. For sampling, 10 stations were selected in the lower tidal line of the Persian Gulf coast where sediment has the most contact with water. Accurate sampling points were determined using the Global Positioning System (GPS). Coastal sediments were collected in the lower tidal line in a transect with a length of 1000 m using 30 x 30 cm quadrats in three replications and two depths of 0-5 and 5-20 cm. During sampling, natural waste pieces such as wood and stone were removed from the sampling area. Then 2 + 0.5 kg of sediment sample was collected from each station using a stainless steel shovel and metal ruler from the surface and subsurface layer. Samples collected from both depths were placed separately in sealed bags and transferred to the laboratory after numbering. The samples taken to the laboratory were dried at room temperature and stored until further analysis.

2.5. Procedure for determination of heavy metals

A composite sample of three replicates in the surface and deep sediments of each station was separated and completely powdered and homogenized by mortar. Then the homogenized sample was passed through a 63-micron sieve. This method was performed because heavy metals are often associated with small grains [12]. One gram of dry sediment was weighed and digested in PTFE tubes using a mixture of 7 ml HNO₃, 5 ml HClO₄ and 2 ml HF at 200 ° C for 8 hours. After cooling, the samples were filtered through Whatman 42 µm filter paper and finally diluted and then adjusted to 25 cc volume using distilled water. The diluted samples were centrifuged at 400 rpm for 6 minutes and stored in special plastic containers. For validation, Some of samples digested by microwave digestion method (MWM) and compared to proposed procedure. 5 replicate samples and 2 blank samples

were used with the aim of accuracy of analytical results and eliminating the error caused by the test process. Also, all plastic and glass containers for digestion and measurement of heavy metals were immersed in 10% nitric acid for 24 hours and then washed three times with distilled water before use. Finally, the concentrations of heavy metals such as, Ni, Pb, Mn and Cu were measured by the flame atomic absorption spectrometer (AAS) GBC model. The results were validated by electrothermal atomic absorption spectrometry (GBC, Pal 3000, ET-AAS).

2.6. Potential environmental risk index

The potential environmental risk index is widely used to evaluate the potential environmental risk of heavy metal pollution in the coastal sediments and the sensitivity of the biological community to toxic substances. Equation 1 was proposed by Hakanson in 1980 [13] for calculating the potential environmental risk was proposed as follows:

$$RI = \sum_{i=1}^n Er = Tr \times Cf = Cs / Cb$$

where Cf is the contamination index of heavy metal, C_s is heavy metal concentration in the sample, C_b is the background value of the each heavy metal (element concentration in shale), RI is the total potential environmental risk of heavy metals in sediment, Er is the potential environmental risk index of each metal and Tr is as a toxicity response factor, by showing the toxicity potential of heavy metals and environmental sensitivity to contamination, indicate the potential risk of heavy metal contamination. toxic response factor values for Pb, Cu, Ni and Mn are 5, 5, 5 and 1, respectively [14]. **Table 3** shows the environmental risk status classification of the studied heavy metals. Also in this study, the average shale presented by Turekian and Wedepohl in 1961[15] was used as the background concentration to determine the amount of sediment contamination to heavy elements (**Table 4**).

Table 3. Classification of heavy metal environmental risk assessment index [16]

risk levels Description	Category	risk levels Description	Category
Low risk	$RI \leq 150$	Low risk	$Er \leq 40$
Moderate risk	$150 \leq RI \leq 300$	Moderate risk	$40 \leq Er \leq 80$
Considerable risk	$300 \leq RI \leq 600$	Considerable risk	$80 \leq Er \leq 160$
High risk	$RI \geq 600$	High risk	$160 \leq Er \leq 320$
-	-	Very high risk	$ER \geq 320$

Table 4. Concentration of metals in average shale (ppm)

Metals	Pb	Cu	Ni	Mn
Average	20	45	68	850

2.7. Statistical analysis

Data analysis was performed using SPSS statistical software version 22. First, the normality of the data was evaluated by Kolmogorov-Smirnov test. Then, in order to understand the changes in the concentration of heavy metals at two depths of 0–5 and 5–20 cm, the mean equality tests of two independent societies were used. Also, the importance of the relationship between heavy metals was analyzed using Pearson correlation analysis. In addition, cluster analysis was used to explain the correlation pattern between heavy metals, identify potential sources and group them based on their similarities and differences. The significance level of statistical tests was considered 5% (95% confidence level).

3. Results and Discussion

3.1. Heavy metal determination in surface and deep sediments

The results of measuring the concentration of heavy metals in surface and deep sediments of 10 sampling stations in Kangan and Siraf ports are presented in **Table 5**. The highest and lowest mean concentrations of the studied metals in surface and deep sediments were related to Mn and

Pb with the amount of 121.47 ± 44.20 and $5.30 \pm 7.09 \mu\text{g g}^{-1}$ dry weight of surface sediment and 131.59 ± 70.64 and $4.88 \pm 8.08 \mu\text{g g}^{-1}$ dry weight of deep sediment, respectively. Among the studied heavy metals in the surface sediments of the study area, Pb and Cu with the variation coefficients of 1.33 and 23 had the highest and lowest values, respectively. Also, in deep sediments, Pb and Cu with the variation coefficients of 1.65 and 0.28 had the highest and lowest values, respectively. A variation coefficient of less than 1 indicates low variability, while a variation coefficient of greater than 1 indicates high variability and non-uniform distribution of the studied heavy metals in sediment [17]. In this study, only lead metal in surface and deep sediments had a variation coefficient of greater than 1. Moreover, the different techniques for heavy metal determination ($\mu\text{g g}^{-1}$) in surface and deep sediments of Kangan and Siraf ports coasts was used and shown in **Table 6**. Also, the results of comparing the concentrations of heavy metals such as, Cu, Mn, Ni and Pb in surface and deep sediments of the coasts of Kangan and Siraf ports showed that there is no significant difference between their average concentrations at two depths ($P > 0.05$) (**Table 7**).

Table 5. Descriptive statistics of heavy metal concentration ($\mu\text{g g}^{-1}$) in surface and deep sediments of Kangan and Siraf ports coasts

Depth of sampling	Descriptive statistics	Heavy metals			
		Pb	Cu	Ni	Mn
Surface sample	minimum	0	7.55	3.27	70.72
	maximum	17.82	16.57	28.37	203.3
	Average	5.30	11.59	11.51	121.47
	Standard deviation	7.09	2.76	7.07	44.20
	Coefficient of variation	1.33	0.23	0.61	0.36
	skewness	1.19	0.32	1.53	0.95
	kurtosis	-0.05	-0.38	3.37	-0.13
	Deep sample	minimum	0	8.77	2.37
maximum		22.25	20.97	28.87	294.6
Average		4.88	12.56	10.81	131.59
Standard deviation		8.08	3.64	7.65	70.64
Coefficient of variation		1.65	0.28	0.70	0.53
skewness		1.71	1.57	1.48	1.44
kurtosis		1.67	2.46	3.06	2.44

Table 6. Different techniques for heavy metal determination ($\mu\text{g g}^{-1}$) in surface and deep sediments of Kangan and Siraf ports coasts ($n=5$, mean SD < 5%)

	Techniques	Heavy metals			
		Pb	Cu	Ni	Mn
Surface sample	F-AAS	5.30	11.59	11.51	121.5
	ICP	5.41	11.06	12.02	119.9
	ET-AAS	5.23	10.93	11.42	125.7
Deep sample	F-AAS	4.88	12.56	10.81	131.59
	ICP	5.12	12.14	11.24	126.82
	ET-AAS	4.73	12.35	11.03	124.27

Table 7. Results of comparing the concentration of heavy metals in surface and deep sediments

Metal	Test statistics	significance level
Pb	0.122	0.904
Cu	-0.671	0.511
Ni	0.210	0.836
Mn	-0.384	0.705

3.2. Correlation analysis and determination of heavy metals origin

The results of Pearson correlation among the studied metals are presented in **Table 8**. Accordingly, in sediment samples, there is a positive and moderate correlation between Cu and Ni as well as Ni and Mn at the level of 1% and 5%, respectively ($P < 0.05$). As the concentration of Ni increases, the concentrations of Cu and Mn increase. This correlation can be the result of geological property, common resources, or similar behaviors of these elements. Also, all metals in cluster analysis were classified into two statistically significant clusters based on the similarity

and dissimilarity among different groups. The first cluster was divided into 2 subgroups. The first subgroup consisted of Cu and Ni with similar geological property which had positive and significant correlation, and the second group included Mn, which may be derived from both human and natural resources. The second cluster contained Pb metal, with less similarity and greater distance compared to the first cluster. Pearson correlation was used for hierarchical cluster analysis and the results were presented as a dendrogram chart (**Fig. 2**). The results of cluster analysis almost confirmed the results of correlation analysis.

Table 8. Pearson correlation coefficient of heavy metals studied

Metal	Pb	Cu	Ni	Mn
Pb	1			
Cu	0.104	1		
Ni	-0.332	0.583**	1	
Mn	-0.263	0.175	0.444*	1

* Significance at the level of 0.05

** Significance at the level of 0.01

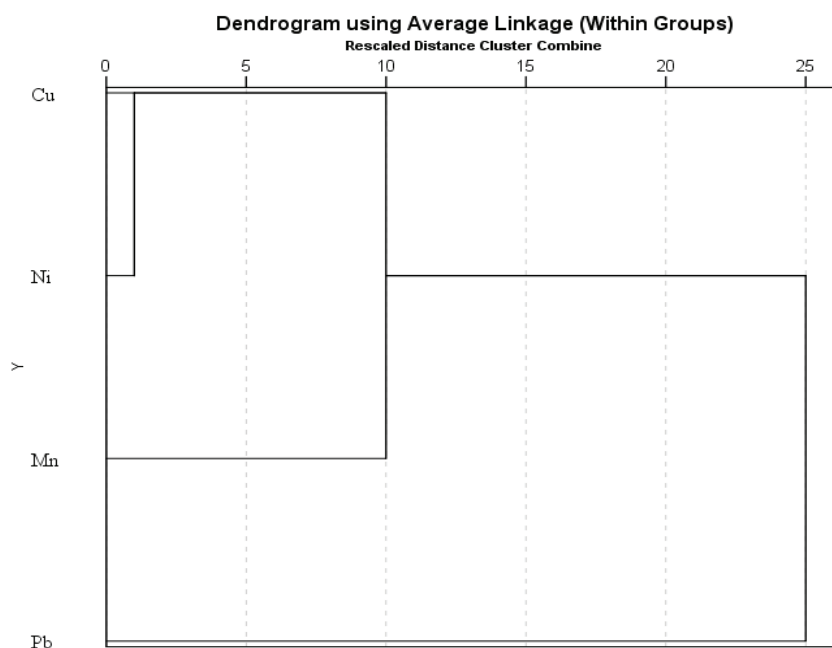


Fig. 2. Results of heavy metal cluster analysis in coastal sediments

3.3. Environmental risk evaluation

The results of environmental risk evaluation of heavy metals in the surface and deep sediments of the studied stations were less than 150, which indicated the low environmental risk of heavy metals in Kangan and Siraf coastal areas. Also, the individual environmental hazard index of the studied metals was less than 40 and showed the descending order of $Pb > Cu > Ni > Mn$ for surface and deep sediments.

3.4. Discussion

Nowadays one of the most important global environmental problems is pollution caused by heavy metals. High concentrations of metals along with high durability, inherent toxicity and consequently accumulation in the food chain play an important role in ecosystems and human health. Therefore, this study has identified the concentration of heavy metals in the collected samples of surface and deep sediments of the Persian Gulf coastal area in Kangan and Siraf ports.

Heavy metals are affected by oil pollution and related industries, ship activity and sewage inflow as the common pollution in the study area. In this study, the highest concentrations of heavy metals in surface and deep sediments include Mn, Cu, Ni and Pb, respectively. Also in other studies conducted in the Persian Gulf coast of Bushehr province, including the study by Hosseini and Habibi et al [18,19], the concentration of Mn, Ni and Cu in the region is higher than Pb. The study by Arfaeinia et al on the concentration of heavy metals in the coasts of Asaloyeh in Persian Gulf showed that due to the high concentration of industries in this region, the concentration of pollutants is much higher than other coasts of the Persian Gulf [3]. The high concentration of heavy metals in industrial and commercial areas compared to non-industrial areas showed that human activities strongly affect the concentration and distribution of heavy metals in the environment. Industrial and agricultural wastewater, solid and liquid wastes and atmospheric emissions increase the concentration of metals in sediments of the area. Atmospheric sediments can affect large

areas according to population distribution and industrial activities [3]. Also, erosion and washing of urban soils by floods and sewage can be other possible sources of sediment pollution and accumulation of heavy metals on the coast [20]. The results of comparing the concentrations of heavy metals in the two coastal areas of Kangan and Siraf showed the existence of concentration differences between them, which can be due to various reasons such as the number and type of pollutants in the environment, the distance from the source of contamination to the sampling site, sediment texture and mineralogical compositions, physical and chemical properties of sediment such as pH and temperature, amount of sediment organic matter and also the effect of environmental factors on metal deposition in sediment. The presence of heavy metals in the stations located in Kangan and Siraf ports can be attributed to various agricultural activities such as vegetables planting in greenhouses, using fertilizers and soil conditioners, drip irrigation pipes, repair of agricultural equipments and the use of pesticides. In addition, the existence of petrochemical and refining industries and their discharge of effluents to the coast, as well as high human activities such as the movement of ships and fishing boats and their discharge of sewage and waste can be considered as the effective factors in the increase of heavy metal concentrations on the coastal areas. Furthermore, the heavy metal pollution in the region could be due to the use of small rivers water to irrigate agricultural lands. Rivers water may be contaminated by discharge of municipal and industrial wastewater from the upstream wastewater treatment plants. Irrigation with contaminated water significantly increases the levels of various pollutants including heavy metals, PAHs and PCBs in coastal sediments [3]. In this study, stations K_7 and K_2 showed the highest concentrations of heavy metals in surface and deep sediments, respectively. Station K_7 is located near an area with high agricultural activities and Station K_2 is adjacent to the commercial wharf of Kangan port. The study by Wang et al also showed that the samples collected from agricultural soil contained large amounts

of heavy metals. The high concentrations of Cu, Ni and Mn in the station K₇ sediments indicated their common sources and similar behavior [21]. In addition, the results of multivariate statistical analyzes showed the common origin of Cu, Ni and Mn and their correlation. The presence of Ni in the sediments of the Persian Gulf coast is probably due to the geological origin and human activities related to oil products in the region [22]. The ground sources of nickel include minerals such as clay, sandstone and basalt [20]. The study by Arfaeinia et al was showed that the origin of Ni in the region is probably due to dyes used in machinery and ships industry [3]. In addition, the concentration of Mn in sediment may increase due to human activities such as discharge of municipal and industrial wastewater, use of agricultural fertilizers and consumption of diesel fuel in motor boats. Also, Mn is easily removed from igneous and metamorphic rocks due to weathering of rocks and in interaction with surface and groundwater, and is released into aquatic environments [23]. Cu is also widely used due to its special physical properties and usually accumulates in soils and sediments following human activities [20]. In this study, the highest concentrations of Cu were identified near residential areas with agricultural activities. As a result, the presence of Cu in the region can be due to the discharge of municipal sewage and agricultural pesticides on the coastal area and also the release of paint used in conveyors, ships and vessels in the water environment which is in line with the study by Haghshenas et al [24]. The concentration of Pb in nature is low, so human activities increase the concentration of Pb in the environment [6]. Pb in the environment comes from the oil industry, lead-containing paints and leaded gasoline. The concentration of Pb metal from dyes is related to the proximity of the structures to the coastal areas and their age. While the amount of Pb due to the displacement of ships and the emission of polluted gases by vehicles depends on the volume of traffic [20]. Among the studied stations, stations S₂ and K₅ showed the highest Pb concentrations in surface and deep sediments, respectively. These two stations are located near the

fishing port, residential and industrial areas. As a result, high concentrations of Pb can result from high-traffic shipping activities, release of paint from the ships' body, proximity to roads and road transport, fishing boat activity, and pollution from industrial wastewater discharge [25]. In general, factors such as high temperature and humidity on the shores of the Persian Gulf accelerate the corrosion process of metal smithereens, which mostly include Cu and Ni alloys. Also, the oil-richness of the region, the existence of activities related to the oil industry and the transport of metal-containing sediment particles by rivers and surface runoff, cause the discharge of metals in the environment and their accumulation in the sediments of the region [3].

4. Conclusions

The coast of the Persian Gulf is an important and strategic region that contributes to the economic growth of the country due to its beautiful scenery and rich resources of oil and gas. However, there is a possibility of contamination of these beaches with heavy metals due to various land and sea activities, mismanagement of solid wastes and discharge of various industrial and municipal wastewaters. The results of this study showed that heavy metals are pervasive in surface and deep sediments of all studied stations and the distance from the source of pollution, environmental conditions and sediment characteristics have caused differences in the frequency and concentration of these pollutants in different stations. The concentrations of heavy metals such as Pb, Cu, Mn and Ni in surface and deep sediments were studied and determined by F-AAS, which almost all stations had the highest concentration of Mn and the lowest concentration of Pb. Observations showed that there is a positive correlation between Cu and Ni as well as Ni and Mn ($P < 0.05$). As the concentration of Ni increases, so does the concentration of Cu and Mn. Also, the results of multivariate statistical analyzes have well confirmed the existence of this relationship. All samples were validated by microwave digestion method coupled to ET-AAS. In addition, the

ecological risk assessment index to determine the environmental risk of heavy metals showed that the sediment contamination status of these metals was not in a dangerous and critical state. However, regular management and preventive measures are necessary to prevent the increase of heavy metal pollutants in the environment.

5. Acknowledgments

The authors wish to thank from the anonymous reviewers for their valuable comments.

6. References

- [1] I. Ahmed, B. Mostefa, A. Bernard, R. Oliver, Levels and ecological risk assessment of heavy metals in surface sediments of fishing grounds along Algerian coast, *Mar. Pollut. Bull.*, 136 (2018) 322-333.
- [2] S. Dobaradaran, T.C. Schmidt, I. Nabipour, N. Khajehmadi, S. Tajbakhsh, R. Saeedi, M.J. Mohammadi, M. Keshtkar, M. Khor-sand, F. Faraji Ghasemi, Characterization of plastic debris and association of metals with microplastics in coastline sediment along the Persian Gulf, *Waste Manag.*, 78 (2018), 649–658.
- [3] H. Arfaeinia, S. Dobaradaran, M. Moradi, H. Pasalari, E. Abouee Mehrizi, F. Taghizadeh, A. Esmaili, M. Ansarizadeh, The effect of land use configurations on concentration, spatial distribution, and ecological risk of heavy metals in coastal sediments of northern part along the Persian Gulf, *Sci. Total Environ.*, 653 (2019) 783-791.
- [4] H. Aslam, T. Ali, M.M. Mortula, A.G. Attaelmanan, Evaluation of microplastics in beach sediments along the coast of Dubai, UAE, *Mar. Pollut. Bull.*, 150 (2020) 110739.
- [5] Atlanta centers for disease control (ACDC) US department of health and human services, national institute for occupational safety and health (NIOSH). Adult blood lead epidemiology and surveillance (ABLES), 2017. <https://www.cdc.gov/niosh/topics/ables/description.html>
- [6] G. Suresh, V. Ramasamy, M. Sundarajan, K. Paramasivam, Spatial and vertical distributions of heavy metals and their potential toxicity levels in various beach sediments from high-background radiation area, Kerala, India, *Mar. Pollut. Bull.*, 91 (2014) 389-400.
- [7] M. Mohammedi Galangash, E. Solgi, Z. Bozorgpanah, The study of heavy metals concentration in pontogammarus maeoticus and surficial sediment in Coastal areas of the Caspian sea; Guilan Province, (Iran. J. Biol.) *J. Animal Res.*, 30 (2017).
- [8] E. Vetrimurugan, V.C. Shruti, M.P. Jonathan, P.D. Roy, B.K. Rawlins, D.M. Rivera-Rivera, Metals and their ecological impact on beach sediments near the marine protected sites of Sodwana Bay and St. Lucia, South Africa, *Mar. Pollut. Bull.*, 127 (2018) 568-575.
- [9] K. Bigus, A. Astel, P. Niedzielski, Seasonal distribution of metals in vertical and horizontal profiles of sheltered and exposed beaches on Polish coast, *Mar. Pollut. Bull.*, 106 (2016) 347-359.
- [10] K.D. Bastami, H. Bagheri, V. Kheirabadi, G. Ghorbanzadeh Zaferani, M.B. Teymori, A. Hamzehpoor, F. Soltani, S. Haghparast, S.R. Moussavi Harami, N. Farzaneh Ghorghani, S. Ganji, Distribution and ecological risk assessment of heavy metals in surface sediments along southeast coast of the Caspian sea, *Mar. Pollut. Bull.*, 81 (2014) 262-267.
- [11] M. Zhang, P. He, G. Qiao, J. Huang, X. Yuan, Q. Li, Heavy metal contamination assessment of surface sediments of the Subei Shoal, China: Spatial distribution, source apportionment and ecological risk, *Chemosphere*, 223 (2019) 211-222.
- [12] N. Harikrishnan, R. Ravisankar, A. Chandrasekaran, M. SureshGandhi, K.V. Kanagasabapathy, M.V.R. Prasad, K.K. Satapathy, Assessment of heavy metal contamination in marine sediments of East coast of Tamil Nadu affected by different pollution sources, *Mar. Pollut. Bull.*, 121 (2017) 418-427.
- [13] L. Hakanson, An ecological risk index for

- aquatic pollution control, a sedimentological approach, *Water Res.*, 14 (1980) 975–1001.
- [14] H. Delshab, P. Farshchi, B. Keshavarzi, Geochemical distribution, fractionation and contamination assessment of heavy metals in marine sediments of the Asaluyeh port, Persian Gulf, *Mar. Pollut. Bull.*, 115 (2016) 401–411.
- [15] K.K. Turekian, K.H. Wedepohl, Distribution of the elements in some major units of the Earth's Crust, *Bull. Geol. Soc. Am.*, 72 (1961) 175–192.
- [16] M. Mohammadzadeh, K.D. Bastami, M. Ehsanpour, M. Afkhami, F. Mohammadzadeh, M. Esmaeilzadeh, Heavy metal accumulation in tissues of two sea cucumbers, *Holothuria leucospilota* and *Holothuria scabra* in the northern part of Qeshm island, Persian gulf, *Mar. Pollut. Bull.*, 103 (2015) 354–359.
- [17] S. Liu, Y. Zhang, S. Bi, X. Zhang, X. Li, M. Lin, G. Hu, Heavy metals distribution and environmental quality assessment for sediments off the southern coast of the Shandong Peninsula, China, *Mar. Pollut. Bull.*, 100 (2015) 483–488.
- [18] M. Hosseini, S.B. Nabavi, R. Golshani, S.N. Nabavi, A. Raeesi sarasiab, The heavy metals pollution (Cd, Co, Pb, Cu and Ni) in sediment, liver and muscles tissues of flounder *Psettodes erumei* from Bushehr Province, Persian Gulf, (Iran. J. Biol.) *J. Animal Res.*, 28 (2014) 441–449.
- [19] S. Habibi, A. Safahieh, H. Pashazanoosi, Determining the level of impurity of coastal sediments in Bushehr province in relation to heavy metals (Cu, Pb, Ni, Cd), *J. Marine Sci. Technol.*, 11 (2013) 84–95.
- [20] A. Ranjbar Jafarabadi, A. Riyahi Bakhtiyari, A. Shadmehri Toosi, C. Jadot, Spatial distribution, ecological and health risk assessment of heavy metals in marine superficial sediments and coastal seawaters of fringing coral reefs of the Persian Gulf, Iran, *Chemosphere*, 185 (2017) 1090–1111.
- [21] Y. Wang, X. Zou, C. Peng, S. Qiao, T. Wang, W. Yu, S. Khokiattiwong, N. Kornkanitnan, Occurrence and distribution of microplastics in surface sediments from the Gulf of Thailand, *Mar. Pollut. Bull.*, 152 (2020) 110916.
- [22] M. Saadati, M. Soleimani, M. Sadeghsaba, M.R. Hemami, Bioaccumulation of heavy metals (Hg, Cd and Ni) by sentinel crab (*Macrophthalmus depressus*) from sediments of Mousa Bay, Persian Gulf, *Ecotoxicol. Environ. Saf.*, 191 (2020) 109986.
- [23] S.M. El Baz, M.M. Khalil, Assessment of trace metals contamination in the coastal sediments of the Egyptian Mediterranean coast, *J. Afr. Earth Sci.*, 143 (2018) 195–200.
- [24] A. Haghshenas, M. Hatami-manesh, M. Sadeghi, M. Mirzaei, B. Mohammadi Bardkashki, Determination and ecological risk assessment of heavy metals (Cd, Pb, Cu, Zn) in surface sediments of coastal regions of Bushehr Province, *J. Environ. Health Eng.*, 5 (2018) 359–374.
- [25] M. Sharifinia, M. Taherizadeh, J. Imanpour Namin, E. Kamrani, Ecological risk assessment of trace metals in the surface sediments of the Persian Gulf and Gulf of Oman: evidence from subtropical estuaries of the Iranian coastal waters, *Chemosphere*, 191 (2018) 485–493.



Separation of aniline from water and wastewater samples based on activated carbon nanoparticles and dispersive solid phase extraction procedure

Saeed Fakhraie^{a,*}, Morteza Mehdipour Rabouri^b and Ahmad Salarifar^c

^a Chemistry Department, Yasouj University, P.O. Box 74831-75918, Yasouj, Iran.

^b Occupational Health Engineering Department, Kerman University of Medical Sciences, Kerman, Iran

^c Environmental Engineering, Faculty of Natural Resources, Islamic Azad University, Bandar Abbas Branch, Iran

ARTICLE INFO:

Received 10 Aug 2020

Revised form 4 Oct 2020

Accepted 22 Nov 2020

Available online 29 Dec 2020

Keywords:

Aniline,
 Activated carbon nanoparticles,
 Ionic liquid,
 Dispersive solid phase extraction
 procedure,
 gas chromatography–mass
 spectrometry

ABSTRACT

The water, wastewater and air are the main sources of aniline in environment. Aniline has a toxic effect in the human body and environment and so, must be determined by novel techniques. In this study, the activated carbon with microwave heating methods (MHM-ACNPs) were used for extraction aniline from waters by dispersive ionic liquid solid phase extraction procedure (D-IL-SPE) and compared to the activated carbon (AC). For this purpose, the mixture of acetone, ionic liquid and 30 mg of MHM-ACNPs/AC added to 100 mL of water samples at pH=8. After sonication for 10 min, the benzene ring in aniline as electron acceptor was chemically adsorbed on carboxylic groups of MHM-ACNPs as electron donors (MHM-ACNPs-COO⁻.....C₆H₅-NH₂) and then, the adsorbent was collected by hydrophobic ionic liquid phase in bottom of conical centrifuging tube. Finally, the aniline was released from MHM-ACNPs in remained solution by changing pH and the concentration of aniline determined by gas chromatography–flame ionization detector (GC-FID). The working range (WR) was obtained from 2.0 to 4000 µg L⁻¹ (RSD % < 1.8). The detection limit (LOD) and preconcentration factor (PF) and linear range (LR) were achieve 0.6 µg L⁻¹, 196.4 and 2.0–950 µg L⁻¹, respectively. The proposed method was validated by spiking of real samples and analysis with gas chromatography mass detector (GC-MS).

1. Introduction

Aromatic amines such as aniline compounds are employed as the chemical in industries (polyurethane foams) and pharmaceutical product. The reduction of nitrobenzene to aromatic amine can be occurred without adding of metal (zinc, tin, or iron) or dihydrogen in polar solvents. Aniline is an aromatic hydrocarbon and discharge into the

environment through certain industrial effluents which thereby cause to water contamination [1, 2]. Aniline (C₆H₅NH₂) with benzene ring and NH₂ bond can be reacted to other chemicals with sulfur and carboxyl groups and removed from waters [3]. The main product of aniline is methylene diphenyl diisocyanate (MDI) which was used in polyurethanes as foams in refrigerator insulation. Aniline use in different industries such as paint, polymers, pesticides, herbicides, resins, chemicals, antioxidants, pharmaceuticals, rubber, plastics,

*Corresponding Author: Saeed Fakhraie

Email: saeedfakhraie@yahoo.com

<https://doi.org/10.24200/amecj.v3.i04.126>

explosives and solvents in perfumes [4]. It should also be noted that the WHO reported the threshold for nitrobenzene in water is 30–110 $\mu\text{g L}^{-1}$. EPA showed, water containing aniline at an average of 6–60 $\mu\text{g L}^{-1}$ is not greater than a one-in-a hundred thousand increased chance of developing cancer. Aniline is toxic in humans and cause to mutagenic or carcinogenic effect in the cells of body and DNA [5]. Aniline cause to myelotoxicity, toxicity of lymphoid organs and hematopoietic tissues in human and faunae [6]. Aniline compounds belong to the blacklist of contaminants material in many countries. Aniline create the reactive oxygen species (ROS) and cause to rise lipid hydroperoxide stages, damage of mitochondrial membrane, damage DNA and lead to variations in hepatocyte feasibility and apoptosis [7]. Also, the acute exposure aniline has toxic reaction in the spleen or liver and cause to splenomegaly, hyperplasia, fibrosis, and cancers with chronic exposure [8]. The toxicity and carcinogenicity of aniline was reported by NIOSH and OSHA [9–11]. The acute toxicity of aniline caused to convert to 4-hydroxyaniline and the formation of aniline compound with hemoglobin (Hb). In erythrocytes(RB), this is associated with the release of iron (Fe) and the accumulation of methemoglobin (MHb) and the development of hemolytic anemia and inflammation of the spleen. Tumor formation is often observed in the spleen on prolonged administration. The International Agency for Research on Cancer (IARC) classifies aniline as a group 2B carcinogenic compound owed to its mutagenic and carcinogenic possible [12] and the concentration of aniline must be evaluated in water samples. So the removal of aniline compounds from wastewater is mainly important for human health and eco-friendly protection. The analytical techniques include, gas chromatography [13], Spectrofluorimetry [14], the capillary zone electrophoresis (CZE) with field-enhanced sample injection [15,16] and high performance liquid chromatography (HPLC) [17] were used for the determination of aniline and derivatives in real samples. The different method include adsorption, the biological degradation, the catalytic oxidation

and the electrochemical procedure was used for eliminating aniline compounds from waters [18–20]. Due to toxicity of aniline and its derivatives, the aniline value must directly evaluate in water sources. As low concentration of aniline compounds in water samples, the pretreatment/preconcentration of the samples was used before analysis by HPLC, GC and liquid chromatography-tandem mass spectrometry [21]. Conventional techniques such as, adsorption, extraction, the chemical oxidation, the catalyzed process the electrochemical, the enzymatic process and the irradiation reported for anilines separation and determination in water samples. You et al. developed a new enzymatic method for the removal of aromatic pollutants from wastewaters by peroxidases [22, 23]. On the other hands, adsorbents such as graphene, graphene oxide, carbon nanotubes, MOF and silica with different physical and chemical properties were used for extraction/adsorption anilines from waters. In this study, the MHM-ACNPs nanoparticles were used for extraction aniline from waters by dispersive ionic liquid solid phase extraction procedure (D-IL-SPE). By procedure, the aniline adsorbed on nanostructure (MHM-ACNPs-COO... NH-C₆H₅) at optimized pH. Then, aniline desorbed from MHM-ACNPs/IL by changing pH and determined by GC-FID.

2. Experimental

2.1. Apparatus

Agilent Gas chromatography with flame ionization detector (GC-FID) and mass detector (GC-MS) based on sample air loop injection (Windows XP Professional) was used (7890A, Netherland). This model of GC based on different detectors and equipped with a split injector was used for aniline analysis. A Hamilton syringe was used for the sample injected to the GC injector. The temperature of the injector tuned for the vaporization of aniline up to 185–200°C. The temperature of the injector port and detector of GC was tuned up to 200°C and 250°C, respectively. The oven temperature was tune up to 120°C and the flow rate of 1.5 mL min⁻¹ for H₂ was adjusted. The sample liquid was

Table 1. Gas chromatography conditions (Agilent, 7890A)

Parameters	Values
Injection Volume	1-10 μL
Split ratio	2:1
Column	30 meter, 0.32mm x 0.25 μm
Temperature Injector	200 $^{\circ}\text{C}$
Detector FID	250 $^{\circ}\text{C}$
Program	30 to 100 $^{\circ}\text{C}$ @ 25 $^{\circ}\text{C}/\text{min}$,
Carrier Gas	H_2 @ 1.5 mL min^{-1}
Gas Makeup	N_2 @ 30 mL min^{-1}
Retention Time N,N-Dimethylaniline	18.1 (min)
Retention Time Aniline	10.9 (min)
Flow Rate N_2	28 (mL min^{-1})
Flow Rate detector H_2	60(mL min^{-1})
Flow Rate air	450(mL min^{-1})

injected into a GC injector with high temperature for vaporizing aniline. The liquids samples inject based on valves to the GC column (0.32 mm \times 0.25 μm). The pressures for inlets and detectors tuned between 35-100 psi for hydrogen with FID detector. The GC-MS was used for validation of aniline results which were adsorbed on MHM-ACNPs adsorbents. The conditions of GC were presented in **Table 1**.

2.2. Reagents

The epoxy resin powders from waste printed circuit boards (WPCB) were provided by Shan-dong Zhonglv Eco-recycle Co. Ltd, China. According to our previous study [10], epoxy resin of WPCBs has low ash content (7%), water ratio (3%), high volatile matter (67%) and fixed carbon (23%). The carbon was measured by an energy dispersive spectrometer instrument (C: 42.16%). Aniline is an aromatic amine that may be used as a reactant in the synthesis of organic intermediates such as pyridine amine, phenyl amine and phenyl benzamide. So the pure Aniline prepared (CAS N: 62-53-3) from Sigma Aldrich. Hydrophobic ionic liquid 1-Butyl-1-methylpyrrolidinium bis(trifluoromethylsulfonyl) imide ($\text{C}_{11}\text{H}_{20}\text{F}_6\text{N}_2\text{O}_4\text{S}_2$, 223437-11-4) with density of 1.4 g cm^{-3} and low solubility in water was used

for collecting of nanoparticles from liquid phase. Acetone, nitric acid and HCl were purchased from Merck, Germany. Ultrapure water was obtained from Millipore Water System (USA), The phosphate buffer ($\text{H}_2\text{PO}_4/\text{HPO}_4$) and ammonium buffer ($\text{NH}_3/\text{NH}_4\text{Cl}$) prepared from Sigma an used for adjusting pH between 6.0–8.2 and 8-9, respectively.

2.3. Synthesis of adsorbent

2.3.1. Carbonization

Activated carbons (ACs) was synthesized by the carbonized method for 2.0 h at 600 $^{\circ}\text{C}$ by activating at 800 $^{\circ}\text{C}$ for 1 h in a furnace. The carbonized chars followed by typically heats biomass feedstock in a kiln (pyrolysis) at temperatures between 300-800 $^{\circ}\text{C}$ in the absence of air. The produced also known as charcoal (porous and carbon-enriched). The carbonization furnace was used for the carbonization. Firstly, 20 g of raw powders prepared and placed in the porcelain crucible, then heated up to 600 $^{\circ}\text{C}$ per minute and hold for 2.0 hours. By decreasing temperature up to 25 $^{\circ}\text{C}$, the product is ready for weight [24].

2.3.2. MHM-ACNPs Synthesis

The activation of ACs based on microwave heating method caused to create the MHM-ACNPs by previous works [24-26]. First, the

carbonized sample was mixed with KOH (CS/KOH; ratio 1:3; wt/wt). By the simple heating, the activation of CS/KOH (ACNPs) was carried out at 800 °C (rate: 25 °C min⁻¹; hold: 1h) in a tube furnace and cooling down to room temperature under N₂ flow (0.5 Lmin⁻¹). In the microwave heating method, the MHM-ACNPs were achieved by microwave furnace at a frequency of 2.45 GHz [25]. The mixture of CS/KOH was placed in the microwave furnace (800 W) and heated for 12 min [26]. The product was cooled up to 25°C under N₂ flow (0.5 Lmin⁻¹). The MHM-ACNPs were washed with 10% HCl and then washed with DW up to pH=7.

2.4. Extraction procedure for aniline

Due to D-IL-SPE method, the acetone, ionic liquid and MHM-ACNPs added to 100 mL of water samples at pH=8. After extraction, the concentration of aniline determined by GC-FID. Firstly, 30 mg of MHM-ACNPs added to mixture of acetone (1 mL) and 1-butyl-1-methylpyrrolidinium bis(trifluoromethylsulfonyl)imide (0.3 g) and then injected to water and standard solution of aniline (2.0 µg L⁻¹ and 950 µg L⁻¹). After sonication for 10 min, the benzene ring in aniline as electron acceptor was chemically adsorbed on carboxylic

groups of MHM-ACNPs as electron donors (MHM-ACNPs-COO⁻.....C₆H₅-NH₂). The MHM-ACNPs trapped in 1-Butyl-1-methylpyrrolidinium bis(trifluoromethylsulfonyl)imide and separated from the liquid phase in the bottom of the conical tube after centrifuging (3.5 min; 4000 rpm). The upper of the liquid sample was removed and then, the aniline back-extracted from MHM-ACNPs in acidic pH (HNO₃, 0.3 mol L⁻¹). After shaking and centrifuging, the remained solution diluted up to 0.5 mL with DW and determined by GC-FID (Fig. 1). The procedure was used for a blank experimental run without any aniline for ten times. The calibration curve for aniline in standards solutions was prepared based on D-IL-SPE/GC-FID procedure (2.0- 950 µg L⁻¹) and GC-FID method (0.4- 800 mg L⁻¹) and preconcentration factor (PF) calculated by curve fitting of calibration curves (m₁/m₂). Each sample was analyzed separately by means of a GC-FID. The aniline was detected with a FID detector. Aniline (mol) were calculated by the following Equations (1) as extraction efficiency and Equations (2) as recovery,

$$\%EE = [\text{Initial aniline} - \text{Final aniline} / \text{Initial aniline}] \times 100 \quad (1)$$

$$\%Recovery = \text{Final aniline amount (mol)} / \text{Initial aniline amount (mol)} \times 100 \quad (2)$$

3. Results and Discussion



Fig. 1. The extraction procedure for aniline in waters by MHM-ACNPs and GC-FID

The FTIR showed that the MHM-ACNPs with high surface area ($2792 \text{ m}^2 \text{ g}^{-1}$) and function groups can be efficiently absorbed/extracted the aniline ($\text{NH}_2\text{-C}_6\text{H}_5$) in water samples as compared to ACs. For optimizing, the important parameters on aniline extraction such as, pH, amount of ionic liquid, sample volume, amount of sorbent, amount of IL, shaking time were studied.

3.1. FTIR of MHM-ACNPs

The FTIR spectrum of MHM-ACNPs is illustrated in **Figure 2**. The band at around 3428 cm^{-1} was attributed to the stretching vibration of hydroxyl. The 2910 and 2840 cm^{-1} bands were respectively assigned to asymmetric and symmetric C-H stretching vibration of methylene. The vibration band at 1710 cm^{-1} was identified as C=O stretching mode of carboxylic groups, while the peak at 1058 cm^{-1} was corresponded to the C-O vibration. The

peak at 1613 is characteristic of stretching vibration of C=C in benzene rings. A group of bands can be seen between 850 and 500 cm^{-1} , which are ascribed to C-H and $\text{CH}=\text{CH}_2$ vibrations in aromatic rings.

3.2. SEM and TEM of MHM-ACNPs

HR-SEM and HRTEM were used for morphological study of prepared MHM-ACNPs (**Fig. 3**). **Figure 3a** and **b** illustrates the FE-SEM images of the synthesized MHM-ACNPs sample. The FE-SEM images of MHM-ACNPs sample displayed small broken pieces of particles with irregular shapes, which can significantly affect the pore characteristics (e.g., pore size distribution and average pore diameter). From **Figure 3b**, MHM-ACNPs appeared to have many different sizes of pores, indicating that the structure had been destroyed and a dense porosity was formed through KOH activation. In order to observe the structure of MHM-ACNPs anoadsorbents, HR-

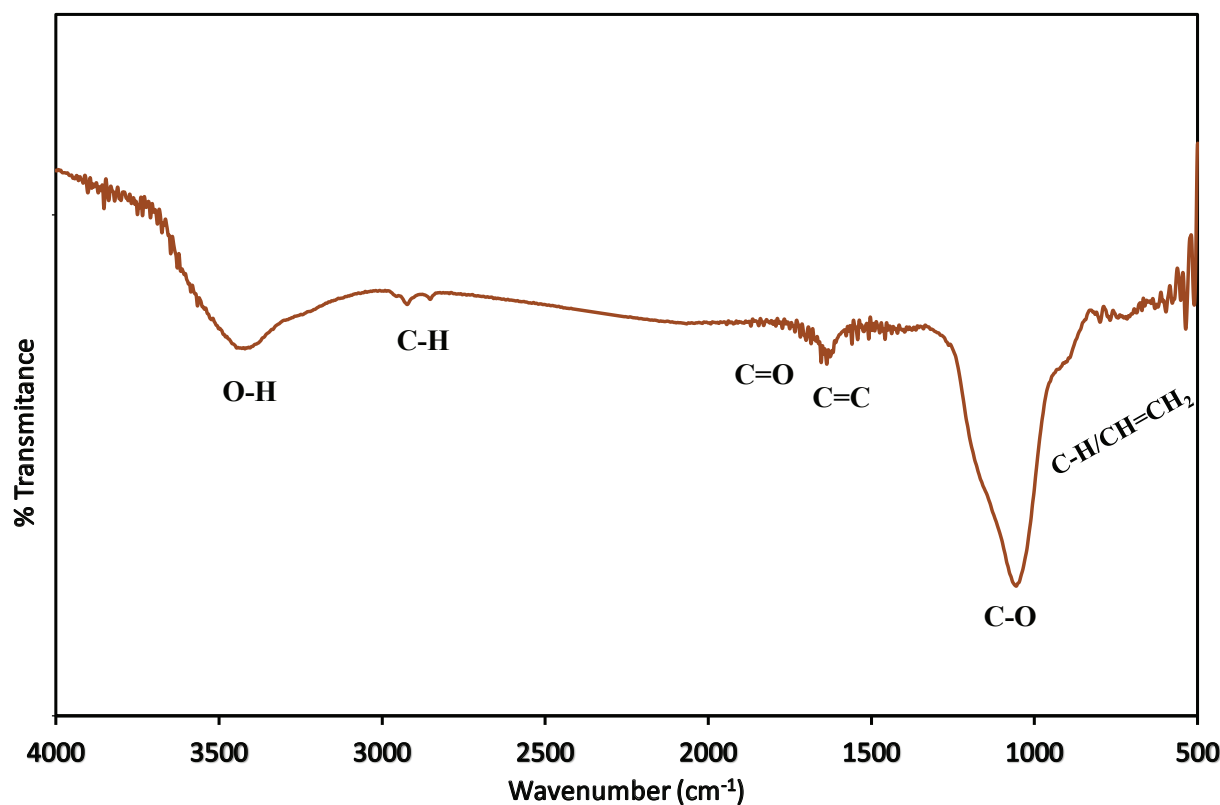


Fig. 2. The FTIR spectrum of MHM-ACNPs adsorbent

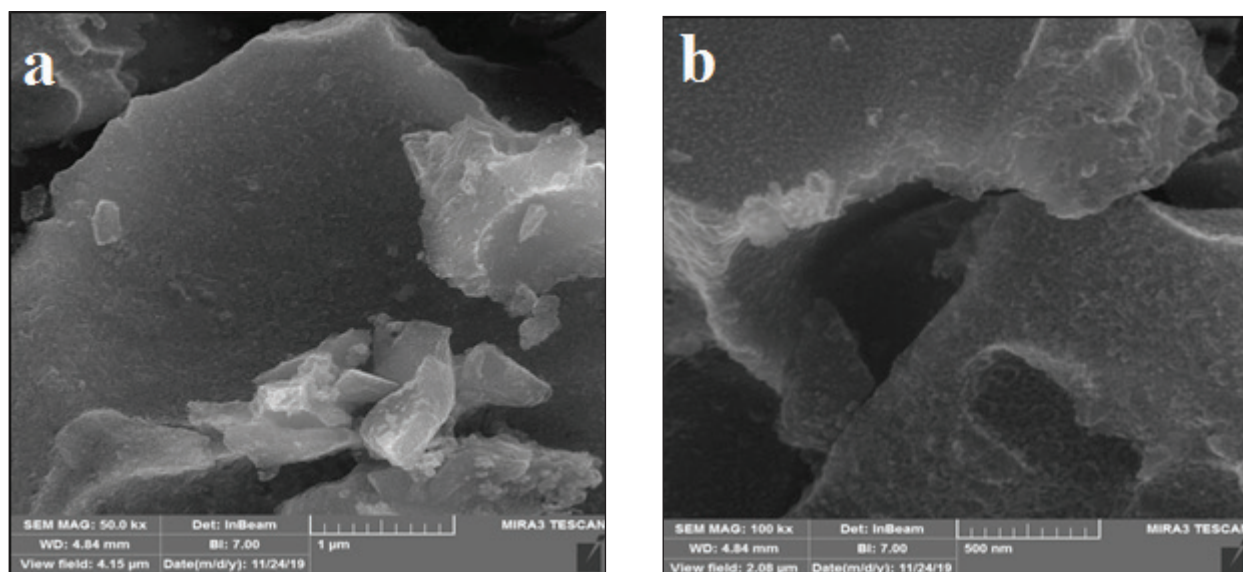


Fig. 3. (a) the FE-SEM images of the synthesized MHM-ACNPs (b) different sizes of pores

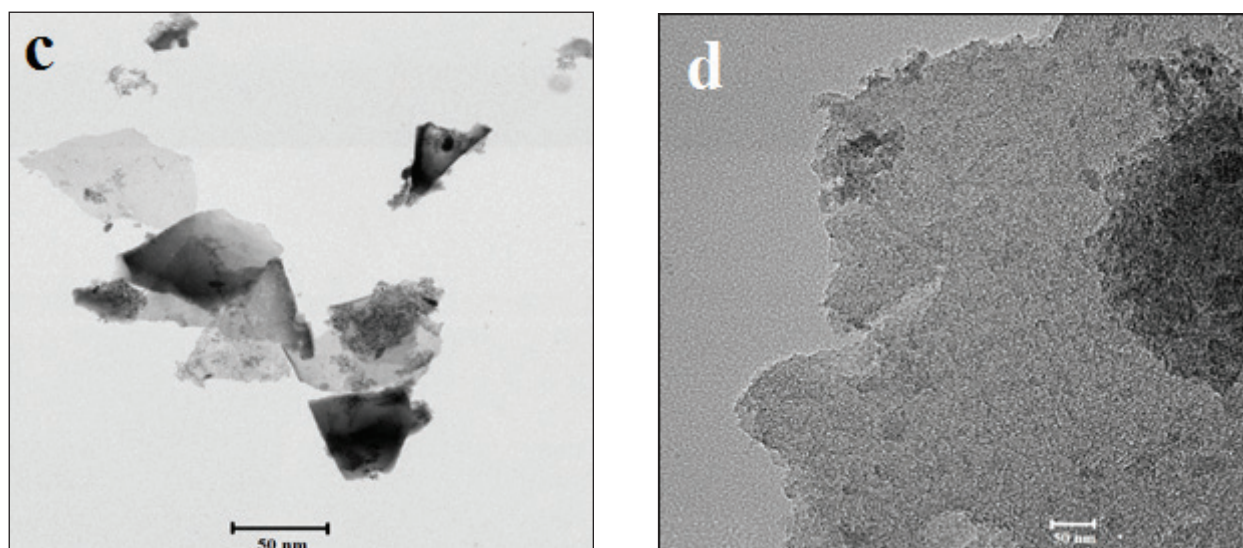


Fig.3. (c)The HR-TEM image of MHM-ACNPs by 2D morphology (d) The HR-TEM image of MHM-ACNPs with intermittent graphitic layers and porous structure

TEM imaging was employed. The HR-TEM image (Fig. 3c) clearly shows the graphene-like structure with a 2D morphology, and the image with 50 nm scale (Fig. 3d) confirms the existence of intermittent graphitic layers and porous structure.

3.3. Optimizations of parameters for extraction aniline

The D-IL-SPE procedure based on MHM-ACNPs nanocomposite was used for extraction of aniline ($\text{NH}_2\text{-C}_6\text{H}_5$) from water and wastewater samples. The main effectiveness parameters such as, pH, amount

of MHM-ACNPs, amount of ionic liquid, sonication time, volume of samples, adsorption capacity of sorbent were evaluated and studied. The mechanism of adsorption depended on the benzene ring in aniline. The benzene ring as electron acceptor was adsorbed on carboxylic groups of sorbent as electron donors ($\text{R-COO}^-\text{.....C}_6\text{H}_5$). After extraction, the sorbent/aniline was collected by 1-butyl-1-methylpyrrolidinium bis(trifluoromethylsulfonyl) imide as a hydrophobic ionic liquid phase in bottom of conical centrifuging tube.

3.3.1. pH effect on aniline extraction

The pH sample is critical factor for aniline extraction in water samples and must be studied. The efficient extraction of aniline based on MHM-ACNPs depended on pH value of water samples which was optimized by D-IL-SPE methods. The pH range from 2 to 11 was examined with different buffer solution and the recovery of aniline extraction in water samples was evaluated in presence of aniline concentration between $2.0\text{--}950\ \mu\text{g L}^{-1}$ for 30 mg of MHM-ACNPs. Based on results, the extraction of aniline was reduced at acidic pH ($\text{pH}<6$) and pH of 7-9 had more extraction for aniline in waters (Fig. 4). So, in this study, the pH of 8.0 was selected as optimized pH for aniline extraction in waters.

3.3.2. The effect of MHM-ACNPs adsorbent on aniline extraction

By proposed method, the amounts of on MHM-ACNPs adsorbent for 100 mL of water and wastewater samples were evaluated. Therefore, the amount of 5-50 mg of MHM-ACNPs and AC was used by D-IL-SPE procedure. The results showed us, aniline efficiently extracted by 25 mg MHM-ACNPs in $\text{pH}=8$. So, the amount of 30 mg of MHM-ACNPs adsorbent was selected for aniline extraction in water samples (Fig. 5).

3.3.3. The effect of sample volume on aniline extraction

The sample volume as an important factor for aniline extraction in water samples. For this proposed, the effect of sample volume for extraction of aniline in waters was evaluated. By procedure, the various sample volumes between 20-150 mL was used for optimizing volume in presence of $2.0\text{--}950\ \mu\text{g L}^{-1}$ of aniline concentration for 30 mg of MHM-ACNPs. The results showed, high recovery obtained for 120 mL of waters. Therefore, 100 mL of sample volume selected for further studies (Fig. 6).

3.3.4. The adsorption capacity

For evaluating of reusability of MHM-ACNPs, the nanoparticles of adsorbent were dispersed in water samples and used for aniline extraction for many times by the D-IL-SPE procedure. The experimental results showed, the aniline was efficiently extracted with MHM-ACNPs adsorbent for 19 cycles of extraction at $\text{pH}=8.0$. So, the MHM-ACNPs adsorbent can be used for 17 extractions/back-extraction steps for aniline in waters. The absorption capacities of adsorbents depended on the structure, surface area (SA) and nanoparticle size (NS) in different samples. For calculating of the absorption capacities, 30 mg of MHM-ACNPs

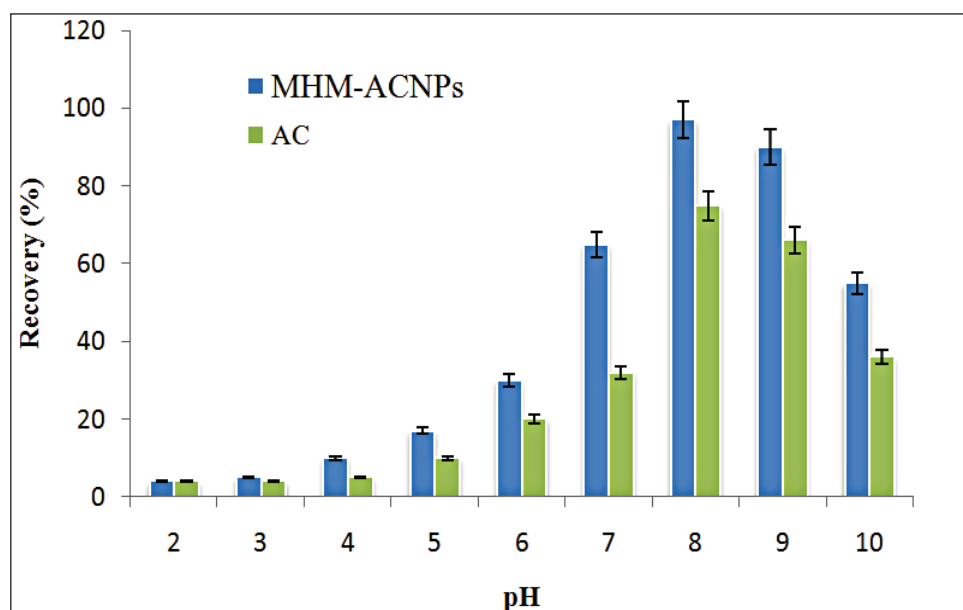


Fig. 4. The effect of pH on aniline extraction by MHM-ACNPs and AC adsorbents from water samples

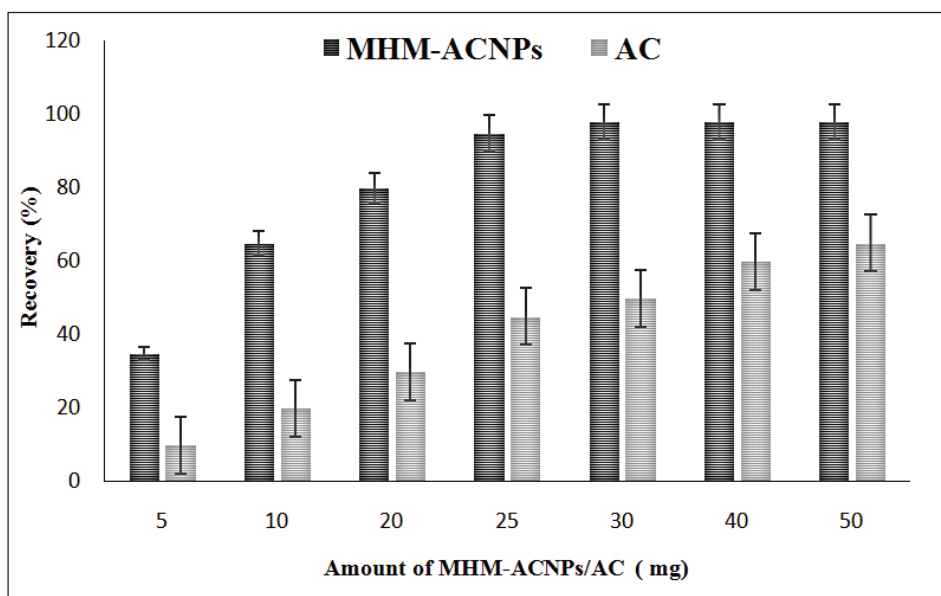


Fig. 5. The effect of MHM-ACNPs and AC adsorbents on aniline extraction by D-IL-SPE method

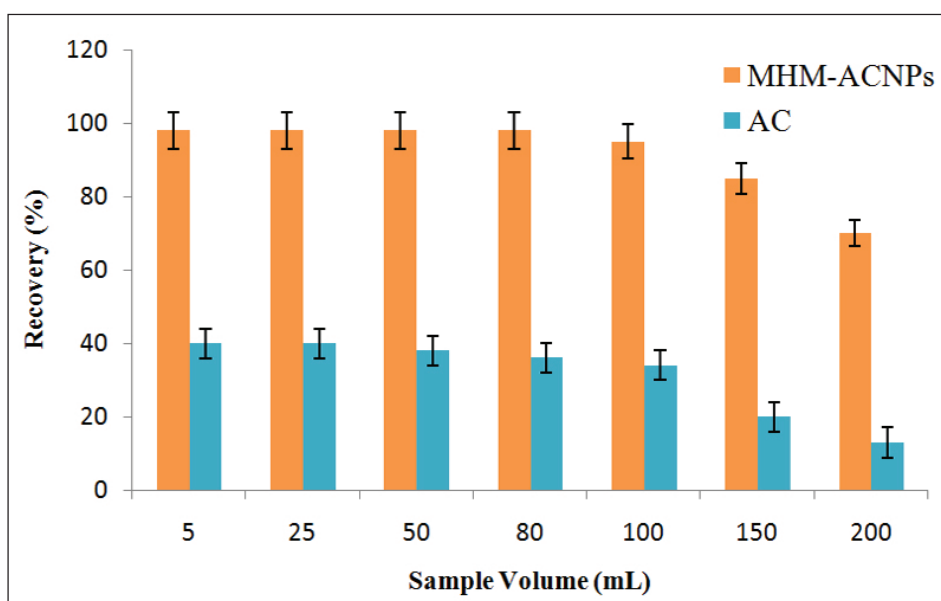


Fig. 6. The effect of sample volume on aniline extraction by MHM-ACNPs and AC adsorbents

and AC nanoparticles was added to 100 mL of water samples with 20 mg L⁻¹ (ppm) of aniline concentration at pH of 8.0. After 30 min sonication, the aniline was extracted by MHM-ACNPs and AC in solutions. Finally, the concentrations of aniline directly determined in remain solution by GC-FID. The adsorption capacities of the MHM-ACNPs and AC structure for aniline were achieved 155.8 mg g⁻¹ and 77.2 mg g⁻¹, respectively in water samples.

3.3.5. Aniline validation in real samples

The MHM-ACNPs adsorbent was used for determination and extraction aniline in water and wastewater samples. The experimental results showed, the aniline was efficiently extracted with proposed procedure and validated by spiking of real samples (**Table 2**). The validation of the results were obtained by spiking of water samples with a standard aniline at pH=8.0.

The extraction efficiency of spiked samples demonstrated that the MHM-ACNPs adsorbent was satisfactory results for aniline extraction and determination in in water and wastewater samples at pH of 8.0. Moreover, the GC-MS were used for validating of methodology based on MHM-ACNPs adsorbent and IL by the D-IL-SPE procedure (Table 3). Also, the aniline extraction based on MHM-ACNPs adsorbent by the D-IL-SPE procedure was compared to other adsorbent and technology which was shown in Table 4.

3.3.6. Discussion

Recently, the aniline was removed/extracted from different matrixes by various technologies by researchers. They showed the different adsorbent and techniques for extraction aniline from water and wastewater samples and the various analytical parameters such as, LOD, LOQ, linear range, RSD% and absorption capacities reported which was shown in Table 4. Kakavandi et al were used the Fe₃O₄-activated carbon magnetic nanoparticles (AC-Fe₃O₄MNPs) for extraction

Table 2. Validation of the D-IL-SPE/GC-FID procedure for determination of aniline in water and wastewater samples by spiking of standard solutions

Sample	Added ($\mu\text{g L}^{-1}$)	*Found ($\mu\text{g L}^{-1}$)	Recovery (%)
Tab water	-----	4.24 \pm 0.22	-----
	5	9.31 \pm 0.24	101.4
Drinking water	-----	ND	-----
	10	9.82 \pm 0.46	98.2
Well water	-----	19.54 \pm 0.95	-----
	20	38.98 \pm 1.84	97.2
wastewater	-----	335.92 \pm 15.11	-----
	300	628.33 \pm 27.65	97.5
Wastewater	-----	188.60 \pm 8.75	-----
	200	379.70 \pm 16.40	95.6

* $\bar{x} \pm ts / \sqrt{n}$ at 95% confidence (n=5)

Table 3. Validation of the D-IL-SPE/GC-FID procedure for determination of aniline in water and wastewater samples by GC-MS

Sample	Added ($\mu\text{g L}^{-1}$)	GC-MS ($\mu\text{g L}^{-1}$)	* D-IL-SPE/GC-FID ($\mu\text{g L}^{-1}$)	Recovery (%)
Water A	-----	11.35 \pm 0.28	10.96 \pm 0.53	96.6
	10	-----	20.78 \pm 0.24	98.2
Water B	-----	53.14 \pm 0.57	53.78 \pm 2.44	101.2
	50	-----	102.66 \pm 4.82	97.8
Water C	-----	98.53 \pm 1.67	101.03 \pm 5.12	102.5
	100	-----	199.87 \pm 9.34	98.8
Water D	-----	202.38 \pm 4.12	195.82 \pm 10.13	96.8
	200	-----	400.08 \pm 18.52	102.1

* $\bar{x} \pm ts / \sqrt{n}$ at 95% confidence (n=5)

Table 4. Comparison of proposed procedure with other published methods

Adsorbent	Matrix	Method	Linear range	Instrument	Recovery (%)	References
C8-column	Water	ESI	0.05- 2 $\mu\text{g L}^{-1}$	LC- MS/MS	99-102%	[27]
AC-Fe ₃ O ₄ MNPs	Water	Adsorbent	50-300 mg L^{-1}	XRD,SEM,TEM	21.1-99%	[28]
Soybean peroxidase	Wastewater	Enzymatic	-----	UV-Vis	95%	[29]
-----	Water	NIAA	50–1000 $\mu\text{g L}^{-1}$	CZE	93-104%	[30]
Activated carbon (AC)	Wastewater	Enzymatic	20-600 mg L^{-1}	UV-Vis	89–94%	[31]
MFH nanocomposites	Wastewater	Electrostatic	50-200 mg L^{-1}	XRD	95.1%	[32]
PFPA	PAAsW	Extraction	0.03–1.4 $\mu\text{g L}^{-1}$	UHPLC-MS/MS	21–110%	[33]
MHM-ACNPs	Water	Adsorption	2.0-950 $\mu\text{g L}^{-1}$	GC-FID/D-IL-SPE	95-102%	This work

NIAA: Non-ionic or anionic analytes

CZE: Capillary zone electrophoresis

PFPA: Mobile phases perfluoropentanoic acid (PFPA) in water and methanol

PAAsW: Primary aromatic amines (PAAs) in Water

of aniline in waters and the characterization of AC-Fe₃O₄MNPs adsorbent obtained by SEM, TEM, XRD, and BET [28]. Also, the results were showed by two kinetic models for adsorption of AC-Fe₃O₄MNPs (Langmuir and Freundlich). The linear range and recovery were achieved 50-300 mg L^{-1} and between 21.1-99%, respectively. Rahdar et al were presented a novel magnetic Fe₂O₃@SiO₂ nanocomposite (Fe@SiNPs) for removal aniline from waters by an electrochemical method. Due to the special characterization of Fe@SiNPs nanocomposite such as, vibrating-sample magnetometry (VSM), XRD, SEM, and FT-IR, the extraction recovery of 71% was obtained. The physical and chemical properties of Fe@SiNPs adsorbent caused to efficient extraction of aniline from the water samples. By optimizing paramours, 50 mg of Fe@SiNp can be removed aniline in waters with absorption capacity of 126.6 mg g^{-1} at pH 6 (50°C) which was lower than the proposed D-IL-SPE procedure. The adsorption of aniline by Fe@SiNp is fast and exothermic which was shown by the kinetic model ($r^2 = 1$) and the Freundlich isotherm model ($r^2 = 0.9986$) [34]. In another study, the polyaniline (PANI)

grafted MWCNTs (PANI/MWCNTs) was used for extraction of aniline in water samples. PANI/MWCNTs were characterized by using ultraviolet–visible spectrophotometry (UV-VIS), X-ray photoelectron spectroscopy (XPS), Raman spectroscopy (RS), the differential thermal analysis (DTA), the differential scanning calorimetry (DSC), and field-emission scanning electron microscopy (FE-SEM). The maximum removal of PANI/MWCNTs adsorbent was achieved around 99% for aniline in waters [35]. Based on our study, the MHM-ACNPs were used for fast, simple and efficient extraction aniline from waters by dispersive ionic liquid solid phase extraction procedure (D-IL-SPE). The aniline adsorbed on nanostructure (MHM-ACNPs -COO.... C₆H₅) with high absorption capacity, the recovery and the extraction as compared to other methods. After back-extraction of aniline, the concentration of aniline is determined by GC-FID and validated by GC-MS. The wide working range was obtained from 2.0 to 4000 $\mu\text{g L}^{-1}$ (RSD% < 1.8) which was higher than other published methods. Based on Table 4, the LOD, PF and linear ranges is better than other presented methods.

4. Conclusions

In this study, a robust procedure based on MHM-ACNPs adsorbent was used for the aniline extraction from water samples. The MHM-ACNPs/aniline was simply separated/collected from water samples in bottom of conical tube by hydrophobic 1-butyl-1-methylpyrrolidinium bis(trifluoromethylsulfonyl) imide. By D-IL-SPE procedure, the efficient extraction, good preconcentration, and the perfect sample preparation was obtained in optimized conditions. By the mixture of IL/ MHM-ACNPs /acetone, the high recovery between 95-102% for aniline extraction were achieved in short time. The developed D-IL-SPE procedure had many advantages such as, the favorite reusability, low LOD and RSD% with accurate and precise results. Therefore, the aniline can be efficiently extracted in water samples based on MHM-ACNPs adsorbent by D-IL-SPE /GC-FID procedure.

5. Acknowledgements

The authors wish to thank from Chemistry Department, Yasouj University, Yasouj, Iran and Islamic Azad University, Bandar Abbas Branch, Iran

6. References

- [1] F. K. Mostafapoor, Sh. Ahmadi, D. Balarak, S. Rahdar, Comparison of dissolved air flotation process function for aniline and penicillin G removal from aqueous solutions, *Hamadan Un. Med. Sci.*, 82 (2016) 203-209.
- [2] U.S.EPA, Environmental Protection Agency, health and environmental effects profile for aniline. office of health and environmental assessment, office of research and development, Cincinnati, OH., 1985.
- [3] J.G. Cai, A. Li, H.Y. Shi, Z.H. Fei, C. Long, Q.X. Zhang, Adsorption characteristics of aniline and 4-methylaniline onto bifunctional polymeric adsorbent modified by sulfonic groups, *J. Hazard. Mater.*, 124 (2005) 173-180.
- [4] T. Kahl, K.W. Schröder, F.R. Lawrence, W.J. Marshall, H. Höke, R. Jäckh, Aniline, in Ullmann, Fritz (ed.). *Ullmann's encyclopedia of industrial chemistry*. John Wiley & Sons: New York, 2007. http://doi:10.1002/14356007.a02_303.
- [5] H. Ma, J. Wang, S.Z. Abdel-Rahman, T.K. Hazra, P.J. Boor, M.F. Khan, Induction of NEIL1 and NEIL2 DNA glycosylases in aniline-induced splenic toxicity, *Toxicol. Appl. Pharmacol.*, 251 (2011) 1-7.
- [6] U. Khairnar, A. Upaganlawar, C. Upasani, Ameliorative effect of chronic supplementation of protocatechuic acid alone and in combination with ascorbic acid in aniline hydrochloride induced spleen toxicity in rats, *Scientifica (Cairo)*, 2016 (2016) 1-9.
- [7] H. Ma, J. Wang, S.Z. Abdel-Rahman, P.J. Boor, M.F. Khan, Oxidative DNA damage and its repair in rat spleen following subchronic exposure to aniline, *Toxicol. Appl. Pharmacol.*, 233 (2008) 247-253.
- [8] P. Makhdomi, H. Hossini, Molecular mechanism of aniline induced spleen toxicity and neuron toxicity in experimental rat exposure, A review, *Curr. Neuropharmacol.*, 17 (2019) 201-213.
- [9] NIOSH, the pocket guide to chemical hazards, Department of health and human services (DHHS), centers for disease control and prevention, National institute for occupational safety and health (NIOSH), Cincinnati, OH. U.S., Publication No. 168c, 2010. <http://www.cdc.gov/niosh/npg/>.
- [10] OSHA, Hazard communication. final rule, Washington, DC. U.S. Department of labor, occupational safety and health administration, OSHA, 77 (2012) 17574-17896. https://osha.gov/pls/oshaweb/owadispl.show_document/.
- [11] T.J. Lentz, M. Seaton, P. Rane, S.J. Gilbert, L.T. McKiernan, C. Whittaker, Technical report, the occupational exposure banding process for chemical risk management, Department of health and human services (DHHS), centers for disease control and prevention

- (CDC), National institute for occupational safety and health (NIOSH), 2019. <https://doi.org/10.26616/NIOSH PUB2019132>.
- [12] IARC, Agents classified by the IARC monographs, the international Agency for research on cancer (IARC) Vol. 1–112, 2015. <http://monographs.iarc.org/Classification/ClassificationsAlphaOrder.pdf>.
- [13] E. Ebrahimpour, A.h. Amir, Poly (indole-co-thiophene) Fe_3O_4 as novel adsorbents for the extraction of aniline derivatives from water samples, *Microchem. J.*, 131 (2017) 174–181.
- [14] H. Bagheri, R. Daliri, A. Roostaie, A novel magnetic poly(aniline-naphthylamine)-based nanocomposite for micro solid phase extraction of rhodamine, *Anal. Chim. Acta*, 794 (2013) 38–46.
- [15] T. Hattori, H. Okamura, S. Asaoka, K. Fukushi, Capillary zone electrophoresis determination of aniline and pyridine in sewage samples using transient isotachopheresis with a system-induced terminator, *J. Chromatog. A*, 1511 (2017) 132–137.
- [16] S. Liu, W. Wang, J. Chen, J. Sun, Determination of aniline and its derivatives in environmental water by capillary electrophoresis with on-line concentration, *Int. J. Mol. Sci.*, 13 (2012) 6863–6872.
- [17] S. Boulahlib, A. Boudina, Development and validation of a fast and simple HPLC method for the simultaneous determination of aniline and its degradation products in wastewater, *Anal. Methods*, 8 (2016) 5949–5956.
- [18] V. Froidevaux, C. Negrell, S. Caillol, J.P. Pascault, B. Boutevin, Biobased amines: from synthesis to polymers, present and future, *Chem. Rev.*, 116 (2016) 14181–14224.
- [19] S. Tadrent, D. Luart, O. Bals, A. Khelfa, R. Luque, C. Len, Metal-free reduction of nitrobenzene to aniline in subcritical water, *J. Org. Chem.*, 83 (2018) 7431–7437.
- [20] N. Galy, R. Nguyen, H. Yalgin, N. Thiebault, D. Luard, C. Len, Glycerol in sub and supercritical solvents, *J. Chem. Technol. Biotechnol.*, 92 (2017) 14–26.
- [21] M.A. Favaro Perez, M. Padula, Primary aromatic amines in kitchenware: Determination by liquid chromatography-tandem mass spectrometry, *J. Chromatogr. A*, 1602 (2019) 217–227.
- [22] X. You, E. Li, J. Liu, S. Li, Using natural biomacromolecules for adsorptive and enzymatic removal of aniline blue from water, *Molecules*, 23 (2018) 1606.
- [23] S. Mazloum, M.M. Al-Ansari, K. Taylor, J.K. Bewtra, N. Biswas, Additive effect on soybean peroxidase-catalyzed removal of anilines from water, *Environ. Eng. Sci.*, 33 (2016) 133–139.
- [24] Y. Kan, Q. Yue, B. Gao, Q. Li, Preparation of epoxy resin-based activated carbons from waste printed circuit boards by steam activation, *Mater. Lett.*, 159 (2015) 443–446.
- [25] J.M. Valente Nabais, P.J.M. Carrott, M.M.L. Ribeiro Carrott, J.A. Menéndez, Preparation and modification of activated carbon fibers by microwave heating, *Carbon*, 42 (2004) 1315–1320.
- [26] L. Huang, Y. Sun, W. Wang, Q. Yue, T. Yang, Comparative study on characterization of activated carbons prepared by microwave and conventional heating methods and application in removal of oxytetracycline (OTC), *Chem. Eng. J.*, 171 (2011) 1446–1453.
- [27] K. Furukawa, M. Hashimoto, S. Kaneco, Optimization of analytical conditions for a rapid determination of aniline in environmental water by liquid chromatography/tandem mass spectrometry, *Anal. Sci.*, 33 (2017) 1189–1191.
- [28] B. Kakavandi, A.J. Jonidi, R.K. Rezaei, S. Nasser, A. Ameri, A. Esrafil, Synthesis and properties of Fe_3O_4 -activated carbon magnetic nanoparticles for removal of aniline

- from aqueous solution, equilibrium, kinetic and thermodynamic studies, Iran. J. Environ. Health Sci. Eng., 10 (2013) 19.
- [29] S. Mazloun, M.M. Al-Ansari, K. Taylor, J.K. Bewtra, N. Biswas, Additive effect on soybean peroxidase-catalyzed removal of anilines from water, Environ. Eng. Sci., 33 (2016) 133-139.
- [30] S. Liu, W. Wang, J. Chen, J. Sun, Determination of aniline and Its derivatives in environmental water by capillary electrophoresis with on-line concentration, Int. J. Mol. Sci., 13 (2012) 6863-6872.
- [31] X. You, E. Li, J. Liu, S. Li, Using natural biomacromolecules for adsorptive and enzymatic removal of aniline blue from water, Molecules, 23 (2018) 1606.
- [32] H. Lu, J. Wang, F.F. Li, X. Huang, B. Tian, H. Hao, Highly efficient and reusable montmorillonite/Fe₃O₄/humic acid nanocomposites for simultaneous removal of Cr(VI) and aniline, Nanomater., 8 (2018) 537.
- [33] O. Yavuz, S. Valzacchi, E. Hoekstra, C. Simoneau, Determination of primary aromatic amines in cold water extract of coloured paper napkin samples by liquid chromatography-tandem mass spectrometry, Food Addit. Contam. Part A, 33 (2016) 1072-1079.
- [34] A. Rahdar, S. Rahdar, G. Labuto, Environmentally friendly synthesis of Fe₂O₃@SiO₂ nanocomposite, characterization and application as an adsorbent to aniline removal from aqueous solution, Environ. Sci. Pollut. Res. Int., 27 (2020) 9181-9191.
- [35] D. Shao, J. Hu, C. Chen, G. Sheng, X. Ren, X. Wang, Polyaniline multiwalled carbon nanotube magnetic composite prepared by plasma-induced graft technique and its application for removal of aniline and phenol, J. Phys. Chem. C, 114 (2010) 21524-21530.